May 2017 UILU-ENG-17-2201

A HIERARCHY OF MODELS FOR INVERTER-BASED MICROGRIDS

Olaoluwapo Ajala, Alejandro D. Domínguez-García, and Peter W. Sauer

Coordinated Science Laboratory
1308 West Main Street, Urbana, IL 61801
University of Illinois at Urbana-Champaign

REPORT DOCUMENTATION PAGE

Form Approved
OMB NO. 0704-0188

1. AGENCY USE ONLY *(Leave blank)*	2. REPORT DATE	3. REPORT TYPE AND DATES COVERED
	May 2017	

4. TITLE AND SUBTITLE
A Hierarchy of Models for Inverter-Based Microgrids

5. FUNDING NUMBERS
(from ARPA-E): DE-AR0000695

6. AUTHOR(S)
Olaoluwapo Ajala, Alejandro D. Domínguez-García, and Peter W. Sauer

7. PERFORMING ORGANIZATION NAME(S) AND ADDRESS(ES)
Coordinated Science Laboratory, University of Illinois at Urbana-Champaign, 1308 W. Main St., Urbana, IL 61801

8. PERFORMING ORGANIZATION REPORT NUMBER
UILU-ENG-17-2201

9. SPONSORING/MONITORING AGENCY NAME(S) AND ADDRESS(ES)
Advanced Research Projects Agency-Energy (ARPA-E), U.S. Department of Energy, within the NODES program; and the MidAmerica Regional Microgrid Education and Training (MARMET) Consortium, U.S. Department of Energy. Both at 1000 Independence Ave SW, Washington, DC 20585

10. SPONSORING/MONITORING AGENCY REPORT NUMBER

11. SUPPLEMENTARY NOTES

12a. DISTRIBUTION/AVAILABILITY STATEMENT

Approved for public release; distribution unlimited.

12b. DISTRIBUTION CODE

13. ABSTRACT *(Maximum 200 words)*

This chapter develops and presents a time resolution based hierarchy of microgrid models for analysis and control design purposes. The focus is on microgrids with distributed generation interfaced via grid-forming inverters. The process of developing the model hierarchy involves two key stages: the formulation of a microgrid high-order model using circuit and control laws, and the systematic reduction of this high-order model to reduced-order models using singular perturbation techniques. The time-scale based hierarchy of models is comprised of the aforementioned microgrid high-order model (μHOm), along with three reduced-order models (microgrid reduced-order model 1 (μROm1), microgrid reduced-order model 2 (μROm2) and microgrid reduced-order model 3 (μROm3)) which are presented in this chapter.

14. SUBJECT TERMS
Microgrid; Distributed energy resource; Reduced-order model; Singular perturbation

15. NUMBER OF PAGES
49

16. PRICE CODE

17. SECURITY CLASSIFICATION OF REPORT	18. SECURITY CLASSIFICATION OF THIS PAGE	19. SECURITY CLASSIFICATION OF ABSTRACT	20. LIMITATION OF ABSTRACT
UNCLASSIFIED	UNCLASSIFIED	UNCLASSIFIED	UL

A Hierarchy of Models for Inverter-Based Microgrids

Olaoluwapo Ajala, Alejandro D. Domínguez-García, and Peter W. Sauer

Abstract This chapter develops and presents a time resolution based hierarchy of microgrid models for analysis and control design purposes. The focus is on microgrids with distributed generation interfaced via grid-forming inverters. The process of developing the model hierarchy involves two key stages: the formulation of a microgrid high-order model using circuit and control laws, and the systematic reduction of this high-order model to reduced-order models using singular perturbation techniques. The time-scale based hierarchy of models is comprised of the aforementioned microgrid high-order model (μHOm), along with three reduced-order models (microgrid reduced-order model 1 (μROm1), microgrid reduced-order model 2 (μROm2) and microgrid reduced-order model 3 (μROm3)) which are presented in this chapter.

Olaoluwapo Ajala
Department of Electrical and Computer Engineering, University of Illinois at Urbana Champaign, 306 N Wright St, Urbana, IL 61801 USA, e-mail: ooajala2@ILLINOIS.EDU

Alejandro D. Domínguez-García
Department of Electrical and Computer Engineering, University of Illinois at Urbana Champaign, 306 N Wright St, Urbana, IL 61801 USA, e-mail: aledan@ILLINOIS.EDU

Peter W. Sauer
Department of Electrical and Computer Engineering, University of Illinois at Urbana Champaign, 306 N Wright St, Urbana, IL 61801 USA, e-mail: psauer@ILLINOIS.EDU

The information, data, or work presented herein was supported by the Advanced Research Projects Agency-Energy (ARPA-E), U.S. Department of Energy, within the NODES program, under Award DE-AR0000695 · The information, data, or work presented herein was supported by the MidAmerica Regional Microgrid Education and Training (MARMET) Consortium, U.S. Department of Energy.

1 Introduction

A microgrid may be defined as a collection of loads and distributed energy resources (DERs), interconnected via an electrical network with a small physical footprint, which is capable of operating in (1) grid-connected mode, as part of a large power system; or (2) islanded mode, as an autonomous power system.

The DERs that constitute a microgrid are often interfaced to the electrical network via a grid-feeding inverter, where the output real and reactive powers are controlled to track a given reference; or via a grid-forming inverter, where the output voltage magnitude and frequency are controlled to track a given reference.

As the popularity and adoption of the microgrid concept in electricity systems increases, it becomes necessary to develop comprehensive mathematical models that can be used for analysis and control design purposes. By utilizing concepts from circuit and control theory, accurate mathematical models may be developed for inverter-based microgrids. However, this in turn leads to the development of highly complex models which are often too detailed for the intended control design or analysis purposes. It therefore becomes necessary to simplify these models to less detailed forms which, though less accurate, can represent the phenomena of interest for each particular application.

The main contribution of this chapter is the development of a time resolution-based hierarchy of models for inverter-based microgrids. Specifically, the focus is on microgrids with grid-forming-inverter-interfaced power supplies interconnected to loads through an electrical network. Using Kirchhoff's laws, Ohms law, and basic control law definitions, a microgrid high-order model (μHOm) is developed. Afterward three reduced-order models (microgrid reduced-order model 1 (μROm1), microgrid reduced-order model 2 (μROm2) and microgrid reduced-order model 3 (μROm3)) are formulated from the μHOm using singular perturbation techniques for model order reduction—the Kuramoto-type model developed in [5] can be extracted from μROm3. The time resolution for which the reduced-order models are valid is also identified, and all four models are explicitly presented with the small parameters used for singular perturbation analysis identified. Finally, a comparison of the models responses, for a given test case, is presented.

The development of high-order and reduced-order models for inverter-based microgrids has received significant attention in the literature recently. More specifically, Pogaku et al. [11] present a high-order model for grid-forming-inverter based microgrids but exclude a discussion on model-order reduction. Anand and Fernandes [1] and Rasheduzzaman et al. [12] present reduced-order models for microgrids but the models are obtained using small-signal analysis, which is only valid within certain operating regions. Kodra et al. [7] discuss the model-order reduction of an islanded microgrid using singular perturbation analysis. However, the electrical network dynamics are not included in the high-order model presented, and a simple linear model, which does not fully capture the dynamics of the islanded microgrid, is used for the singular perturbation analysis. Dörfler and Bullo [5] present a Kuramoto-type model for a grid-forming-inverter developed using singular perturbation analysis. The electrical network is considered in the analysis and sufficient

conditions for which the reduced-order Kuramoto-type model is valid are presented. However, the analysis is not as detailed as that presented in this chapter. More specifically, the time-scale resolution associated with the Kuramoto-type is not discussed, the analysis is performed for a lossless electrical network, and the high-order model, on which singular perturbation analysis is performed, is not rigorously developed. Schiffer et al. [14] develop a detailed high-order model for grid-forming-inverter-based microgrids. Singular perturbation analysis is then employed to perform time-scale separation and model-order reduction, as done in this chapter with underlying assumptions stated. However, though the authors claim that the model-order reduction can be performed, the small parameters used for singular perturbation analysis are not explicitly identified, and details of the singular perturbation analysis are not presented. Also, the time resolution associated with the reduced-order model developed is not identified. Luo and Dhople [10] present three models for a grid-forming-inverter-based microgrid which are obtained by performing successive model reduction steps on a high-order model, using singular perturbation analysis. However, the singular perturbation analysis is presented in a much less detailed form as is in this chapter, the time scales associated with each reduced model are not identified, and the high-order model from which all other models are derived is not explicitly stated with all the small parameters used for singular perturbation analysis identified.

The remainder of this chapter is organized as follows. In Section 2, the following relevant concepts, to be used in later developments, are introduced: (1) the $qd0$ transformation of three-phase variables [9], (2) graph-theoretic notions, and (3) singular perturbation analysis techniques for time-scale modeling and model-order reduction [8] . In Section 3, the microgrid high-order model (μHOm) is developed. Circuit laws and control design definitions are used to formulate mathematical models for: (1) the three-phase grid-forming inverter (2) the electrical network of the microgrid and (3) the interconnected loads . Afterwards the models are combined to result in the so-called μHOm. In Sections 4–6, small parameters $\varepsilon_1 = 1 \times 10^{-5}$, $\varepsilon_2 = 1 \times 10^{-3}$ and $\varepsilon_3 = 1 \times 10^{-1}$ are chosen respectively, and in each case, the small parameter is used to perform time-scale separation and model-order reduction of the μHOm, using singular perturbation techniques, to obtain μROm1, μROm2 and μROm3, respectively. Finally, in Section 7, the time resolutions of μROm1, μROm2 and μROm3 are identified, and a comparison between the models responses, for a given test case, is presented.

2 Preliminaries

In this section, we first introduce the $qd0$ transformation of three-phase variables to arbitrary and synchronous reference frames. Next, we introduce graph-theoretic notions used in later developments to develop models for an electrical network and its interconnected electrical loads. Finally, a primer on singular perturbation analysis for time-scale modeling and model-order reduction is presented.

2.1 The $qd0$ Transformation

Let $\alpha^{(j)}(t)$ denote the angular position of a reference frame rotating at angular velocity $\omega^{(j)}(t)$, and let $\mathbf{f}^{(j)}_{qd0[\alpha^{(j)}(t)]}(t) = \left[f^{(j)}_{q[\alpha^{(j)}(t)]}(t)\ f^{(j)}_{d[\alpha^{(j)}(t)]}(t)\ f^{(j)}_{0[\alpha^{(j)}(t)]}(t)\right]^{\mathrm{T}}$ denote the $qd0$ transform of a three-phase variable, $\mathbf{f}^{(j)}_{abc}(t) = \left[f^{(j)}_{a}(t)\ f^{(j)}_{b}(t)\ f^{(j)}_{c}(t)\right]^{\mathrm{T}}$, to the rotating reference frame. From [9], the general form of the $qd0$ transformation is given by:

$$\mathbf{f}^{(j)}_{qd0[\alpha^{(j)}(t)]}(t) = \mathbf{K}_1(\alpha^{(j)}(t))\mathbf{f}^{(j)}_{abc}(t), \tag{1}$$

where:

$$\begin{aligned}\mathbf{K}_1(\alpha^{(j)}(t)) &= \frac{2}{3}\begin{bmatrix}\cos(\alpha^{(j)}(t)) & \cos(\alpha^{(j)}(t)-\frac{2\pi}{3}) & \cos(\alpha^{(j)}(t)+\frac{2\pi}{3})\\ \sin(\alpha^{(j)}(t)) & \sin(\alpha^{(j)}(t)-\frac{2\pi}{3}) & \sin(\alpha^{(j)}(t)+\frac{2\pi}{3})\\ \frac{1}{2} & \frac{1}{2} & \frac{1}{2}\end{bmatrix},\\ \alpha^{(j)}(t) &= \int_0^t \omega^{(j)}(\tau)\,d\tau + \alpha^{(j)}(0).\end{aligned} \tag{2}$$

Let $\mathbf{f}^{(j)}_{qd0[\omega_0 t]}(t) = \left[f^{(j)}_{q[\omega_0 t]}(t)\ f^{(j)}_{d[\omega_0 t]}(t)\ f^{(j)}_{0[\omega_0 t]}(t)\right]^{\mathrm{T}}$ denote the $qd0$ transformation of $\mathbf{f}^{(j)}_{abc}(t)$ to a reference frame with angular position $\omega_0 t$. Then we have that:

$$\mathbf{f}^{(j)}_{qd0[\omega_0 t]}(t) = \mathbf{K}_1(\omega_0 t)\mathbf{f}^{(j)}_{abc}(t), \tag{3}$$

where ω_0 denotes the synchronous frequency, and:

$$\mathbf{K}_1(\omega_0 t) = \frac{2}{3}\begin{bmatrix}\cos(\omega_0 t) & \cos(\omega_0 t-\frac{2\pi}{3}) & \cos(\omega_0 t+\frac{2\pi}{3})\\ \sin(\omega_0 t) & \sin(\omega_0 t-\frac{2\pi}{3}) & \sin(\omega_0 t+\frac{2\pi}{3})\\ \frac{1}{2} & \frac{1}{2} & \frac{1}{2}\end{bmatrix}. \tag{4}$$

In a balanced three-phase system the element $f^{(j)}_{0[.]}(t)$ of $\mathbf{f}^{(j)}_{qd0[.]}(t)$ is equal to zero (see [9], pp. 98–99). The $qd0$ reference frames in Eqs. 1 and 3 are referred to as the arbitrary reference frame and the synchronous reference frame respectively [9].

Synchronous Reference Frame to Arbitrary Reference Frame Transformation

Consider a three phase sinusoidal variable, $\mathbf{f}^{(j)}_{abc[\alpha^{(j)}(t)]}(t)$. Let $\overrightarrow{\mathbf{f}}^{(j)}_{qd0[\omega_0 t]}(t)$ and $\overrightarrow{\mathbf{f}}^{(j)}_{qd0[\alpha^{(j)}(t)]}(t)$ denote its phasor representation in the synchronous reference frame and the arbitrary reference frame of the inverter at bus j respectively, and let $\left|\overrightarrow{\mathbf{f}}^{(j)}_{qd0[.]}(t)\right|$ denote the phasor magnitude accordingly, so that:

$$\overrightarrow{\mathbf{f}}^{(j)}_{qd0[\omega_0 t]}(t) := f^{(j)}_{q[\omega_0 t]}(t) - \mathrm{j} f^{(j)}_{d[\omega_0 t]}(t), \tag{5}$$

$$\overrightarrow{\mathbf{f}}^{(j)}_{qd0[\alpha^{(j)}(t)]}(t) := f^{(j)}_{q[\alpha^{(j)}(t)]}(t) - \mathrm{j} f^{(j)}_{d[\alpha^{(j)}(t)]}(t), \tag{6}$$

where j denotes the complex variable, i.e., $\mathrm{j} = \sqrt{-1}$. The phasor representations are related through the expression:

$$\overrightarrow{\mathbf{f}}^{(j)}_{qd0[\alpha^{(j)}(t)]}(t) = \overrightarrow{\mathbf{f}}^{(j)}_{qd0[\omega_0 t]}(t) \exp(-\mathrm{j}\delta^{(j)}(t)), \tag{7}$$

with

$$\delta^{(j)}(t) := \alpha^{(j)}(t) - \omega_0 t. \tag{8}$$

From Eqs. 5–7, it follows that:

$$f^{(j)}_{q[\alpha^{(j)}(t)]}(t) = f^{(j)}_{q[\omega_0 t]}(t)\cos(\delta^{(j)}(t)) - f^{(j)}_{d[\omega_0 t]}(t)\sin(\delta^{(j)}(t)), \tag{9}$$

$$f^{(j)}_{d[\alpha^{(j)}(t)]}(t) = f^{(j)}_{q[\omega_0 t]}(t)\sin(\delta^{(j)}(t)) + f^{(j)}_{d[\omega_0 t]}(t)\cos(\delta^{(j)}(t)), \tag{10}$$

and

$$f^{(j)}_{q[\omega_0 t]}(t) = f^{(j)}_{q[\alpha^{(j)}(t)]}(t)\cos(\delta^{(j)}(t)) + f^{(j)}_{d[\alpha^{(j)}(t)]}(t)\sin(\delta^{(j)}(t)), \tag{11}$$

$$f^{(j)}_{d[\omega_0 t]}(t) = -f^{(j)}_{q[\alpha^{(j)}(t)]}(t)\sin(\delta^{(j)}(t)) + f^{(j)}_{d[\alpha^{(j)}(t)]}(t)\cos(\delta^{(j)}(t)), \tag{12}$$

which can be compactly written as:

$$\mathbf{f}^{(j)}_{qd0[\alpha^{(j)}(t)]}(t) = \mathbf{K}_2(\delta^{(j)}(t))\mathbf{f}^{(j)}_{qd0[\omega_0 t]}(t), \tag{13}$$

$$\mathbf{f}^{(j)}_{qd0[\omega_0 t]}(t) = \left(\mathbf{K}_2(\delta^{(j)}(t))\right)^{-1}\mathbf{f}^{(j)}_{qd0[\alpha^{(j)}(t)]}(t), \tag{14}$$

with

$$\mathbf{K}_2(\delta^{(j)}(t)) = \begin{bmatrix} \cos(\delta^{(j)}(t)) & -\sin(\delta^{(j)}(t)) \\ \sin(\delta^{(j)}(t)) & \cos(\delta^{(j)}(t)) \end{bmatrix}. \tag{15}$$

Figure 1 is a graphical representation of Eqs. 13–14, from where it follows that:

$$\begin{aligned} f^{(j)}_{q[\omega_0 t]}(t) - \mathrm{j} f^{(j)}_{d[\omega_0 t]}(t) &= \left(f^{(j)}_{q[\alpha^{(j)}(t)]}(t) - \mathrm{j} f^{(j)}_{d[\alpha^{(j)}(t)]}(t)\right)\exp(\mathrm{j}\delta^{(j)}(t)) \\ &= \left(f^{(j)}_{d[\alpha^{(j)}(t)]}(t) + \mathrm{j} f^{(j)}_{q[\alpha^{(j)}(t)]}(t)\right)\exp\left(\mathrm{j}\left(\delta^{(j)}(t) - \frac{\pi}{2}\right)\right) \end{aligned} \tag{16}$$

and

$$
\begin{aligned}
f^{(j)}_{q[\alpha^{(j)}(t)]}(t) - \mathrm{j} f^{(j)}_{d[\alpha^{(j)}(t)]}(t) &= \left(f^{(j)}_{q[\omega_0 t]}(t) - \mathrm{j} f^{(j)}_{d[\omega_0 t]}(t) \right) \exp(-\mathrm{j}\delta^{(j)}(t)) \\
&= \left(f^{(j)}_{d[\omega_0 t]}(t) + \mathrm{j} f^{(j)}_{q[\omega_0 t]}(t) \right) \exp\left(-\mathrm{j} \left(\delta^{(j)}(t) + \frac{\pi}{2} \right) \right)
\end{aligned} \tag{17}
$$

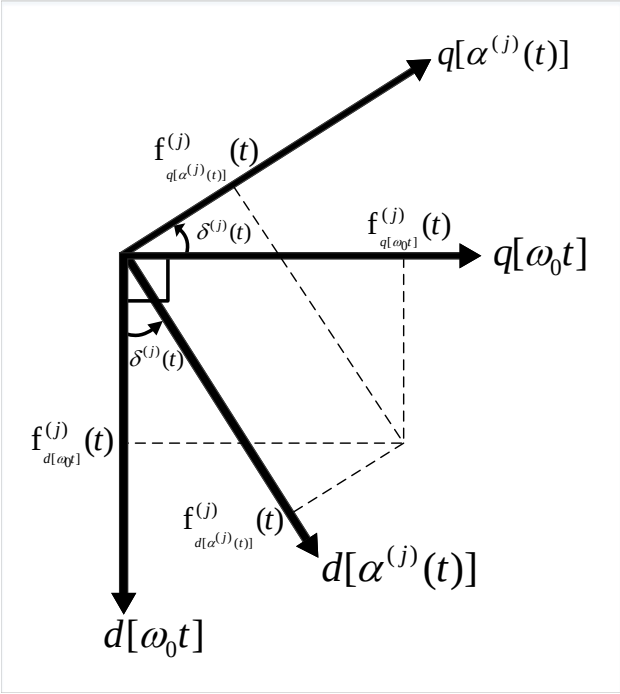

Fig. 1: Graphical representation.

Phase Angle Dynamics

The transformation matrix in Eq. 15 is a function of $\delta^{(j)}(t)$. From Eq. 8, the evolution of $\delta^{(j)}(t)$ is governed by:

$$
\frac{d\delta^{(j)}(t)}{dt} = \frac{d\alpha^{(j)}(t)}{dt} - \omega_0, \tag{18}
$$

and since from Eq. 2 we have that $\omega^{(j)}(t) = \frac{d\alpha^{(j)}(t)}{dt}$, it follows that:

$$\frac{d\delta^{(j)}(t)}{dt} = \omega^{(j)}(t) - \omega_0. \tag{19}$$

2.2 Graph-Theoretic Notions

The topology of an electrical network can be described by a connected undirected graph, $\mathscr{G} = (\mathscr{V}, \mathscr{E})$, with $\mathscr{V}$ denoting the set of buses in the network, so that $\mathscr{V} := \{1, 2, \ldots, |\mathscr{V}|\}$, and $\mathscr{E} \subset \mathscr{V} \times \mathscr{V}$, so that $\{j,k\} \in \mathscr{E}$ if buses j and k are electrically connected. For a graph $\mathscr{G}$ with $|\mathscr{E}|$ directed edges and n nodes, we define the incidence matrix to be a $|\mathscr{E}| \times n$ matrix

$$M = [m_{ij}].$$

where

$$\begin{aligned}
&[m_{ij}] = 1 \quad \text{if edge } j \text{ is directed into node } i,\\
&[m_{ij}] = -1 \quad \text{if edge } j \text{ is directed away from node } i,\\
&[m_{ij}] = 0 \quad \text{if edge } j \text{ is not incident on node } i.
\end{aligned}$$

Let $\mathbb{S} := \{|\mathscr{V}| + 1, \ldots, |\mathscr{V}| + |\mathscr{E}|\}$ and define a one-to-one map, $p : \mathscr{E} \to \mathbb{S}$ such that every $e \in \mathbb{S}$ is arbitrarily assigned to exactly one edge $\{j,k\} \in \mathscr{E}$, so that $p\left(\{j,k\}\right) = e$. Consequently, we can represent the resistance, inductance and current across a line extending from bus j to bus k as: $R^{(e)}$, $L^{(e)}$ and $I^{(e)}(t)$ respectively.

Without loss of generality, we assume that a net load is connected to each bus of an electrical network (if no load is connected, the net load connected is zero). Let $\mathscr{V}^{(\mathscr{I})} \subseteq \mathscr{V}$ denote the set of buses connected to an inverter-interfaced source, and let $\mathscr{V}^{(\mathscr{N})} \subseteq \mathscr{V}$ denote the set of buses not connected to an inverter-interfaced source, so that $\mathscr{V}^{(\mathscr{I})} \cup \mathscr{V}^{(\mathscr{N})} = \mathscr{V}$ and $\mathscr{V}^{(\mathscr{I})} \cap \mathscr{V}^{(\mathscr{N})} = \emptyset$, with $\mathscr{V}^{(\mathscr{I})} := \{1, 2, \ldots, |\mathscr{V}^{(\mathscr{I})}|\}$, and $\mathscr{V}^{(\mathscr{N})} := \{|\mathscr{V}^{(\mathscr{I})}| + 1, |\mathscr{V}^{(\mathscr{I})}| + 2, \ldots, |\mathscr{V}|\}$. For a network with n nodes, let $\mathbb{S}' := \{|\mathscr{V}| + |\mathscr{E}| + 1, \ldots, |\mathscr{V}| + |\mathscr{E}| + |\mathscr{V}^{(\mathscr{I})}|\}$, and define a one-to-one map, $p' : \mathscr{V}^{(\mathscr{I})} \to \mathbb{S}'$, $p' : \mathscr{V}^{(\mathscr{N})} \to \mathscr{V}^{(\mathscr{N})}$ such that:

- for bus $j \in \mathscr{V}^{(\mathscr{I})}$, $p'(j) = e'$ where $e' \in \mathbb{S}'$ is arbitrarily assigned to exactly one node $j \in \mathscr{V}^{(\mathscr{I})}$; and
- for bus $j \in \mathscr{V}^{(\mathscr{N})}$, $p'(j) = e'$ where $e' = j$.

Consequently, we can represent the resistance, inductance and current injection of the net load at bus j as: $R^{(e')}$, $L^{(e')}$ and $I^{(e')}(t)$ respectively, where $e' \in \mathbb{S}'$ if $j \in \mathscr{V}^{(\mathscr{I})}$ and $e' = j$ if $j \in \mathscr{V}^{(\mathscr{N})}$.

2.3 A Primer on Singular Perturbation Analysis

For the development of reduced-order model i, we consider the high-order model

$$\dot{\mathbf{x}}_i(t) = f_i\left(\mathbf{x}_i(t), \mathbf{z}_i(t), \mathbf{w}_i(t), \varepsilon_i\right), \tag{20}$$

$$\varepsilon_i \dot{\mathbf{z}}_i(t) = g_i\left(\mathbf{x}_i(t), \mathbf{z}_i(t), \mathbf{w}_i(t), \varepsilon_i\right), \tag{21}$$

$$\mathbf{0} = h_i\left(\mathbf{x}_i(t), \mathbf{z}_i(t), \mathbf{w}_i(t), \varepsilon_i\right). \tag{22}$$

Standard Form. When we set $\varepsilon_i = 0$, the state space dimension of the high-order model reduces because Eq. 21 degenerates into an algebraic or transcendental equation, and it follows that:

$$\mathbf{0} = g_i\left(\bar{\mathbf{x}}_i(t), \bar{\mathbf{z}}_i(t), \bar{\mathbf{w}}_i(t), 0\right), \tag{23}$$

$$\mathbf{0} = h_i\left(\bar{\mathbf{x}}_i(t), \bar{\mathbf{z}}_i(t), \bar{\mathbf{w}}_i(t), 0\right), \tag{24}$$

where the bar ($\bar{}$) notation is used to indicate that the variables belong to a system with $\varepsilon_i = 0$.

The high-order model is in standard form if and only if, in a domain of interest, Eqs. 23–24 have $r \geq 1$ isolated real roots for $\bar{\mathbf{z}}_i(t)$ and $\bar{\mathbf{w}}_i(t)$. Let $\bar{\mathbf{z}}_i(t) = \bar{\zeta}_i\left(\bar{\mathbf{x}}_i(t)\right)$ and $\bar{\mathbf{w}}_i(t) = \bar{v}_i\left(\bar{\mathbf{x}}_i(t)\right)$ be isolated roots of Eqs. 23–24, it follows that:

$$\begin{aligned}\dot{\bar{\mathbf{x}}}_i(t) &= f_i\left(\bar{\mathbf{x}}_i(t), \bar{\mathbf{z}}_i(t), \bar{\mathbf{w}}_i(t), 0\right) \\ &= f_i\left(\bar{\mathbf{x}}_i(t), \bar{\zeta}_i\left(\bar{\mathbf{x}}_i(t)\right), \bar{v}_i\left(\bar{\mathbf{x}}_i(t)\right), 0\right).\end{aligned} \tag{25}$$

Time-Scale Separation. Let $\tau_i = \frac{t}{\varepsilon_i}$. We perform a two-time-scale asymptotic expansion of $\mathbf{x}_i$, $\mathbf{z}_i$ and $\mathbf{w}_i$, having some terms defined in a t-scale and others in a τ_i-scale.

General asymptotic expansion procedures use two power series in ε_i to represent $\mathbf{x}_i$, $\mathbf{z}_i$ and $\mathbf{w}_i$, individually. The coefficients of the first series are functions of t, and those of the second are functions of τ_i (see [8], pp. 11-12).

Truncating the asymptotic expansions to only the first terms, it follows that:

$$\mathbf{x}_i(t) \approx \bar{\mathbf{x}}_i(t) + \tilde{\mathbf{x}}_i(\tau_i), \tag{26}$$

$$\mathbf{z}_i(t) \approx \bar{\mathbf{z}}_i(t) + \tilde{\mathbf{z}}_i(\tau_i), \tag{27}$$

$$\mathbf{w}_i(t) \approx \bar{\mathbf{w}}_i(t) + \tilde{\mathbf{w}}_i(\tau_i), \tag{28}$$

where the bar ($\bar{}$) and tilde ($\tilde{}$) notations are used to describe the t-scale and τ_i-scale variables respectively. Substituting the truncated expansions into the high-order model, we obtain:

$$\dot{\bar{\mathbf{x}}}_i(t) + \frac{1}{\varepsilon_i}\frac{d\tilde{\mathbf{x}}_i(\tau_i)}{d\tau_i} = f_i\left(\bar{\mathbf{x}}_i(t) + \tilde{\mathbf{x}}_i(\tau_i), \bar{\mathbf{z}}_i(t) + \tilde{\mathbf{z}}_i(\tau_i), \bar{\mathbf{w}}_i(t) + \tilde{\mathbf{w}}_i(\tau_i), \varepsilon_i\right), \tag{29}$$

$$\varepsilon_i \dot{\bar{\mathbf{z}}}_i(t) + \frac{d\tilde{\mathbf{z}}_i(\tau_i)}{d\tau_i} = g_i\left(\bar{\mathbf{x}}_i(t) + \tilde{\mathbf{x}}_i(\tau_i), \bar{\mathbf{z}}_i(t) + \tilde{\mathbf{z}}_i(\tau_i), \bar{\mathbf{w}}_i(t) + \tilde{\mathbf{w}}_i(\tau_i), \varepsilon_i\right), \tag{30}$$

$$\mathbf{0} = h_i\left(\bar{\mathbf{x}}_i(t) + \tilde{\mathbf{x}}_i(\tau_i), \bar{\mathbf{z}}_i(t) + \tilde{\mathbf{z}}_i(\tau_i), \bar{\mathbf{w}}_i(t) + \tilde{\mathbf{w}}_i(\tau_i), \varepsilon_i\right). \tag{31}$$

Assumption 2.1 $\tilde{\mathbf{x}}_i(0) = \mathbf{0}$*, and* $\bar{\mathbf{x}}_i(t)$ *satisfies Eq. 25*

Given the above assumptions and setting $\varepsilon_i = 0$, it follows that $\tilde{\mathbf{x}}_i(\tau_i) \equiv \mathbf{0}$, and

$$\dot{\bar{\mathbf{x}}}_i(t) = f_i\left(\bar{\mathbf{x}}_i(t), \bar{\mathbf{z}}_i(t) + \tilde{\mathbf{z}}_i(\tau_i), \bar{\mathbf{w}}_i(t) + \tilde{\mathbf{w}}_i(\tau_i), 0\right), \tag{32}$$

$$\frac{d\tilde{\mathbf{z}}_i(\tau_i)}{d\tau_i} = g_i\left(\bar{\mathbf{x}}_i(0), \bar{\mathbf{z}}_i(0) + \tilde{\mathbf{z}}_i(\tau_i), \bar{\mathbf{w}}_i(0) + \tilde{\mathbf{w}}_i(\tau_i), 0\right), \tag{33}$$

$$\mathbf{0} = h_i\left(\bar{\mathbf{x}}_i(0), \bar{\mathbf{z}}_i(0) + \tilde{\mathbf{z}}_i(\tau_i), \bar{\mathbf{w}}_i(0) + \tilde{\mathbf{w}}_i(\tau_i), 0\right), \tag{34}$$

where

$$\bar{\mathbf{x}}_i(0) = \mathbf{x}_i(0), \quad \bar{\mathbf{z}}_i(t) = \bar{\zeta}_i\left(\bar{\mathbf{x}}_i(t)\right), \quad \bar{\mathbf{w}}_i(t) = \bar{\nu}_i\left(\bar{\mathbf{x}}_i(t)\right) \quad \text{and} \quad \tilde{\mathbf{z}}_i(0) = \mathbf{z}_i(0) - \bar{\mathbf{z}}_i(0).$$

For the standard high-order model, a distinct solution $\tilde{\mathbf{w}}_i(\tau_i) = \tilde{\nu}_i\left(\tilde{\mathbf{z}}_i(\tau_i)\right)$ exists for Eq. 34, and the model can be simplified to:

$$\dot{\bar{\mathbf{x}}}_i(t) = f_i\left(\bar{\mathbf{x}}_i(t), \bar{\mathbf{z}}_i(t) + \tilde{\mathbf{z}}_i(\tau_i), \bar{\mathbf{w}}_i(t) + \tilde{\nu}_i\left(\tilde{\mathbf{z}}_i(\tau_i)\right), 0\right), \tag{35}$$

$$\frac{d\tilde{\mathbf{z}}_i(\tau_i)}{d\tau_i} = g_i\left(\bar{\mathbf{x}}_i(0), \bar{\mathbf{z}}_i(0) + \tilde{\mathbf{z}}_i(\tau_i), \bar{\mathbf{w}}_i(0) + \tilde{\nu}_i\left(\tilde{\mathbf{z}}_i(\tau_i), 0\right)\right). \tag{36}$$

The expressions in Eqs. 35–36 represent an approximate time-scale separation of the high-order model dynamics to fast-time-scale, τ_i, and slow-time-scale, t, dynamics.

Sufficient Conditions for Model-Order Reduction. Tikhonov's theorem provides sufficient conditions for which the approximate time-scale separation above is valid for model-order reduction (see [8], pp. 10–11).

Assumption 2.2 *The equilibrium* $\tilde{\mathbf{z}}_i(\tau_i) = 0$ *of Eq. 36 is asymptotically stable in* $\bar{\mathbf{x}}_i(0)$*, and* $\tilde{\mathbf{z}}_i(0)$ *belongs to its domain of attraction.*

Assumption 2.3 *The eigenvalues of* $\frac{\partial \mathbf{g}_i}{\partial \mathbf{z}_i}$ *evaluated, for* $\varepsilon_i = 0$*, along* $\bar{\mathbf{x}}_i(t)$*,* $\bar{\mathbf{z}}_i(t)$*, have real parts smaller than a fixed negative number.*

Tikhonov's theorem states that if the high-order model is in standard form, and Assumptions 2.2 and 2.3 are satisfied, then, with error $O(\varepsilon_i)$, the high-order model can be approximately described by a slow model,

$$\dot{\bar{\mathbf{x}}}_i(t) = f_i\left(\bar{\mathbf{x}}_i(t), \bar{\zeta}_i\left(\bar{\mathbf{x}}_i(t)\right), \bar{\nu}_i\left(\bar{\mathbf{x}}_i(t)\right) + \tilde{\nu}_i\left(\mathbf{0}\right), 0\right), \tag{37}$$

and a fast model,

$$\frac{d\tilde{\mathbf{z}}_i(\tau_i)}{d\tau_i} = g_i\left(\bar{\mathbf{x}}_i(0), \bar{\zeta}_i\left(\bar{\mathbf{x}}_i(0)\right) + \tilde{\mathbf{z}}_i(\tau_i), \bar{\nu}_i\left(\bar{\mathbf{x}}_i(0)\right) + \tilde{\nu}_i\left(\tilde{\mathbf{z}}_i(\tau_i)\right), 0\right), \tag{38}$$

where

$$\bar{\mathbf{x}}_i(0) = \mathbf{x}_i(0) \qquad \text{and} \qquad \tilde{\mathbf{z}}_i(0) = \mathbf{z}_i(0) - \bar{\zeta}_i\left(\bar{\mathbf{x}}_i(0)\right),$$

so that

$$\mathbf{x}_i(t) = \bar{\mathbf{x}}_i(t) + O(\varepsilon_i) \qquad \text{and} \qquad \mathbf{z}_i(t) = \tilde{\mathbf{z}}_i(\tau_i) + \bar{\zeta}_i\left(\bar{\mathbf{x}}_i(t)\right) + O(\varepsilon_i).$$

The high-order model may be reduced to the form in Eq. 37, which is independent of $\tilde{\mathbf{z}}_i(\tau_i)$. In subsequent chapters, Eq. 37 is called *Reduced-Order Model i*.

Time Resolution of Reduced-Order Model i. Given Assumptions 2.2–2.3, it follows that the eigenvalues associated with the fast dynamics in the high-order model have strictly negative real parts. Choosing a small parameter ε_i such that $-\frac{1}{\varepsilon_i}$ is greater than the real part of eigenvalues associated with the fast dynamics, then the fast model in Eq. 38 reaches equilibrium $\tilde{\mathbf{z}}_i(\tau_i) = 0$ in $5\varepsilon_i$ seconds, after it is perturbed from an equilibrium state. As a result, *the time resolution for reduced-order model i is approximately* $5\varepsilon_i$ *seconds*.

3 Microgrid High-Order Model (μHO)

In this section, basic circuit laws are used in conjunction with notions introduced in Section 2 to develop a High-Order model for a grid-forming-inverter-based AC microgrid operating in islanded mode. First, a model is developed for the three-phase grid-forming-inverter which includes a three-phase inverter model, a *LCL* filter model and a voltage magnitude controller model. Next, a model for the three-phase electrical network is developed, and afterward a three-phase load model is introduced. Finally, the three-phase grid-forming-inverter model, the network model and the load model are combined to form the μHOm.

3.1 Inverter Model

A 3-phase inverter coupled with a battery, an *LCL* filter and a voltage magnitude controller is adopted in this work (see Fig. 2 for a diagram). An averaged model, as opposed to a switched model, is used to describe the 3-phase inverter dynamics (see [15], pp. 27–38, for more details).

Inverter Averaged Model

For an inverter connected to bus j of a microgrid, let $V_{DC}^{(j)}$, $u^{(j)}(t)$, $e^{(j)}(t)$, $\hat{e}^{(j)}(t)$ and $v^{(j)}(t)$ denote the dc voltage at the inverter input, the Pulse Width Modulation (PWM) output voltage of the inverter, the internal voltage of the inverter, the *LCL* capacitor voltage and the voltage at bus j of the network respectively. Additionally,

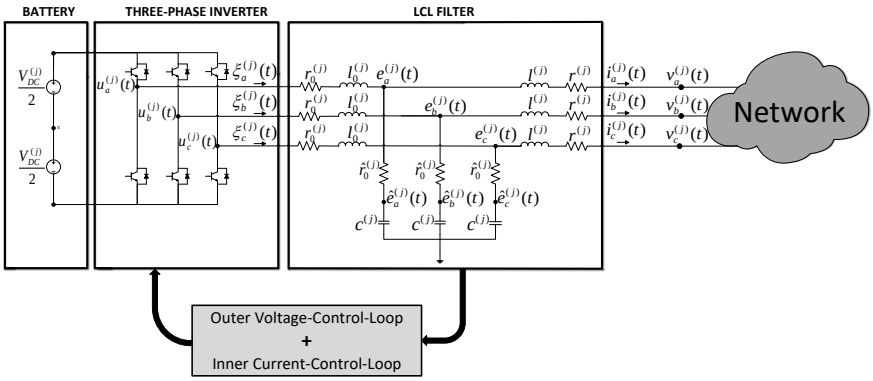

Fig. 2: 3-phase voltage-sourced inverter at bus j.

let $\xi^{(j)}(t)$ and $i^{(j)}(t)$ denote the inverter output current and the filtered inverter output current respectively. Then the dynamics of the *LCL* filter, shown in Fig. 3, can be described by:

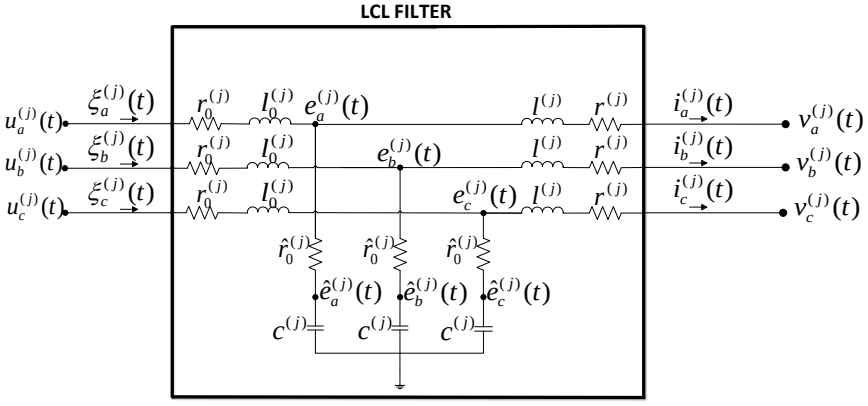

Fig. 3: *LCL* Filter at bus j.

$$l^{(j)}\frac{di_a^{(j)}(t)}{dt} = -r^{(j)}i_a^{(j)}(t) + e_a^{(j)}(t) - v_a^{(j)}(t), \tag{39}$$

$$l^{(j)}\frac{di_b^{(j)}(t)}{dt} = -r^{(j)}i_b^{(j)}(t) + e_b^{(j)}(t) - v_b^{(j)}(t), \tag{40}$$

$$l^{(j)}\frac{di_c^{(j)}(t)}{dt} = -r^{(j)}i_c^{(j)}(t) + e_c^{(j)}(t) - v_c^{(j)}(t), \tag{41}$$

$$c^{(j)}\frac{d\hat{e}_a^{(j)}(t)}{dt} = -i_a^{(j)}(t) + \xi_a^{(j)}(t), \tag{42}$$

$$c^{(j)}\frac{d\hat{e}_b^{(j)}(t)}{dt} = -i_b^{(j)}(t) + \xi_b^{(j)}(t), \tag{43}$$

$$c^{(j)}\frac{d\hat{e}_c^{(j)}(t)}{dt} = -i_c^{(j)}(t) + \xi_c^{(j)}(t), \tag{44}$$

$$l_0^{(j)}\frac{d\xi_a^{(j)}(t)}{dt} = -e_a^{(j)}(t) - r_0^{(j)}\xi_a^{(j)}(t) + u_a^{(j)}(t), \tag{45}$$

$$l_0^{(j)}\frac{d\xi_b^{(j)}(t)}{dt} = -e_b^{(j)}(t) - r_0^{(j)}\xi_b^{(j)}(t) + u_b^{(j)}(t), \tag{46}$$

$$l_0^{(j)}\frac{d\xi_c^{(j)}(t)}{dt} = -e_c^{(j)}(t) - r_0^{(j)}\xi_c^{(j)}(t) + u_c^{(j)}(t), \tag{47}$$

$$e_a^{(j)}(t) = \left(-i_a^{(j)}(t) + \xi_a^{(j)}(t)\right)\hat{r}_0^{(j)} + \hat{e}_a^{(j)}(t), \tag{48}$$

$$e_b^{(j)}(t) = \left(-i_b^{(j)}(t) + \xi_b^{(j)}(t)\right)\hat{r}_0^{(j)} + \hat{e}_b^{(j)}(t), \tag{49}$$

$$e_c^{(j)}(t) = \left(-i_c^{(j)}(t) + \xi_c^{(j)}(t)\right)\hat{r}_0^{(j)} + \hat{e}_c^{(j)}(t). \tag{50}$$

where $l_0^{(j)}$, $l^{(j)}$ and $c^{(j)}$ denote the inductances and capacitance of the *LCL* filter respectively, and $r_0^{(j)}$, $\hat{r}_0^{(j)}$ and $r^{(j)}$ denote the inverter and filter resistances.

In a balanced three-phase system, the 0 axis component of the $qd0$ transformation is equal to zero (see [9], pp. 98–99). To reduce the dimension of the model in Eqs. 39–47 and describe the controller dynamics (to be presented later) as a DC command tracking task instead of a sinusoidal command tracking task, the model in Eqs. 39–47 is transformed to a two-phase model using the $qd0$ transformation presented in Section 2.1.

Then, by using the expression in Eq. 1, the *LCL* filter dynamics for the inverter at bus j, in its arbitrary reference frame, is given by:

$$\begin{aligned} l^{(j)}\frac{di^{(j)}_{q[\alpha^{(j)}(t)]}(t)}{dt} =& -r^{(j)}i^{(j)}_{q[\alpha^{(j)}(t)]}(t) - \omega^{(j)}(t)l^{(j)}i^{(j)}_{d[\alpha^{(j)}(t)]}(t) + e^{(j)}_{q[\alpha^{(j)}(t)]}(t) \\ & - v^{(j)}_{q[\alpha^{(j)}(t)]}(t), \end{aligned} \tag{51}$$

$$\begin{aligned} l^{(j)}\frac{di^{(j)}_{d[\alpha^{(j)}(t)]}(t)}{dt} =& \omega^{(j)}(t)l^{(j)}i^{(j)}_{q[\alpha^{(j)}(t)]}(t) - r^{(j)}i^{(j)}_{d[\alpha^{(j)}(t)]}(t) + e^{(j)}_{d[\alpha^{(j)}(t)]}(t) \\ & - v^{(j)}_{d[\alpha^{(j)}(t)]}(t), \end{aligned} \tag{52}$$

$$c^{(j)}\frac{d\hat{e}^{(j)}_{q[\alpha^{(j)}(t)]}(t)}{dt} = -i^{(j)}_{q[\alpha^{(j)}(t)]}(t) - \omega^{(j)}(t)c^{(j)}\hat{e}^{(j)}_{d[\alpha^{(j)}(t)]}(t) + \xi^{(j)}_{q[\alpha^{(j)}(t)]}(t), \tag{53}$$

$$c^{(j)}\frac{d\hat{e}^{(j)}_{d[\alpha^{(j)}(t)]}(t)}{dt} = -i^{(j)}_{d[\alpha^{(j)}(t)]}(t) + \omega^{(j)}(t)c^{(j)}\hat{e}^{(j)}_{q[\alpha^{(j)}(t)]}(t) + \xi^{(j)}_{d[\alpha^{(j)}(t)]}(t), \quad (54)$$

$$l^{(j)}_0\frac{d\xi^{(j)}_{q[\alpha^{(j)}(t)]}(t)}{dt} = -e^{(j)}_{q[\alpha^{(j)}(t)]}(t) - r^{(j)}_0\xi^{(j)}_{q[\alpha^{(j)}(t)]}(t) - \omega^{(j)}(t)l^{(j)}_0\xi^{(j)}_{d[\alpha^{(j)}(t)]}(t) + u^{(j)}_{q[\alpha^{(j)}(t)]}(t), \quad (55)$$

$$l^{(j)}_0\frac{d\xi^{(j)}_{d[\alpha^{(j)}(t)]}(t)}{dt} = -e^{(j)}_{d[\alpha^{(j)}(t)]}(t) + \omega^{(j)}(t)l^{(j)}_0\xi^{(j)}_{q[\alpha^{(j)}(t)]}(t) - r^{(j)}_0\xi^{(j)}_{d[\alpha^{(j)}(t)]}(t) + u^{(j)}_{d[\alpha^{(j)}(t)]}(t), \quad (56)$$

$$e^{(j)}_{q[\alpha^{(j)}(t)]}(t) = \left(-i^{(j)}_{q[\alpha^{(j)}(t)]}(t) + \xi^{(j)}_{q[\alpha^{(j)}(t)]}(t)\right)\hat{r}^{(j)}_0 + \hat{e}^{(j)}_{q[\alpha^{(j)}(t)]}(t), \quad (57)$$

$$e^{(j)}_{d[\alpha^{(j)}(t)]}(t) = \left(-i^{(j)}_{d[\alpha^{(j)}(t)]}(t) + \xi^{(j)}_{d[\alpha^{(j)}(t)]}(t)\right)\hat{r}^{(j)}_0 + \hat{e}^{(j)}_{d[\alpha^{(j)}(t)]}(t). \quad (58)$$

Henceforth, the dynamics of the filtered inverter output current, the *LCL* capacitor voltage and the internal voltage of the inverter at bus j, as given in Eqs. 51–54 and Eqs. 57–58, are expressed in the synchronous reference frame, using Eq. 14, as follows:

$$l^{(j)}\frac{di^{(j)}_{q[\omega_0 t]}(t)}{dt} = -r^{(j)}i^{(j)}_{q[\omega_0 t]}(t) - \omega_0 l^{(j)}i^{(j)}_{d[\omega_0 t]}(t) + e^{(j)}_{q[\omega_0 t]}(t) - v^{(j)}_{q[\omega_0 t]}(t), \quad (59)$$

$$l^{(j)}\frac{di^{(j)}_{d[\omega_0 t]}(t)}{dt} = \omega_0 l^{(j)}i^{(j)}_{q[\omega_0 t]}(t) - r^{(j)}i^{(j)}_{d[\omega_0 t]}(t) + e^{(j)}_{d[\omega_0 t]}(t) - v^{(j)}_{d[\omega_0 t]}(t), \quad (60)$$

$$c^{(j)}\frac{d\hat{e}^{(j)}_{q[\omega_0 t]}(t)}{dt} = -i^{(j)}_{q[\omega_0 t]}(t) - \omega_0 c^{(j)}\hat{e}^{(j)}_{d[\omega_0 t]}(t) + \xi^{(j)}_{q[\omega_0 t]}(t), \quad (61)$$

$$c^{(j)}\frac{d\hat{e}^{(j)}_{d[\omega_0 t]}(t)}{dt} = -i^{(j)}_{d[\omega_0 t]}(t) + \omega_0 c^{(j)}\hat{e}^{(j)}_{q[\omega_0 t]}(t) + \xi^{(j)}_{d[\omega_0 t]}(t), \quad (62)$$

$$e^{(j)}_{q[\omega_0 t]}(t) = \left(-i^{(j)}_{q[\omega_0 t]}(t) + \xi^{(j)}_{q[\omega_0 t]}(t)\right)\hat{r}^{(j)}_0 + \hat{e}^{(j)}_{q[\omega_0 t]}(t), \quad (63)$$

$$e^{(j)}_{d[\omega_0 t]}(t) = \left(-i^{(j)}_{d[\omega_0 t]}(t) + \xi^{(j)}_{d[\omega_0 t]}(t)\right)\hat{r}^{(j)}_0 + \hat{e}^{(j)}_{d[\omega_0 t]}(t). \quad (64)$$

Inverter Voltage Magnitude Controller

For voltage magnitude control, we adopt an outer voltage-control-loop and inner current-control-loop structure (see, e.g., [6]). Let $\phi^{(j)}_{[\alpha^{(j)}(t)]}(t)$ and $\gamma^{(j)}_{[\alpha^{(j)}(t)]}(t)$ denote the state variables for the voltage and current Proportional-Integral (PI) controllers respectively, let $e^{(j)}_{r[\alpha^{(j)}(t)]}(t) = e^{(j)}_{rq[\alpha^{(j)}(t)]}(t)$ denote the voltage magnitude controller reference, which implies that $e^{(j)}_{rd[\alpha^{(j)}(t)]}(t) = 0$, and let $\xi^{(j)}_{r[\alpha^{(j)}(t)]}(t) =$

$\xi^{(j)}_{rq[\alpha^{(j)}(t)]}(t) - \mathrm{j}\xi^{(j)}_{rd[\alpha^{(j)}(t)]}(t)$ denote the current controller reference. We define the following variables:

$$\hat{e}^{(j)}_{rq[\alpha^{(j)}(t)]}(t) \coloneqq e^{(j)}_{rq[\alpha^{(j)}(t)]}(t) + \left(i^{(j)}_{q[\alpha^{(j)}(t)]}(t) - \xi^{(j)}_{q[\alpha^{(j)}(t)]}(t) \right) \hat{r}^{(j)}_0, \tag{65}$$

$$\hat{e}^{(j)}_{rd[\alpha^{(j)}(t)]}(t) \coloneqq \left(i^{(j)}_{d[\alpha^{(j)}(t)]}(t) - \xi^{(j)}_{d[\alpha^{(j)}(t)]}(t) \right) \hat{r}^{(j)}_0. \tag{66}$$

The controller dynamics can be described by:

$$\frac{d\phi^{(j)}_{q[\alpha^{(j)}(t)]}(t)}{dt} = \hat{e}^{(j)}_{rq[\alpha^{(j)}(t)]}(t) - \hat{e}^{(j)}_{q[\alpha^{(j)}(t)]}(t), \tag{67}$$

$$\frac{d\phi^{(j)}_{d[\alpha^{(j)}(t)]}(t)}{dt} = \hat{e}^{(j)}_{rd[\alpha^{(j)}(t)]}(t) - \hat{e}^{(j)}_{d[\alpha^{(j)}(t)]}(t), \tag{68}$$

$$\frac{d\gamma^{(j)}_{q[\alpha^{(j)}(t)]}(t)}{dt} = \xi^{(j)}_{rq[\alpha^{(j)}(t)]}(t) - \xi^{(j)}_{q[\alpha^{(j)}(t)]}(t), \tag{69}$$

$$\frac{d\gamma^{(j)}_{d[\alpha^{(j)}(t)]}(t)}{dt} = \xi^{(j)}_{rd[\alpha^{(j)}(t)]}(t) - \xi^{(j)}_{d[\alpha^{(j)}(t)]}(t). \tag{70}$$

Feedback Linearization To implement the adopted control structure, feedback linearization is employed [3, 15]. Let $\kappa^{(j)}_{P\phi}$ and $\kappa^{(j)}_{P\gamma}$ denote the proportional controller gains for the voltage and current controllers respectively, and let $\kappa^{(j)}_{I\phi}$ and $\kappa^{(j)}_{I\gamma}$ denote the corresponding integral controller gains. Let $\xi^{(j)}_{rq[\alpha^{(j)}(t)]}(t)$ and $\xi^{(j)}_{rd[\alpha^{(j)}(t)]}(t)$ denote the q-axis and d-axis current-control-loop outputs respectively, and let $u^{(j)}_{rq[\alpha^{(j)}(t)]}(t)$ and $u^{(j)}_{rd[\alpha^{(j)}(t)]}(t)$ denote the q-axis and d-axis voltage-control-loop outputs respectively. Using identical controllers on the q-axis and d-axis, and employing feedback linearization, the controller outputs are given by:

$$\begin{aligned}\xi^{(j)}_{rq[\alpha^{(j)}(t)]}(t) = {} & \kappa^{(j)}_{P\phi} \left(\hat{e}^{(j)}_{rq[\alpha^{(j)}(t)]}(t) - \hat{e}^{(j)}_{q[\alpha^{(j)}(t)]}(t) \right) + \kappa^{(j)}_{I\phi} \phi^{(j)}_{q[\alpha^{(j)}(t)]}(t) \\ & + \frac{2}{V^{(j)}_{DC}} \left(i^{(j)}_{q[\alpha^{(j)}(t)]}(t) + \omega^{(j)}(t) c^{(j)} \hat{e}^{(j)}_{d[\alpha^{(j)}(t)]}(t) \right),\end{aligned} \tag{71}$$

$$\begin{aligned}\xi^{(j)}_{rd[\alpha^{(j)}(t)]}(t) = {} & \kappa^{(j)}_{P\phi} \left(\hat{e}^{(j)}_{rd[\alpha^{(j)}(t)]}(t) - \hat{e}^{(j)}_{d[\alpha^{(j)}(t)]}(t) \right) + \kappa^{(j)}_{I\phi} \phi^{(j)}_{d[\alpha^{(j)}(t)]}(t) \\ & + \frac{2}{V^{(j)}_{DC}} \left(i^{(j)}_{d[\alpha^{(j)}(t)]}(t) - \omega^{(j)}(t) c^{(j)} \hat{e}^{(j)}_{q[\alpha^{(j)}(t)]}(t) \right),\end{aligned} \tag{72}$$

$$u^{(j)}_{rq[\alpha^{(j)}(t)]}(t) = \frac{V^{(j)}_{DC}}{2} \left(\kappa^{(j)}_{P\gamma} \left(\xi^{(j)}_{rq[\alpha^{(j)}(t)]}(t) - \xi^{(j)}_{q[\alpha^{(j)}(t)]}(t) \right) + \kappa^{(j)}_{I\gamma} \gamma^{(j)}_{q[\alpha^{(j)}(t)]}(t) \right)$$

$$+\omega^{(j)}(t)l_0^{(j)}\xi^{(j)}_{d[\alpha^{(j)}(t)]}(t)+e^{(j)}_{q[\alpha^{(j)}(t)]}(t) \tag{73}$$

$$=\frac{V_{DC}^{(j)}}{2}\left(\kappa_{P\gamma}^{(j)}\left(\kappa_{P\phi}^{(j)}\left(\hat{e}^{(j)}_{rq[\alpha^{(j)}(t)]}(t)-\hat{e}^{(j)}_{q[\alpha^{(j)}(t)]}(t)\right)+\kappa_{I\phi}^{(j)}\phi^{(j)}_{q[\alpha^{(j)}(t)]}(t)\right.\right.$$

$$\left.\left.-\xi^{(j)}_{q[\alpha^{(j)}(t)]}(t)\right)+\kappa_{I\gamma}^{(j)}\gamma^{(j)}_{q[\alpha^{(j)}(t)]}(t)\right)+\omega^{(j)}(t)\kappa_{P\gamma}^{(j)}c^{(j)}\hat{e}^{(j)}_{d[\alpha^{(j)}(t)]}(t)$$

$$+\kappa_{P\gamma}^{(j)}i^{(j)}_{q[\alpha^{(j)}(t)]}(t)+\omega^{(j)}(t)l_0^{(j)}\xi^{(j)}_{d[\alpha^{(j)}(t)]}(t)+e^{(j)}_{q[\alpha^{(j)}(t)]}(t), \tag{74}$$

$$u^{(j)}_{rd[\alpha^{(j)}(t)]}(t)=\frac{V_{DC}^{(j)}}{2}\left(\kappa_{P\gamma}^{(j)}\left(\xi^{(j)}_{rd[\alpha^{(j)}(t)]}(t)-\xi^{(j)}_{d[\alpha^{(j)}(t)]}(t)\right)+\kappa_{I\gamma}^{(j)}\gamma^{(j)}_{d[\alpha^{(j)}(t)]}(t)\right)$$

$$-\omega^{(j)}(t)l_0^{(j)}\xi^{(j)}_{q[\alpha^{(j)}(t)]}(t)+e^{(j)}_{d[\alpha^{(j)}(t)]}(t) \tag{75}$$

$$=\frac{V_{DC}^{(j)}}{2}\left(\kappa_{P\gamma}^{(j)}\left(\kappa_{P\phi}^{(j)}\left(\hat{e}^{(j)}_{rd[\alpha^{(j)}(t)]}(t)-\hat{e}^{(j)}_{d[\alpha^{(j)}(t)]}(t)\right)+\kappa_{I\phi}^{(j)}\phi^{(j)}_{d[\alpha^{(j)}(t)]}(t)\right.\right.$$

$$\left.\left.-\xi^{(j)}_{d[\alpha^{(j)}(t)]}(t)\right)+\kappa_{I\gamma}^{(j)}\gamma^{(j)}_{d[\alpha^{(j)}(t)]}(t)\right)-\omega^{(j)}(t)\kappa_{P\gamma}^{(j)}c^{(j)}\hat{e}^{(j)}_{q[\alpha^{(j)}(t)]}(t)$$

$$+\kappa_{P\gamma}^{(j)}i^{(j)}_{d[\alpha^{(j)}(t)]}(t)-\omega^{(j)}(t)l_0^{(j)}\xi^{(j)}_{q[\alpha^{(j)}(t)]}(t)+e^{(j)}_{d[\alpha^{(j)}(t)]}(t). \tag{76}$$

Assumption 3.1 *The voltage* $u^{(j)}_{rq[\alpha^{(j)}(t)]}(t)-\mathrm{j}u^{(j)}_{rd[\alpha^{(j)}(t)]}(t)$ *is synthesized instantaneously by the inverter PWM mechanism, so that* $u^{(j)}_{q[\alpha^{(j)}(t)]}(t)=u^{(j)}_{rq[\alpha^{(j)}(t)]}(t)$ *and* $u^{(j)}_{d[\alpha^{(j)}(t)]}(t)=u^{(j)}_{rd[\alpha^{(j)}(t)]}(t)$.

Normalized Inverter Model

For ease of analysis in subsequent developments, we normalize the inverter model using the base variables $V_{DQ}^{(j)}$, $S^{(j)}$ and ω_0, where $V_{DQ}^{(j)}$ denotes the rated peak line to neutral voltage of the inverter at bus j, $S^{(j)}$ denotes the rated three-phase voltamperes of the inverter at bus j, and ω_0 denotes the nominal or synchronous frequency. We define the base variables $I_{DQ}^{(j)}:=\frac{2S^{(j)}}{3V_{DQ}^{(j)}}$, $Z_{DQ}^{(j)}:=\frac{V_{DQ}^{(j)}}{I_{DQ}^{(j)}}$, $L_{DQ}^{(j)}:=\frac{Z_{DQ}^{(j)}}{\omega_0}$, $C_{DQ}^{(j)}:=\frac{1}{\omega_0 Z_{DQ}^{(j)}}$, $\Phi_{DQ}^{(j)}:=\frac{V_{DQ}^{(j)}}{\omega_0}$ and $\Gamma_{DQ}^{(j)}:=\frac{I_{DQ}^{(j)}}{\omega_0}$ for current, resistance, inductance, capacitance, voltage controller state variable, and current controller state variable of the inverter at bus j respectively. Henceforth, capitalized notation is used to indicate normalized quantities.

Substituting Eqs. 71, 72, 74 and 76 into Eqs. 55–64 and normalizing the resulting system of equations, it follows that the *LCL* filter dynamics can be described by:

$$\frac{L^{(j)}}{\omega_0}\frac{dI^{(j)}_{q[\omega_0 t]}(t)}{dt} = -R^{(j)}I^{(j)}_{q[\omega_0 t]}(t) - L^{(j)}I^{(j)}_{d[\omega_0 t]}(t) + E^{(j)}_{q[\omega_0 t]}(t) - V^{(j)}_{q[\omega_0 t]}(t), \quad (77)$$

$$\frac{L^{(j)}}{\omega_0}\frac{dI^{(j)}_{d[\omega_0 t]}(t)}{dt} = L^{(j)}I^{(j)}_{q[\omega_0 t]}(t) - R^{(j)}I^{(j)}_{d[\omega_0 t]}(t) + E^{(j)}_{d[\omega_0 t]}(t) - V^{(j)}_{d[\omega_0 t]}(t), \quad (78)$$

$$\frac{C^{(j)}}{\omega_0}\frac{d\hat{E}^{(j)}_{q[\omega_0 t]}(t)}{dt} = -I^{(j)}_{q[\omega_0 t]}(t) - C^{(j)}\hat{E}^{(j)}_{d[\omega_0 t]}(t) + \Xi^{(j)}_{q[\omega_0 t]}(t), \quad (79)$$

$$\frac{C^{(j)}}{\omega_0}\frac{d\hat{E}^{(j)}_{d[\omega_0 t]}(t)}{dt} = -I^{(j)}_{d[\omega_0 t]}(t) + C^{(j)}\hat{E}^{(j)}_{q[\omega_0 t]}(t) + \Xi^{(j)}_{d[\omega_0 t]}(t), \quad (80)$$

$$\begin{aligned}\frac{L^{(j)}_0}{\omega_0}\frac{d\Xi^{(j)}_{q[\alpha^{(j)}(t)]}(t)}{dt} &= K^{(j)}_{P\gamma}I^{(j)}_{q[\alpha^{(j)}(t)]}(t) - \frac{V^{(j)}_{DC}K^{(j)}_{P\gamma}K^{(j)}_{P\phi}}{2}\hat{E}^{(j)}_{q[\alpha^{(j)}(t)]}(t)\\ &+ K^{(j)}_{P\gamma}\frac{\omega^{(j)}(t)}{\omega_0}C^{(j)}\hat{E}^{(j)}_{d[\alpha^{(j)}(t)]}(t) + \frac{V^{(j)}_{DC}K^{(j)}_{I\gamma}}{2}\Gamma^{(j)}_{q[\alpha^{(j)}(t)]}\\ &+ \frac{V^{(j)}_{DC}K^{(j)}_{P\gamma}K^{(j)}_{P\phi}}{2}\hat{E}^{(j)}_{rq[\alpha^{(j)}(t)]}(t) + \frac{V^{(j)}_{DC}K^{(j)}_{P\gamma}K^{(j)}_{I\phi}}{2}\Phi^{(j)}_{q[\alpha^{(j)}(t)]}(t)\\ &- \left(R^{(j)}_0 + \frac{V^{(j)}_{DC}K^{(j)}_{P\gamma}}{2}\right)\Xi^{(j)}_{q[\alpha^{(j)}(t)]}(t), \end{aligned} \quad (81)$$

$$\begin{aligned}\frac{L^{(j)}_0}{\omega_0}\frac{d\Xi^{(j)}_{d[\alpha^{(j)}(t)]}(t)}{dt} &= K^{(j)}_{P\gamma}I^{(j)}_{d[\alpha^{(j)}(t)]}(t) - \frac{V^{(j)}_{DC}K^{(j)}_{P\gamma}K^{(j)}_{P\phi}}{2}\hat{E}^{(j)}_{d[\alpha^{(j)}(t)]}(t)\\ &- K^{(j)}_{P\gamma}\frac{\omega^{(j)}(t)}{\omega_0}C^{(j)}\hat{E}^{(j)}_{q[\alpha^{(j)}(t)]}(t) + \frac{V^{(j)}_{DC}K^{(j)}_{I\gamma}}{2}\Gamma^{(j)}_{d[\alpha^{(j)}(t)]}\\ &+ \frac{V^{(j)}_{DC}K^{(j)}_{P\gamma}K^{(j)}_{P\phi}}{2}\hat{E}^{(j)}_{rd[\alpha^{(j)}(t)]}(t) + \frac{V^{(j)}_{DC}K^{(j)}_{P\gamma}K^{(j)}_{I\phi}}{2}\Phi^{(j)}_{d[\alpha^{(j)}(t)]}(t)\\ &- \left(R^{(j)}_0 + \frac{V^{(j)}_{DC}K^{(j)}_{P\gamma}}{2}\right)\Xi^{(j)}_{d[\alpha^{(j)}(t)]}(t), \end{aligned} \quad (82)$$

$$E^{(j)}_{q[\omega_0 t]}(t) = \left(-I^{(j)}_{q[\omega_0 t]}(t) + \Xi^{(j)}_{q[\omega_0 t]}(t)\right)\hat{R}^{(j)}_0 + \hat{E}^{(j)}_{q[\omega_0 t]}(t), \quad (83)$$

$$E^{(j)}_{d[\omega_0 t]}(t) = \left(-I^{(j)}_{d[\omega_0 t]}(t) + \Xi^{(j)}_{d[\omega_0 t]}(t)\right)\hat{R}^{(j)}_0 + \hat{E}^{(j)}_{d[\omega_0 t]}(t), \quad (84)$$

and the controller dynamics can be described by:

$$\frac{1}{\omega_0}\frac{d\Phi^{(j)}_{q[\alpha^{(j)}(t)]}(t)}{dt} = -\hat{E}^{(j)}_{q[\alpha^{(j)}(t)]}(t) + \hat{E}^{(j)}_{rq[\alpha^{(j)}(t)]}(t), \quad (85)$$

$$\frac{1}{\omega_0}\frac{d\Phi^{(j)}_{d[\alpha^{(j)}(t)]}(t)}{dt} = -\hat{E}^{(j)}_{d[\alpha^{(j)}(t)]}(t) + \hat{E}^{(j)}_{rd[\alpha^{(j)}(t)]}(t), \quad (86)$$

$$\frac{1}{\omega_0}\frac{d\Gamma^{(j)}_{q[\alpha^{(j)}(t)]}(t)}{dt} = \frac{2}{V_{DC}} I^{(j)}_{q[\alpha^{(j)}(t)]}(t) - K^{(j)}_{P\phi}\hat{E}^{(j)}_{q[\alpha^{(j)}(t)]}(t) + \frac{2\omega^{(j)}(t)}{\omega_0 V_{DC}} C^{(j)}\hat{E}^{(j)}_{d[\alpha^{(j)}(t)]}(t) - \Xi^{(j)}_{q[\alpha^{(j)}(t)]}(t) + K^{(j)}_{I\phi}\Phi^{(j)}_{q[\alpha^{(j)}(t)]}(t) + K^{(j)}_{P\phi}\hat{E}^{(j)}_{rq[\alpha^{(j)}(t)]}(t), \quad (87)$$

$$\frac{1}{\omega_0}\frac{d\Gamma^{(j)}_{d[\alpha^{(j)}(t)]}(t)}{dt} = \frac{2}{V_{DC}} I^{(j)}_{d[\alpha^{(j)}(t)]}(t) - \frac{2\omega^{(j)}(t)}{\omega_0 V_{DC}} C^{(j)}\hat{E}^{(j)}_{q[\alpha^{(j)}(t)]}(t) - K^{(j)}_{P\phi}\hat{E}^{(j)}_{d[\alpha^{(j)}(t)]}(t) - \Xi^{(j)}_{d[\alpha^{(j)}(t)]}(t) + K^{(j)}_{I\phi}\Phi^{(j)}_{d[\alpha^{(j)}(t)]}(t) + K^{(j)}_{P\phi}\hat{E}^{(j)}_{rd[\alpha^{(j)}(t)]}(t), \quad (88)$$

where

$$K^{(j)}_{P\gamma} = \frac{\kappa^{(j)}_{P\gamma}}{Z^{(j)}_{DQ}}, \qquad K^{(j)}_{I\gamma} = \frac{\kappa^{(j)}_{I\gamma}}{\omega_0 Z^{(j)}_{DQ}}, \qquad K^{(j)}_{P\phi} = \kappa^{(j)}_{P\phi} Z^{(j)}_{DQ}, \qquad K^{(j)}_{I\phi} = \frac{\kappa^{(j)}_{I\phi} Z^{(j)}_{DQ}}{\omega_0}.$$

Voltage and Frequency Droop

Let $D^{(j)}_E$ and $D^{(j)}_\omega$ respectively denote voltage and frequency droop coefficients. Following [4], we assume that the reference voltage $E^{(j)}_{rq[\alpha^{(j)}(t)]}(t)$ and the frequency set-point $\omega^{(j)}(t)$ for each inverter are obtained from the following droop laws:

$$E^{(j)}_{rq[\alpha^{(j)}(t)]}(t) = E^{(j)}_0 + \frac{1}{D^{(j)}_E}\left(Q^{(j)}_r - Q^{(j)}_f(t)\right), \quad (89)$$

$$\omega^{(j)}(t) = \omega_0 + \frac{1}{D^{(j)}_\omega}\left(P^{(j)}_r - P^{(j)}_f(t)\right). \quad (90)$$

with the dynamics of the filtered reactive power, $Q^{(j)}_f(t)$, and real power, $P^{(j)}_f(t)$, described by:

$$\frac{1}{\omega^{(j)}_c}\frac{dQ^{(j)}_f(t)}{dt} = -Q^{(j)}_f(t) + E^{(j)}_{q[\omega_0 t]}(t) I^{(j)}_{d[\omega_0 t]}(t) - E^{(j)}_{d[\omega_0 t]}(t) I^{(j)}_{q[\omega_0 t]}(t), \quad (91)$$

$$\frac{1}{\omega^{(j)}_c}\frac{dP^{(j)}_f(t)}{dt} = -P^{(j)}_f(t) + E^{(j)}_{q[\omega_0 t]}(t) I^{(j)}_{q[\omega_0 t]}(t) + E^{(j)}_{d[\omega_0 t]}(t) I^{(j)}_{d[\omega_0 t]}(t). \quad (92)$$

where, for the inverter at bus j, $E^{(j)}_0$ is the voltage droop law constant, $\omega^{(j)}_c$ is the filter cut-off frequency, and $P^{(j)}_r$ and $Q^{(j)}_r$ are real and reactive power generation set-points respectively.

Substituting Eq. 90 into Eq. 19, the time evolution of $\delta^{(j)}(t)$ can be described by:

$$D^{(j)}_\omega \frac{d\delta^{(j)}(t)}{dt} = P^{(j)}_r - P^{(j)}_f(t). \quad (93)$$

3.2 Network Model

Assumption 3.2 *All lines connecting the network buses are less than 50 miles long.*

Given Assumption 3.2, [2] shows that the short transmission line model is a good approximation to describe the terminal behavior of the network. Using the per-unit normalization (see [2], pp. 157–163), let $V^{(j)}_{q[\omega_0 t]}(t) - \mathrm{j}V^{(j)}_{d[\omega_0 t]}(t)$ denote the normalized voltage at bus j, and let $R^{(e)}$, $L^{(e)}$ and $I^{(e)}_{q[\omega_0 t]}(t) - \mathrm{j}I^{(e)}_{d[\omega_0 t]}(t)$ denote the normalized resistance, normalized inductance and normalized current across line (j,k), respectively, where $p\left(\{j,k\}\right) = e$ as introduced in Section 2.2,

$$\begin{aligned} V^{(j)}_{q[\omega_0 t]}(t) - \mathrm{j}V^{(j)}_{d[\omega_0 t]}(t) &= \left(V^{(j)}_{q[\alpha^{(j)}(t)]}(t) - \mathrm{j}V^{(j)}_{d[\alpha^{(j)}(t)]}(t)\right)\exp(\mathrm{j}\delta^{(j)}(t)) \\ &= \left(V^{(j)}_{d[\alpha^{(j)}(t)]}(t) + \mathrm{j}V^{(j)}_{q[\alpha^{(j)}(t)]}(t)\right)\exp\left(\mathrm{j}\left(\delta^{(j)}(t) - \frac{\pi}{2}\right)\right), \end{aligned} \tag{94}$$

and

$$\begin{aligned} I^{(e)}_{q[\omega_0 t]}(t) - \mathrm{j}I^{(e)}_{d[\omega_0 t]}(t) &= \left(I^{(e)}_{q[\alpha^{(j)}(t)]}(t) - \mathrm{j}I^{(e)}_{d[\alpha^{(j)}(t)]}(t)\right)\exp(\mathrm{j}\delta^{(j)}(t)) \\ &= \left(I^{(e)}_{d[\alpha^{(j)}(t)]}(t) + \mathrm{j}I^{(e)}_{q[\alpha^{(j)}(t)]}(t)\right)\exp\left(\mathrm{j}\left(\delta^{(j)}(t) - \frac{\pi}{2}\right)\right). \end{aligned} \tag{95}$$

The short transmission line model is depicted in Fig. 4.

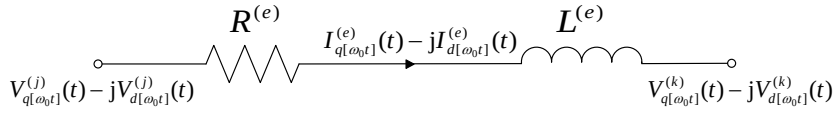

Fig. 4: Short transmission line model (bus j to bus k).

From Fig. 4, the voltage across a line connecting bus j and bus k of the network can be described by:

$$V^{(j)}_{q[\omega_0 t]}(t) - V^{(k)}_{q[\omega_0 t]}(t) = \frac{L^{(e)}}{\omega_0}\frac{dI^{(e)}_{q[\omega_0 t]}(t)}{dt} + R^{(e)}I^{(e)}_{q[\omega_0 t]}(t) + L^{(e)}I^{(e)}_{d[\omega_0 t]}(t), \tag{96}$$

$$V^{(j)}_{d[\omega_0 t]}(t) - V^{(k)}_{d[\omega_0 t]}(t) = \frac{L^{(e)}}{\omega_0}\frac{dI^{(e)}_{d[\omega_0 t]}(t)}{dt} + R^{(e)} I^{(e)}_{d[\omega_0 t]}(t) - L^{(e)} I^{(e)}_{q[\omega_0 t]}(t). \tag{97}$$

Generalized Network Model

Using the concepts presented in Section 2.2, we provide the following definitions for the network with n buses.

$$\mathbf{V}^{(\mathscr{V})}_{q[\omega_0 t]}(t) \coloneqq \begin{bmatrix} V^{(1)}_{q[\omega_0 t]}(t) \\ \vdots \\ V^{(n)}_{q[\omega_0 t]}(t) \end{bmatrix}, \qquad \mathbf{V}^{(\mathscr{V})}_{d[\omega_0 t]}(t) \coloneqq \begin{bmatrix} V^{(1)}_{d[\omega_0 t]}(t) \\ \vdots \\ V^{(n)}_{d[\omega_0 t]}(t) \end{bmatrix}. \tag{98}$$

For $e = |\mathscr{V}^{(\mathscr{I})}| + 1$:

$$\mathbf{I}^{(\mathscr{E})}_{q[\omega_0 t]}(t) \coloneqq \begin{bmatrix} I^{(e)}_{q[\omega_0 t]}(t) \\ I^{(e+1)}_{q[\omega_0 t]}(t) \\ \vdots \\ I^{(e+|\mathscr{E}|-1)}_{q[\omega_0 t]}(t) \end{bmatrix}, \qquad \mathbf{I}^{(\mathscr{E})}_{d[\omega_0 t]}(t) \coloneqq \begin{bmatrix} I^{(e)}_{d[\omega_0 t]}(t) \\ I^{(e+1)}_{d[\omega_0 t]}(t) \\ \vdots \\ I^{(e+|\mathscr{E}|-1)}_{d[\omega_0 t]}(t) \end{bmatrix} \tag{99}$$

$$\mathbf{R}^{(\mathscr{E})} \coloneqq \begin{bmatrix} R^{(e)} & 0 & \cdots & 0 \\ 0 & R^{(e+1)} & \cdots & 0 \\ \vdots & \vdots & \ddots & \vdots \\ 0 & 0 & \cdots & R^{(e+|\mathscr{E}|-1)} \end{bmatrix}, \tag{100}$$

$$\mathbf{L}^{(\mathscr{E})} \coloneqq \begin{bmatrix} L^{(e)} & 0 & \cdots & 0 \\ 0 & L^{(e+1)} & \cdots & 0 \\ \vdots & \vdots & \ddots & \vdots \\ 0 & 0 & \cdots & L^{(e+|\mathscr{E}|-1)} \end{bmatrix}. \tag{101}$$

Let $\mathbf{M}$ denote the incidence matrix of the network; then the network dynamics are described by:

$$\mathbf{M}\mathbf{V}^{(\mathscr{V})}_{q[\omega_0 t]}(t) = \frac{1}{\omega_0}\mathbf{L}^{(\mathscr{E})}\frac{d\mathbf{I}^{(\mathscr{E})}_{q[\omega_0 t]}(t)}{dt} + \mathbf{R}^{(\mathscr{E})}\mathbf{I}^{(\mathscr{E})}_{q[\omega_0 t]}(t) + \mathbf{L}^{(\mathscr{E})}\mathbf{I}^{(\mathscr{E})}_{d[\omega_0 t]}(t), \tag{102}$$

$$\mathbf{M}\mathbf{V}^{(\mathscr{V})}_{d[\omega_0 t]}(t) = \frac{1}{\omega_0}\mathbf{L}^{(\mathscr{E})}\frac{d\mathbf{I}^{(\mathscr{E})}_{d[\omega_0 t]}(t)}{dt} + \mathbf{R}^{(\mathscr{E})}\mathbf{I}^{(\mathscr{E})}_{d[\omega_0 t]}(t) - \mathbf{L}^{(\mathscr{E})}\mathbf{I}^{(\mathscr{E})}_{q[\omega_0 t]}(t). \tag{103}$$

3.3 Load Model

Using the notation presented in Section 2.2, let $V^{((j)}_{q[\omega_0 t]}(t) - \mathrm{j}V^{((j)}_{d[\omega_0 t]}(t)$ denote the normalized voltage at bus j, and let $I^{(e')}_{q[\omega_0 t]}(t) - \mathrm{j}I^{(e')}_{d[\omega_0 t]}(t)$ denote the normalized current injection by the net load at bus j. The load dynamics can be described by a non-linear system of differential equations which we assume to be of the form:

$$\mu^{(j)}\dot{V}^{(j)}_{q[\omega_0 t]}(t) = q_V\left(V^{(j)}_{q[\omega_0 t]}(t), V^{(j)}_{d[\omega_0 t]}(t), I^{(e')}_{q[\omega_0 t]}(t), I^{(e')}_{d[\omega_0 t]}(t)\right), \tag{104}$$

$$\mu^{(j)}\dot{V}^{(j)}_{d[\omega_0 t]}(t) = d_V\left(V^{(j)}_{q[\omega_0 t]}(t), V^{(j)}_{d[\omega_0 t]}(t), I^{(e')}_{q[\omega_0 t]}(t), I^{(e')}_{d[\omega_0 t]}(t)\right), \tag{105}$$

$$\mu^{(j)}\dot{I}^{(e')}_{q[\omega_0 t]}(t) = q_I\left(V^{(j)}_{q[\omega_0 t]}(t), V^{(j)}_{d[\omega_0 t]}(t), I^{(e')}_{q[\omega_0 t]}(t), I^{(e')}_{d[\omega_0 t]}(t)\right), \tag{106}$$

$$\mu^{(j)}\dot{I}^{(e')}_{d[\omega_0 t]}(t) = d_I\left(V^{(j)}_{q[\omega_0 t]}(t), V^{(j)}_{d[\omega_0 t]}(t), I^{(e')}_{q[\omega_0 t]}(t), I^{(e')}_{d[\omega_0 t]}(t)\right). \tag{107}$$

where $\mu^{(j)}$ denotes the largest time constant of the net load at bus j, $q_V\left(\cdot,\cdot,\cdot,\cdot\right)$, $d_V\left(\cdot,\cdot,\cdot,\cdot\right)$, $q_I\left(\cdot,\cdot,\cdot,\cdot\right)$ and $d_I\left(\cdot,\cdot,\cdot,\cdot\right)$ are nonlinear functions of the load state variables, $p'(j) = e'$, as discussed in Section 2.2, and

$$V^{(j)}_{q[\omega_0 t]}(t) - \mathrm{j}V^{(j)}_{d[\omega_0 t]}(t) = \left(V^{(j)}_{d[\alpha^{(j)}(t)]}(t) + \mathrm{j}V^{(j)}_{q[\alpha^{(j)}(t)]}(t)\right)\exp\left(\mathrm{j}\left(\delta^{(j)}(t) - \frac{\pi}{2}\right)\right), \tag{108}$$

$$I^{(e')}_{q[\omega_0 t]}(t) - \mathrm{j}I^{(e')}_{d[\omega_0 t]}(t) = \left(I^{(e')}_{d[\alpha^{(j)}(t)]}(t) + \mathrm{j}I^{(e')}_{q[\alpha^{(j)}(t)]}(t)\right)\exp\left(\mathrm{j}\left(\delta^{(j)}(t) - \frac{\pi}{2}\right)\right). \tag{109}$$

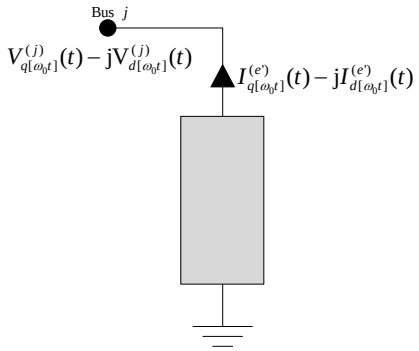

Fig. 5: Load model (net load at bus j).

3.4 μHO Model

We consider a microgrid with n buses. Let the microgrid have $m \leq n$ generator buses, with each bus connected to an inverter-interfaced power supply. Combining the models in Sections 3.1–3.3, we can develop a microgrid dynamical model; we refer to this model as the microgrid High-Order model (μHO).

At each generator bus $j = 1, 2..., m$, the dynamics of the connected inverter-interfaced power supply are described by:

$$D_{\omega}^{(j)} \frac{d\delta^{(j)}(t)}{dt} = P_r^{(j)} - P_f^{(j)}(t), \tag{110}$$

$$\frac{1}{\omega_c^{(j)}} \frac{dQ_f^{(j)}(t)}{dt} = -Q_f^{(j)}(t) + E_{q[\omega_0 t]}^{(j)}(t) I_{d[\omega_0 t]}^{(j)}(t) - E_{d[\omega_0 t]}^{(j)}(t) I_{q[\omega_0 t]}^{(j)}(t), \tag{111}$$

$$\frac{1}{\omega_c^{(j)}} \frac{dP_f^{(j)}(t)}{dt} = -P_f^{(j)}(t) + E_{q[\omega_0 t]}^{(j)}(t) I_{q[\omega_0 t]}^{(j)}(t) + E_{d[\omega_0 t]}^{(j)}(t) I_{d[\omega_0 t]}^{(j)}(t), \tag{112}$$

$$\frac{L^{(j)}}{\omega_0} \frac{dI_{q[\omega_0 t]}^{(j)}(t)}{dt} = -R^{(j)} I_{q[\omega_0 t]}^{(j)}(t) - L^{(j)} I_{d[\omega_0 t]}^{(j)}(t) + E_{q[\omega_0 t]}^{(j)}(t) - V_{q[\omega_0 t]}^{(j)}(t), \tag{113}$$

$$\frac{L^{(j)}}{\omega_0} \frac{dI_{d[\omega_0 t]}^{(j)}(t)}{dt} = L^{(j)} I_{q[\omega_0 t]}^{(j)}(t) - R^{(j)} I_{d[\omega_0 t]}^{(j)}(t) + E_{d[\omega_0 t]}^{(j)}(t) - V_{d[\omega_0 t]}^{(j)}(t), \tag{114}$$

$$\begin{aligned} \frac{1}{\omega_0} \frac{d\Phi_{q[\alpha^{(j)}(t)]}^{(j)}(t)}{dt} = & -\hat{E}_{q[\omega_0 t]}^{(j)}(t) \cos(\delta^{(j)}(t)) + \hat{E}_{d[\omega_0 t]}^{(j)}(t) \sin(\delta^{(j)}(t)) \\ & + \hat{R}_0^{(j)} I_{q[\omega_0 t]}^{(j)}(t) \cos(\delta^{(j)}(t)) - \hat{R}_0^{(j)} I_{d[\omega_0 t]}^{(j)}(t) \sin(\delta^{(j)}(t)) \\ & - \hat{R}_0^{(j)} \Xi_{q[\alpha^{(j)}(t)]}^{(j)}(t) - \frac{1}{D_E^{(j)}} Q_f^{(j)}(t) + E_0^{(j)} + \frac{1}{D_E^{(j)}} Q_r^{(j)}, \end{aligned} \tag{115}$$

$$\begin{aligned} \frac{1}{\omega_0} \frac{d\Phi_{d[\alpha^{(j)}(t)]}^{(j)}(t)}{dt} = & -\hat{E}_{q[\omega_0 t]}^{(j)}(t) \sin(\delta^{(j)}(t)) - \hat{E}_{d[\omega_0 t]}^{(j)}(t) \cos(\delta^{(j)}(t)) \\ & + \hat{R}_0^{(j)} I_{q[\omega_0 t]}^{(j)}(t) \sin(\delta^{(j)}(t)) + \hat{R}_0^{(j)} I_{d[\omega_0 t]}^{(j)}(t) \cos(\delta^{(j)}(t)) \\ & - \hat{R}_0^{(j)} \Xi_{d[\alpha^{(j)}(t)]}^{(j)}(t), \end{aligned} \tag{116}$$

$$\frac{C^{(j)}}{\omega_0}\frac{d\hat{E}^{(j)}_{q[\omega_0 t]}(t)}{dt} = -I^{(j)}_{q[\omega_0 t]}(t) - C^{(j)}\hat{E}^{(j)}_{d[\omega_0 t]}(t) + \Xi^{(j)}_{q[\alpha^{(j)}(t)]}(t)\cos(\delta^{(j)}(t)) + \Xi^{(j)}_{d[\alpha^{(j)}(t)]}(t)\sin(\delta^{(j)}(t)), \tag{117}$$

$$\frac{C^{(j)}}{\omega_0}\frac{d\hat{E}^{(j)}_{d[\omega_0 t]}(t)}{dt} = -I^{(j)}_{d[\omega_0 t]}(t) + C^{(j)}\hat{E}^{(j)}_{q[\omega_0 t]}(t) - \Xi^{(j)}_{q[\alpha^{(j)}(t)]}(t)\sin(\delta^{(j)}(t)) + \Xi^{(j)}_{d[\alpha^{(j)}(t)]}(t)\cos(\delta^{(j)}(t)), \tag{118}$$

$$\begin{aligned}\frac{L^{(j)}_0}{\omega_0}\frac{d\Xi^{(j)}_{q[\alpha^{(j)}(t)]}(t)}{dt} &= K^{(j)}_{P\gamma}\left(1+\frac{V^{(j)}_{DC}K^{(j)}_{P\phi}\hat{R}^{(j)}_0}{2}\right)I^{(j)}_{q[\omega_0 t]}(t)\cos(\delta^{(j)}(t)) \\ &- K^{(j)}_{P\gamma}\left(1+\frac{V^{(j)}_{DC}K^{(j)}_{P\phi}\hat{R}^{(j)}_0}{2}\right)I^{(j)}_{d[\omega_0 t]}(t)\sin(\delta^{(j)}(t)) \\ &- \left(R^{(j)}_0+\frac{V^{(j)}_{DC}K^{(j)}_{P\gamma}}{2}\left(1+K^{(j)}_{P\phi}\hat{R}^{(j)}_0\right)\right)\Xi^{(j)}_{q[\alpha^{(j)}(t)]}(t) \\ &- \frac{V^{(j)}_{DC}K^{(j)}_{P\gamma}K^{(j)}_{P\phi}}{2}\hat{E}^{(j)}_{q[\omega_0 t]}(t)\cos(\delta^{(j)}(t)) + \frac{V^{(j)}_{DC}K^{(j)}_{I\gamma}}{2}\Gamma^{(j)}_{q[\alpha^{(j)}(t)]} \\ &+ \frac{V^{(j)}_{DC}K^{(j)}_{P\gamma}K^{(j)}_{P\phi}}{2}\hat{E}^{(j)}_{d[\omega_0 t]}(t)\sin(\delta^{(j)}(t)) + \frac{V^{(j)}_{DC}K^{(j)}_{P\gamma}K^{(j)}_{P\phi}}{2}E^{(j)}_0 \\ &+ \frac{V^{(j)}_{DC}K^{(j)}_{P\gamma}K^{(j)}_{I\phi}}{2}\Phi^{(j)}_{q[\alpha^{(j)}(t)]}(t) + \frac{V^{(j)}_{DC}K^{(j)}_{P\gamma}K^{(j)}_{P\phi}}{2D^{(j)}_E}Q^{(j)}_r \\ &- \frac{V^{(j)}_{DC}K^{(j)}_{P\gamma}K^{(j)}_{P\phi}}{2D^{(j)}_E}Q^{(j)}_f(t) + K^{(j)}_{P\gamma}C^{(j)}\hat{E}^{(j)}_{q[\omega_0 t]}(t)\sin(\delta^{(j)}(t)) \\ &+ \frac{K^{(j)}_{P\gamma}C^{(j)}}{D^{(j)}_\omega\omega_0}\left(P^{(j)}_r - P^{(j)}_f(t)\right)\hat{E}^{(j)}_{q[\omega_0 t]}(t)\sin(\delta^{(j)}(t)) \\ &+ K^{(j)}_{P\gamma}C^{(j)}\hat{E}^{(j)}_{d[\omega_0 t]}(t)\cos(\delta^{(j)}(t)) \\ &+ \frac{K^{(j)}_{P\gamma}C^{(j)}}{D^{(j)}_\omega\omega_0}\left(P^{(j)}_r - P^{(j)}_f(t)\right)\hat{E}^{(j)}_{d[\omega_0 t]}(t)\cos(\delta^{(j)}(t)),\end{aligned} \tag{119}$$

$$\frac{L^{(j)}_0}{\omega_0}\frac{d\Xi^{(j)}_{d[\alpha^{(j)}(t)]}(t)}{dt} = K^{(j)}_{P\gamma}\left(1+\frac{V^{(j)}_{DC}K^{(j)}_{P\phi}\hat{R}^{(j)}_0}{2}\right)I^{(j)}_{q[\omega_0 t]}(t)\sin(\delta^{(j)}(t))$$

$$
\begin{aligned}
&+K_{P\gamma}^{(j)}\left(1+\frac{V_{DC}^{(j)}K_{P\phi}^{(j)}\hat{R}_0^{(j)}}{2}\right)I_{d[\omega_0 t]}^{(j)}(t)\cos(\delta^{(j)}(t))\\
&-\left(R_0^{(j)}+\frac{V_{DC}^{(j)}K_{P\gamma}^{(j)}}{2}\left(1+K_{P\phi}^{(j)}\hat{R}_0^{(j)}\right)\right)\Xi_{d[\alpha^{(j)}(t)]}^{(j)}(t)\\
&-\frac{V_{DC}^{(j)}K_{P\gamma}^{(j)}K_{P\phi}^{(j)}}{2}\hat{E}_{q[\omega_0 t]}^{(j)}(t)\sin(\delta^{(j)}(t))+\frac{V_{DC}^{(j)}K_{I\gamma}^{(j)}}{2}\Gamma_{d[\alpha^{(j)}(t)]}^{(j)}\\
&-\frac{V_{DC}^{(j)}K_{P\gamma}^{(j)}K_{P\phi}^{(j)}}{2}\hat{E}_{d[\omega_0 t]}^{(j)}(t)\cos(\delta^{(j)}(t))\\
&-\frac{K_{P\gamma}^{(j)}C^{(j)}}{D_\omega^{(j)}\omega_0}\left(P_r^{(j)}-P_f^{(j)}(t)\right)\hat{E}_{q[\omega_0 t]}^{(j)}(t)\cos(\delta^{(j)}(t))\\
&+\frac{K_{P\gamma}^{(j)}C^{(j)}}{D_\omega^{(j)}\omega_0}\left(P_r^{(j)}-P_f^{(j)}(t)\right)\hat{E}_{d[\omega_0 t]}^{(j)}(t)\sin(\delta^{(j)}(t))\\
&-K_{P\gamma}^{(j)}C^{(j)}\hat{E}_{q[\omega_0 t]}^{(j)}(t)\cos(\delta^{(j)}(t))\\
&+K_{P\gamma}^{(j)}C^{(j)}\hat{E}_{d[\omega_0 t]}^{(j)}(t)\sin(\delta^{(j)}(t))\\
&+\frac{V_{DC}^{(j)}K_{P\gamma}^{(j)}K_{I\phi}^{(j)}}{2}\Phi_{d[\alpha^{(j)}(t)]}^{(j)}(t),
\end{aligned}
\tag{120}
$$

$$
\begin{aligned}
\frac{1}{\omega_0}\frac{d\Gamma_{q[\alpha^{(j)}(t)]}^{(j)}(t)}{dt}=&\left(\frac{2}{V_{DC}}+K_{P\phi}^{(j)}\hat{R}_0^{(j)}\right)I_{q[\omega_0 t]}^{(j)}(t)\cos(\delta^{(j)}(t))\\
&-\left(\frac{2}{V_{DC}}+K_{P\phi}^{(j)}\hat{R}_0^{(j)}\right)I_{d[\omega_0 t]}^{(j)}(t)\sin(\delta^{(j)}(t))+K_{P\phi}^{(j)}E_0^{(j)}\\
&-K_{P\phi}^{(j)}\hat{E}_{q[\omega_0 t]}^{(j)}(t)\cos(\delta^{(j)}(t))+K_{P\phi}^{(j)}\hat{E}_{d[\omega_0 t]}^{(j)}(t)\sin(\delta^{(j)}(t))\\
&-\left(1+K_{P\phi}^{(j)}\hat{R}_0^{(j)}\right)\Xi_{q[\alpha^{(j)}(t)]}^{(j)}(t)+\frac{K_{P\phi}^{(j)}}{D_E^{(j)}}\left(Q_r^{(j)}-Q_f^{(j)}(t)\right)\\
&+\frac{2C^{(j)}}{V_{DC}}\left(P_r^{(j)}-P_f^{(j)}(t)\right)\hat{E}_{q[\omega_0 t]}^{(j)}(t)\sin(\delta^{(j)}(t))\\
&+\frac{2C^{(j)}}{V_{DC}D_\omega^{(j)}\omega_0}\left(P_r^{(j)}-P_f^{(j)}(t)\right)\hat{E}_{q[\omega_0 t]}^{(j)}(t)\sin(\delta^{(j)}(t))\\
&+\frac{2C^{(j)}}{V_{DC}}\left(P_r^{(j)}-P_f^{(j)}(t)\right)\hat{E}_{q[\omega_0 t]}^{(j)}(t)\sin(\delta^{(j)}(t))\\
&+\frac{2C^{(j)}}{V_{DC}D_\omega^{(j)}\omega_0}\left(P_r^{(j)}-P_f^{(j)}(t)\right)\hat{E}_{d[\omega_0 t]}^{(j)}(t)\cos(\delta^{(j)}(t))
\end{aligned}
$$

$$+ K_{I\phi}^{(j)} \Phi_{q[\alpha^{(j)}(t)]}^{(j)}(t), \tag{121}$$

$$\begin{aligned}
\frac{1}{\omega_0}\frac{d\Gamma_{d[\alpha^{(j)}(t)]}^{(j)}(t)}{dt} = &\left(\frac{2}{V_{DC}} + K_{P\phi}^{(j)}\hat{R}_0^{(j)}\right) I_{q[\omega_0 t]}^{(j)}(t)\sin(\delta^{(j)}(t)) \\
&+ \left(\frac{2}{V_{DC}} + K_{P\phi}^{(j)}\hat{R}_0^{(j)}\right) I_{d[\omega_0 t]}^{(j)}(t)\cos(\delta^{(j)}(t)) \\
&- K_{P\phi}^{(j)}\hat{E}_{q[\omega_0 t]}^{(j)}(t)\sin(\delta^{(j)}(t)) - K_{P\phi}^{(j)}\hat{E}_{d[\omega_0 t]}^{(j)}(t)\cos(\delta^{(j)}(t)) \\
&- \left(1 + K_{P\phi}^{(j)}\hat{R}_0^{(j)}\right) \Xi_{d[\alpha^{(j)}(t)]}^{(j)}(t) + K_{I\phi}^{(j)} \Phi_{d[\alpha^{(j)}(t)]}^{(j)}(t) \\
&- \frac{2C^{(j)}}{V_{DC}}\hat{E}_{q[\omega_0 t]}^{(j)}(t)\cos(\delta^{(j)}(t)) \\
&- \frac{2C^{(j)}}{V_{DC}D_\omega^{(j)}\omega_0}\left(P_r^{(j)} - P_f^{(j)}(t)\right)\hat{E}_{q[\omega_0 t]}^{(j)}(t)\cos(\delta^{(j)}(t)) \\
&+ \frac{2C^{(j)}}{V_{DC}}\hat{E}_{d[\omega_0 t]}^{(j)}(t)\sin(\delta^{(j)}(t)) \\
&+ \frac{2C^{(j)}}{V_{DC}D_\omega^{(j)}\omega_0}\left(P_r^{(j)} - P_f^{(j)}(t)\right)\hat{E}_{d[\omega_0 t]}^{(j)}(t)\sin(\delta^{(j)}(t)),
\end{aligned} \tag{122}$$

where

$$\begin{aligned}
E_{q[\omega_0 t]}^{(j)}(t) = &-\hat{R}_0^{(j)} I_{q[\omega_0 t]}^{(j)}(t) + \hat{R}_0^{(j)} \Xi_{q[\alpha^{(j)}(t)]}^{(j)}(t)\cos(\delta^{(j)}(t)) \\
&+ \hat{R}_0^{(j)} \Xi_{d[\alpha^{(j)}(t)]}^{(j)}(t)\sin(\delta^{(j)}(t)) + \hat{E}_{q[\omega_0 t]}^{(j)}(t),
\end{aligned} \tag{123}$$

$$\begin{aligned}
E_{d[\omega_0 t]}^{(j)}(t) = &-\hat{R}_0^{(j)} I_{d[\omega_0 t]}^{(j)}(t) - \hat{R}_0^{(j)} \Xi_{q[\alpha^{(j)}(t)]}^{(j)}(t)\sin(\delta^{(j)}(t)) \\
&+ \hat{R}_0^{(j)} \Xi_{d[\alpha^{(j)}(t)]}^{(j)}(t)\cos(\delta^{(j)}(t)) + \hat{E}_{d[\omega_0 t]}^{(j)}(t),
\end{aligned} \tag{124}$$

From Section 3.2, the microgrid network dynamics are described by:

$$\frac{1}{\omega_0}\mathbf{L}^{(\mathscr{E})}\frac{d\mathbf{I}_{q[\omega_0 t]}^{(\mathscr{E})}(t)}{dt} = -\mathbf{R}^{(\mathscr{E})}\mathbf{I}_{q[\omega_0 t]}^{(\mathscr{E})}(t) - \mathbf{L}^{(\mathscr{E})}\mathbf{I}_{d[\omega_0 t]}^{(\mathscr{E})}(t) + \mathbf{M}\mathbf{V}_{q[\omega_0 t]}^{(\mathscr{V})}(t), \tag{125}$$

$$\frac{1}{\omega_0}\mathbf{L}^{(\mathscr{E})}\frac{d\mathbf{I}_{d[\omega_0 t]}^{(\mathscr{E})}(t)}{dt} = -\mathbf{R}^{(\mathscr{E})}\mathbf{I}_{d[\omega_0 t]}^{(\mathscr{E})}(t) + \mathbf{L}^{(\mathscr{E})}\mathbf{I}_{q[\omega_0 t]}^{(\mathscr{E})}(t) + \mathbf{M}\mathbf{V}_{d[\omega_0 t]}^{(\mathscr{V})}(t). \tag{126}$$

From Section 3.3, the load dynamics are described by:

$$\mu^{(j)}\dot{V}^{(j)}_{q[\omega_0 t]}(t) = q_V\left(V^{(j)}_{q[\omega_0 t]}(t), V^{(j)}_{d[\omega_0 t]}(t), I^{(e')}_{q[\omega_0 t]}(t), I^{(e')}_{d[\omega_0 t]}(t)\right), \tag{127}$$

$$\mu^{(j)}\dot{V}^{(j)}_{d[\omega_0 t]}(t) = d_V\left(V^{(j)}_{q[\omega_0 t]}(t), V^{(j)}_{d[\omega_0 t]}(t), I^{(e')}_{q[\omega_0 t]}(t), I^{(e')}_{d[\omega_0 t]}(t)\right), \tag{128}$$

$$\mu^{(j)}\dot{I}^{(e')}_{q[\omega_0 t]}(t) = q_I\left(V^{(j)}_{q[\omega_0 t]}(t), V^{(j)}_{d[\omega_0 t]}(t), I^{(e')}_{q[\omega_0 t]}(t), I^{(e')}_{d[\omega_0 t]}(t)\right), \tag{129}$$

$$\mu^{(j)}\dot{I}^{(e')}_{d[\omega_0 t]}(t) = d_I\left(V^{(j)}_{q[\omega_0 t]}(t), V^{(j)}_{d[\omega_0 t]}(t), I^{(e')}_{q[\omega_0 t]}(t), I^{(e')}_{d[\omega_0 t]}(t)\right). \tag{130}$$

Henceforth, Eqs. 110–130 are referred to as the microgrid High-Order (μHOm) model.

4 Microgrid Reduced-Order Model 1 (μROm1)

In this section, the singular perturbation techniques discussed in Section 2.3 are used to reduce the order (state-space dimension) of the μHOm to obtain μROm1.

Assumption 4.1 *For $\varepsilon_1 = 1\times 10^{-5}$, the dynamic properties of the μHOm are such that for:*

$$\mathbf{x}_1(t) = \Big[\delta^{(j)}(t)\ Q^{(j)}_f(t)\ P^{(j)}_f(t)\ I^{(e')}_{q[\omega_0 t]}(t)\ I^{(e')}_{d[\omega_0 t]}(t)\ V^{(j)}_{q[\omega_0 t]}(t)\ V^{(j)}_{d[\omega_0 t]}(t)\ \mathbf{I}^{(\mathscr{E})}_{q[\omega_0 t]}(t)\ \mathbf{I}^{(\mathscr{E})}_{d[\omega_0 t]}(t)\ I^{(j)}_{q[\omega_0 t]}(t)\ I^{(j)}_{d[\omega_0 t]}(t)\ \Phi^{(j)}_{q[\alpha^{(j)}(t)]}(t)\ \Phi^{(j)}_{d[\alpha^{(j)}(t)]}(t)\Big]^T,$$

$$\mathbf{z}_1(t) = \Big[\Gamma^{(j)}_{q[\alpha^{(j)}(t)]}(t)\ \Gamma^{(j)}_{d[\alpha^{(j)}(t)]}(t)\ \Xi^{(j)}_{q[\alpha^{(j)}(t)]}(t)\ \Xi^{(j)}_{d[\alpha^{(j)}(t)]}(t)\ \hat{E}^{(j)}_{q[\omega_0 t]}(t)\ \hat{E}^{(j)}_{d[\omega_0 t]}(t)\Big]^T,$$

and $\mathbf{w}_1(t) = \Big[E^{(j)}_{q[\omega_0 t]}(t)\ E^{(j)}_{d[\omega_0 t]}(t)\Big]^T$, the dynamics of $\mathbf{z}_1(t)$ are at least $\frac{1}{\varepsilon_1}$ times faster than those of $\mathbf{x}_1(t)$, and the μHOm can be expressed compactly as follows:

$$\dot{\mathbf{x}}_1(t) = f_1\left(\mathbf{x}_1(t), \mathbf{z}_1(t), \mathbf{w}_1(t), \varepsilon_1\right), \tag{131}$$

$$\varepsilon_1\dot{\mathbf{z}}_1(t) = g_1\left(\mathbf{x}_1(t), \mathbf{z}_1(t), \mathbf{w}_1(t), \varepsilon_1\right), \tag{132}$$

$$\mathbf{0} = h_1\left(\mathbf{x}_1(t), \mathbf{z}_1(t), \mathbf{w}_1(t), \varepsilon_1\right). \tag{133}$$

Assumption 4.2 *Equations 131–133 are in standard form and satisfy Assumptions 2.1–2.3, according to the formulations in Section 2.3*

Assumption 4.3 *For $i = 1, 2, \ldots$, there exists $k_i^{(j)} \in (0, 10)$ such that:*

$$\frac{K^{(j)}_{P\gamma}C^{(j)}}{D^{(j)}_{\omega}\omega_0} = k^{(j)}_1\varepsilon_1, \quad \frac{2C^{(j)}}{V_{DC}D^{(j)}_{\omega}\omega_0} = k^{(j)}_2\varepsilon_1, \quad \frac{2\omega_0\varepsilon_1}{V_{DC}} = k^{(j)}_3\varepsilon_1, \quad \frac{2C^{(j)}\omega_0\varepsilon_1}{V_{DC}} = k^{(j)}_4\varepsilon_1,$$

$$\frac{C^{(j)}K^{(j)}_{P\phi}\hat{R}^{(j)}_0\left(1+K^{(j)}_{P\phi}\hat{R}^{(j)}_0\right)}{{C^{(j)}}^2\left(1+K^{(j)}_{P\phi}\hat{R}^{(j)}_0\right)^2+\left(K^{(j)}_{P\phi}\right)^2} = k^{(j)}_5\varepsilon_1, \quad \frac{C^{(j)}K^{(j)}_{I\phi}\hat{R}^{(j)}_0\left(1+K^{(j)}_{P\phi}\hat{R}^{(j)}_0\right)}{{C^{(j)}}^2\left(1+K^{(j)}_{P\phi}\hat{R}^{(j)}_0\right)^2+\left(K^{(j)}_{P\phi}\right)^2} = k^{(j)}_6\varepsilon_1,$$

$\frac{C^{(j)}K_{P\phi}^{(j)}\hat{R}_0^{(j)}}{{C^{(j)}}^2\left(1+K_{P\phi}^{(j)}\hat{R}_0^{(j)}\right)^2+\left(K_{P\phi}^{(j)}\right)^2}=k_7^{(j)}\varepsilon_1,\quad \frac{C^{(j)}\left(1+K_{P\phi}^{(j)}\hat{R}_0^{(j)}\right)^2}{{C^{(j)}}^2\left(1+K_{P\phi}^{(j)}\hat{R}_0^{(j)}\right)^2+\left(K_{P\phi}^{(j)}\right)^2}=k_8^{(j)}\varepsilon_1,\quad \frac{2R_0^{(j)}}{V_{DC}^{(j)}K_{I\gamma}^{(j)}}=k_9^{(j)}\varepsilon_1.$

Given Assumption 4.2, the μHOm can be approximately described by a slow model,

$$\dot{\bar{\mathbf{x}}}_1(t)=f_1\left(\bar{\mathbf{x}}_1(t),\bar{\zeta}_1\left(\bar{\mathbf{x}}_1(t)\right),\bar{\nu}_1\left(\bar{\mathbf{x}}_1(t)\right)+\tilde{\nu}_1\left(\mathbf{0}\right),0\right), \tag{134}$$

and a fast model,

$$\frac{d\tilde{\mathbf{z}}_1(\tau_1)}{d\tau}=g_1\left(\bar{\mathbf{x}}_1(0),\bar{\zeta}_1\left(\bar{\mathbf{x}}_1(0)\right)+\tilde{\mathbf{z}}_1(\tau_1),\bar{\nu}_1\left(\bar{\mathbf{x}}_1(0)\right)+\tilde{\nu}_1\left(\tilde{\mathbf{z}}_1(\tau_1)\right),0\right), \tag{135}$$

where

$$\bar{\mathbf{x}}_1(0)=\mathbf{x}_1(0)\qquad\text{and}\qquad\tilde{\mathbf{z}}_1(0)=\mathbf{z}_1(0)-\bar{\zeta}_1\left(\bar{\mathbf{x}}_1(0)\right)$$

so that:

$$\mathbf{x}_1(t)=\bar{\mathbf{x}}_1(t)+O(\varepsilon_1)\qquad\text{and}\qquad\mathbf{z}_1(0)=\tilde{\mathbf{z}}_1(\tau_1)+\bar{\zeta}_1\left(\bar{\mathbf{x}}_1(t)\right)+O(\varepsilon_1).$$

The μHOm is reduced to the expression in Eq. 134, which is independent of $\tilde{\mathbf{z}}_1(\tau_1)$. This is the so-called *Microgrid Reduced-Order Model 1 (μROm1).*

Next, the explicit ordinary differential equations (ODEs) that constitute μROm1 are derived. For $i=1$, Eqs. 23–24 are expressed explicitly, and the isolated real roots for $\bar{\mathbf{z}}_i(t)$ and $\bar{\mathbf{w}}_i(t)$ are given by:

$$\begin{aligned}
\Gamma_{q[\alpha^{(j)}(t)]}^{(j)}(t)=&-\frac{2K_{P\gamma}^{(j)}}{V_{DC}^{(j)}K_{I\gamma}^{(j)}}\left(1+\frac{V_{DC}^{(j)}K_{P\phi}^{(j)}\hat{R}_0^{(j)}}{2}\right)I_{q[\omega_0 t]}^{(j)}(t)\cos(\delta^{(j)}(t))\\
&+\frac{2K_{P\gamma}^{(j)}}{V_{DC}^{(j)}K_{I\gamma}^{(j)}}\left(1+\frac{V_{DC}^{(j)}K_{P\phi}^{(j)}\hat{R}_0^{(j)}}{2}\right)I_{d[\omega_0 t]}^{(j)}(t)\sin(\delta^{(j)}(t))\\
&+\frac{K_{P\gamma}^{(j)}}{K_{I\gamma}^{(j)}}\left(1+K_{P\phi}^{(j)}\hat{R}_0^{(j)}\right)\Xi_{q[\alpha^{(j)}(t)]}^{(j)}(t)\\
&+\frac{K_{P\gamma}^{(j)}K_{P\phi}^{(j)}}{K_{I\gamma}^{(j)}}\hat{E}_{q[\omega_0 t]}^{(j)}(t)\cos(\delta^{(j)}(t))-\frac{K_{P\gamma}^{(j)}K_{P\phi}^{(j)}}{K_{I\gamma}^{(j)}}E_0^{(j)}\\
&-\frac{K_{P\gamma}^{(j)}K_{P\phi}^{(j)}}{K_{I\gamma}^{(j)}}\hat{E}_{d[\omega_0 t]}^{(j)}(t)\sin(\delta^{(j)}(t))-\frac{K_{P\gamma}^{(j)}K_{P\phi}^{(j)}}{D_E^{(j)}K_{I\gamma}^{(j)}}\left(Q_r^{(j)}-Q_f^{(j)}(t)\right)\\
&-\frac{K_{P\gamma}^{(j)}K_{I\phi}^{(j)}}{K_{I\gamma}^{(j)}}\Phi_{q[\alpha^{(j)}(t)]}^{(j)}(t)-\frac{2K_{P\gamma}^{(j)}C^{(j)}}{V_{DC}^{(j)}K_{I\gamma}^{(j)}}\hat{E}_{d[\omega_0 t]}^{(j)}(t)\cos(\delta^{(j)}(t))
\end{aligned}$$

$$
\begin{aligned}
&- \frac{2K_{P\gamma}^{(j)}C^{(j)}}{V_{DC}^{(j)}K_{I\gamma}^{(j)}}\hat{E}_{q[\omega_0 t]}^{(j)}(t)\sin(\delta^{(j)}(t)), \qquad (136)\\
\Gamma_{d[\alpha^{(j)}(t)]}^{(j)}(t) =& -\frac{2K_{P\gamma}^{(j)}}{V_{DC}^{(j)}K_{I\gamma}^{(j)}}\left(1+\frac{V_{DC}^{(j)}K_{P\phi}^{(j)}\hat{R}_0^{(j)}}{2}\right)I_{q[\omega_0 t]}^{(j)}(t)\sin(\delta^{(j)}(t))\\
&- \frac{2K_{P\gamma}^{(j)}}{V_{DC}^{(j)}K_{I\gamma}^{(j)}}\left(1+\frac{V_{DC}^{(j)}K_{P\phi}^{(j)}\hat{R}_0^{(j)}}{2}\right)I_{d[\omega_0 t]}^{(j)}(t)\cos(\delta^{(j)}(t))\\
&+ \frac{K_{P\gamma}^{(j)}}{K_{I\gamma}^{(j)}}\left(1+K_{P\phi}^{(j)}\hat{R}_0^{(j)}\right)\Xi_{d[\alpha^{(j)}(t)]}^{(j)}(t)\\
&+ \frac{K_{P\gamma}^{(j)}K_{P\phi}^{(j)}}{K_{I\gamma}^{(j)}}\hat{E}_{q[\omega_0 t]}^{(j)}(t)\sin(\delta^{(j)}(t)) - \frac{K_{P\gamma}^{(j)}K_{I\phi}^{(j)}}{K_{I\gamma}^{(j)}}\Phi_{d[\alpha^{(j)}(t)]}^{(j)}(t)\\
&+ \frac{K_{P\gamma}^{(j)}K_{P\phi}^{(j)}}{K_{I\gamma}^{(j)}}\hat{E}_{d[\omega_0 t]}^{(j)}(t)\cos(\delta^{(j)}(t)) - \frac{2K_{P\gamma}^{(j)}C^{(j)}}{V_{DC}^{(j)}K_{I\gamma}^{(j)}}\hat{E}_{d[\omega_0 t]}^{(j)}(t)\sin(\delta^{(j)}(t))\\
&+ \frac{2K_{P\gamma}^{(j)}C^{(j)}}{V_{DC}^{(j)}K_{I\gamma}^{(j)}}\hat{E}_{q[\omega_0 t]}^{(j)}(t)\cos(\delta^{(j)}(t)), \qquad (137)\\
\Xi_{q[\alpha^{(j)}(t)]}^{(j)}(t) =& \frac{K_{P\phi}^{(j)}\hat{R}_0^{(j)}}{1+K_{P\phi}^{(j)}\hat{R}_0^{(j)}}I_{q[\omega_0 t]}^{(j)}(t)\cos(\delta^{(j)}(t)) + \frac{K_{I\phi}^{(j)}}{1+K_{P\phi}^{(j)}\hat{R}_0^{(j)}}\Phi_{q[\alpha^{(j)}(t)]}^{(j)}(t)\\
&- \frac{K_{P\phi}^{(j)}\hat{R}_0^{(j)}}{1+K_{P\phi}^{(j)}\hat{R}_0^{(j)}}I_{d[\omega_0 t]}^{(j)}(t)\sin(\delta^{(j)}(t)) + \frac{K_{P\phi}^{(j)}}{1+K_{P\phi}^{(j)}\hat{R}_0^{(j)}}E_0^{(j)}\\
&- \frac{K_{P\phi}^{(j)}}{1+K_{P\phi}^{(j)}\hat{R}_0^{(j)}}\hat{E}_{q[\omega_0 t]}^{(j)}(t)\cos(\delta^{(j)}(t))\\
&+ \frac{K_{P\phi}^{(j)}}{1+K_{P\phi}^{(j)}\hat{R}_0^{(j)}}\hat{E}_{d[\omega_0 t]}^{(j)}(t)\sin(\delta^{(j)}(t))\\
&+ \frac{K_{P\phi}^{(j)}}{D_E^{(j)}\left(1+K_{P\phi}^{(j)}\hat{R}_0^{(j)}\right)}\left(Q_r^{(j)}-Q_f^{(j)}(t)\right), \qquad (138)\\
\Xi_{d[\alpha^{(j)}(t)]}^{(j)}(t) =& \frac{K_{P\phi}^{(j)}\hat{R}_0^{(j)}}{1+K_{P\phi}^{(j)}\hat{R}_0^{(j)}}I_{q[\omega_0 t]}^{(j)}(t)\sin(\delta^{(j)}(t)) + \frac{K_{I\phi}^{(j)}}{1+K_{P\phi}^{(j)}\hat{R}_0^{(j)}}\Phi_{d[\alpha^{(j)}(t)]}^{(j)}(t)\\
&+ \frac{K_{P\phi}^{(j)}\hat{R}_0^{(j)}}{1+K_{P\phi}^{(j)}\hat{R}_0^{(j)}}I_{d[\omega_0 t]}^{(j)}(t)\cos(\delta^{(j)}(t))
\end{aligned}
$$

$$- \frac{K_{P\phi}^{(j)}}{1+K_{P\phi}^{(j)}\hat{R}_0^{(j)}}\hat{E}_{q[\omega_0 t]}^{(j)}(t)\sin(\delta^{(j)}(t)) - \frac{K_{P\phi}^{(j)}}{1+K_{P\phi}^{(j)}\hat{R}_0^{(j)}}\hat{E}_{d[\omega_0 t]}^{(j)}(t)\cos(\delta^{(j)}(t)), \tag{139}$$

$$\hat{E}_{q[\omega_0 t]}^{(j)}(t) = \frac{1}{C^{(j)}}I_{d[\omega_0 t]}^{(j)}(t) + \frac{1}{C^{(j)}}\Xi_{q[\alpha^{(j)}(t)]}^{(j)}(t)\sin(\delta^{(j)}(t)) - \frac{1}{C^{(j)}}\Xi_{d[\alpha^{(j)}(t)]}^{(j)}(t)\cos(\delta^{(j)}(t)), \tag{140}$$

$$\hat{E}_{d[\omega_0 t]}^{(j)}(t) = -\frac{1}{C^{(j)}}I_{q[\omega_0 t]}^{(j)}(t) + \frac{1}{C^{(j)}}\Xi_{q[\alpha^{(j)}(t)]}^{(j)}(t)\cos(\delta^{(j)}(t)) + \frac{1}{C^{(j)}}\Xi_{d[\alpha^{(j)}(t)]}^{(j)}(t)\sin(\delta^{(j)}(t)), \tag{141}$$

$$E_{q[\omega_0 t]}^{(j)}(t) = -\hat{R}_0^{(j)}I_{q[\omega_0 t]}^{(j)}(t) + \hat{R}_0^{(j)}\Xi_{q[\alpha^{(j)}(t)]}^{(j)}(t)\cos(\delta^{(j)}(t)) + \hat{R}_0^{(j)}\Xi_{d[\alpha^{(j)}(t)]}^{(j)}(t)\sin(\delta^{(j)}(t)) + \hat{E}_{q[\omega_0 t]}^{(j)}(t), \tag{142}$$

$$E_{d[\omega_0 t]}^{(j)}(t) = -\hat{R}_0^{(j)}I_{d[\omega_0 t]}^{(j)}(t) - \hat{R}_0^{(j)}\Xi_{q[\alpha^{(j)}(t)]}^{(j)}(t)\sin(\delta^{(j)}(t)) + \hat{R}_0^{(j)}\Xi_{d[\alpha^{(j)}(t)]}^{(j)}(t)\cos(\delta^{(j)}(t)) + \hat{E}_{d[\omega_0 t]}^{(j)}(t). \tag{143}$$

Next, we reduce the system of equations by substituting Eqs 136–141 into the μH0 Model given in Eqs. 110–130. Then, μR0 Model-1 can be explicitly expressed as follows:

$$D_\omega^{(j)}\frac{d\delta^{(j)}(t)}{dt} = P_r^{(j)} - P_f^{(j)}(t), \tag{144}$$

$$\frac{1}{\omega_c^{(j)}}\frac{dQ_f^{(j)}(t)}{dt} = -Q_f^{(j)}(t) + E_{q[\omega_0 t]}^{(j)}(t)I_{d[\omega_0 t]}^{(j)}(t) - E_{d[\omega_0 t]}^{(j)}(t)I_{q[\omega_0 t]}^{(j)}(t), \tag{145}$$

$$\frac{1}{\omega_c^{(j)}}\frac{dP_f^{(j)}(t)}{dt} = -P_f^{(j)}(t) + E_{q[\omega_0 t]}^{(j)}(t)I_{q[\omega_0 t]}^{(j)}(t) + E_{d[\omega_0 t]}^{(j)}(t)I_{d[\omega_0 t]}^{(j)}(t), \tag{146}$$

$$\mu^{(j)}\dot{V}_{q[\omega_0 t]}^{(j)}(t) = q_V\left(V_{q[\omega_0 t]}^{(j)}(t), V_{d[\omega_0 t]}^{(j)}(t), I_{q[\omega_0 t]}^{(e')}(t), I_{d[\omega_0 t]}^{(e')}(t)\right), \tag{147}$$

$$\mu^{(j)}\dot{V}_{d[\omega_0 t]}^{(j)}(t) = d_V\left(V_{q[\omega_0 t]}^{(j)}(t), V_{d[\omega_0 t]}^{(j)}(t), I_{q[\omega_0 t]}^{(e')}(t), I_{d[\omega_0 t]}^{(e')}(t)\right), \tag{148}$$

$$\mu^{(j)}\dot{I}_{q[\omega_0 t]}^{(e')}(t) = q_I\left(V_{q[\omega_0 t]}^{(j)}(t), V_{d[\omega_0 t]}^{(j)}(t), I_{q[\omega_0 t]}^{(e')}(t), I_{d[\omega_0 t]}^{(e')}(t)\right), \tag{149}$$

$$\mu^{(j)}\dot{I}_{d[\omega_0 t]}^{(e')}(t) = d_I\left(V_{q[\omega_0 t]}^{(j)}(t), V_{d[\omega_0 t]}^{(j)}(t), I_{q[\omega_0 t]}^{(e')}(t), I_{d[\omega_0 t]}^{(e')}(t)\right), \tag{150}$$

$$\frac{1}{\omega_0}\mathbf{L}^{(\mathscr{E})}\frac{d\mathbf{I}^{(\mathscr{E})}_{q[\omega_0 t]}(t)}{dt} = -\mathbf{R}^{(\mathscr{E})}\mathbf{I}^{(\mathscr{E})}_{q[\omega_0 t]}(t) - \mathbf{L}^{(\mathscr{E})}\mathbf{I}^{(\mathscr{E})}_{d[\omega_0 t]}(t) + \mathbf{M}\mathbf{V}^{(\mathscr{V})}_{q[\omega_0 t]}(t), \tag{151}$$

$$\frac{1}{\omega_0}\mathbf{L}^{(\mathscr{E})}\frac{d\mathbf{I}^{(\mathscr{E})}_{d[\omega_0 t]}(t)}{dt} = -\mathbf{R}^{(\mathscr{E})}\mathbf{I}^{(\mathscr{E})}_{d[\omega_0 t]}(t) + \mathbf{L}^{(\mathscr{E})}\mathbf{I}^{(\mathscr{E})}_{q[\omega_0 t]}(t) + \mathbf{M}\mathbf{V}^{(\mathscr{V})}_{d[\omega_0 t]}(t), \tag{152}$$

$$\frac{L^{(j)}}{\omega_0}\frac{dI^{(j)}_{q[\omega_0 t]}(t)}{dt} = -R^{(j)}I^{(j)}_{q[\omega_0 t]}(t) - L^{(j)}I^{(j)}_{d[\omega_0 t]}(t) + E^{(j)}_{q[\omega_0 t]}(t) - V^{(j)}_{q[\omega_0 t]}(t), \tag{153}$$

$$\frac{L^{(j)}}{\omega_0}\frac{dI^{(j)}_{d[\omega_0 t]}(t)}{dt} = L^{(j)}I^{(j)}_{q[\omega_0 t]}(t) - R^{(j)}I^{(j)}_{d[\omega_0 t]}(t) + E^{(j)}_{d[\omega_0 t]}(t) - V^{(j)}_{d[\omega_0 t]}(t), \tag{154}$$

$$\begin{aligned}\frac{1}{\omega_0}\frac{d\Phi^{(j)}_{q[\alpha^{(j)}(t)]}(t)}{dt} =& -\frac{K^{(j)}_{I\phi}K^{(j)}_{P\phi}}{C^{(j)2}\left(1+K^{(j)}_{P\phi}\hat{R}^{(j)}_0\right)^2+\left(K^{(j)}_{P\phi}\right)^2}\Phi^{(j)}_{q[\alpha^{(j)}(t)]}(t)\\ &+\frac{C^{(j)}K^{(j)}_{I\phi}}{C^{(j)2}\left(1+K^{(j)}_{P\phi}\hat{R}^{(j)}_0\right)^2+\left(K^{(j)}_{P\phi}\right)^2}\Phi^{(j)}_{d[\alpha^{(j)}(t)]}(t)\\ &+\frac{K^{(j)}_{P\phi}\left(I^{(j)}_{q[\omega_0 t]}(t)\cos(\delta^{(j)}(t))-I^{(j)}_{d[\omega_0 t]}(t)\sin(\delta^{(j)}(t))\right)}{C^{(j)2}\left(1+K^{(j)}_{P\phi}\hat{R}^{(j)}_0\right)^2+\left(K^{(j)}_{P\phi}\right)^2}\\ &+\frac{C^{(j)2}\left(1+K^{(j)}_{P\phi}\hat{R}^{(j)}_0\right)^2E^{(j)}_0}{C^{(j)2}\left(1+K^{(j)}_{P\phi}\hat{R}^{(j)}_0\right)^2+\left(K^{(j)}_{P\phi}\right)^2}\\ &+\frac{C^{(j)2}\left(1+K^{(j)}_{P\phi}\hat{R}^{(j)}_0\right)^2\left(Q^{(j)}_r-Q^{(j)}_f(t)\right)}{D^{(j)}_E C^{(j)2}\left(1+K^{(j)}_{P\phi}\hat{R}^{(j)}_0\right)^2+D^{(j)}_E\left(K^{(j)}_{P\phi}\right)^2},\end{aligned} \tag{155}$$

$$\begin{aligned}\frac{1}{\omega_0}\frac{d\Phi^{(j)}_{d[\alpha^{(j)}(t)]}(t)}{dt} =& -\frac{K^{(j)}_{I\phi}K^{(j)}_{P\phi}}{C^{(j)2}\left(1+K^{(j)}_{P\phi}\hat{R}^{(j)}_0\right)^2+\left(K^{(j)}_{P\phi}\right)^2}\Phi^{(j)}_{d[\alpha^{(j)}(t)]}(t)\\ &+\frac{C^{(j)}K^{(j)}_{I\phi}}{C^{(j)2}\left(1+K^{(j)}_{P\phi}\hat{R}^{(j)}_0\right)^2+\left(K^{(j)}_{P\phi}\right)^2}\Phi^{(j)}_{q[\alpha^{(j)}(t)]}(t)\end{aligned}$$

$$+\frac{K_{P\phi}^{(j)}\left(I_{q[\omega_0 t]}^{(j)}(t)\sin(\delta^{(j)}(t))+I_{d[\omega_0 t]}^{(j)}(t)cos(\delta^{(j)}(t))\right)}{C^{(j)^2}\left(1+K_{P\phi}^{(j)}\hat{R}_0^{(j)}\right)^2+\left(K_{P\phi}^{(j)}\right)^2}$$
$$-\frac{C^{(j)}K_{P\phi}^{(j)}\left(E_0^{(j)}+\frac{1}{D_E^{(j)}}\left(Q_r^{(j)}-Q_f^{(j)}(t)\right)\right)}{C^{(j)^2}\left(1+K_{P\phi}^{(j)}\hat{R}_0^{(j)}\right)^2+\left(K_{P\phi}^{(j)}\right)^2}, \quad (156)$$

where

$$\begin{aligned}
E_{q[\omega_0 t]}^{(j)}(t) =& -\frac{K_{P\phi}^{(j)}}{C^{(j)^2}\left(1+K_{P\phi}^{(j)}\hat{R}_0^{(j)}\right)^2+\left(K_{P\phi}^{(j)}\right)^2}I_{q[\omega_0 t]}^{(j)}(t)\\
&+\frac{C^{(j)}K_{I\phi}^{(j)}\left(\Phi_{q[\alpha^{(j)}(t)]}^{(j)}(t)\sin(\delta^{(j)}(t))-\Phi_{d[\alpha^{(j)}(t)]}^{(j)}(t)\cos(\delta^{(j)}(t))\right)}{C^{(j)^2}\left(1+K_{P\phi}^{(j)}\hat{R}_0^{(j)}\right)^2+\left(K_{P\phi}^{(j)}\right)^2}\\
&+\frac{K_{I\phi}^{(j)}K_{P\phi}^{(j)}\left(\Phi_{q[\alpha^{(j)}(t)]}^{(j)}(t)\cos(\delta^{(j)}(t))+\Phi_{d[\alpha^{(j)}(t)]}^{(j)}(t)\sin(\delta^{(j)}(t))\right)}{C^{(j)^2}\left(1+K_{P\phi}^{(j)}\hat{R}_0^{(j)}\right)^2+\left(K_{P\phi}^{(j)}\right)^2}\\
&+\frac{E_0^{(j)}C^{(j)}K_{P\phi}^{(j)}\left(1+K_{P\phi}^{(j)}\hat{R}_0^{(j)}\right)\sin(\delta^{(j)}(t))}{C^{(j)^2}\left(1+K_{P\phi}^{(j)}\hat{R}_0^{(j)}\right)^2+\left(K_{P\phi}^{(j)}\right)^2}\\
&+\frac{C^{(j)}K_{P\phi}^{(j)}\left(1+K_{P\phi}^{(j)}\hat{R}_0^{(j)}\right)\left(Q_r^{(j)}-Q_f^{(j)}(t)\right)\sin(\delta^{(j)}(t))}{D_E^{(j)}C^{(j)^2}\left(1+K_{P\phi}^{(j)}\hat{R}_0^{(j)}\right)^2+D_E^{(j)}\left(K_{P\phi}^{(j)}\right)^2}\\
&+\frac{\left(K_{P\phi}^{(j)}\right)^2\cos(\delta^{(j)}(t))\left(E_0^{(j)}+\frac{1}{D_E^{(j)}}\left(Q_r^{(j)}-Q_f^{(j)}(t)\right)\right)}{C^{(j)^2}\left(1+K_{P\phi}^{(j)}\hat{R}_0^{(j)}\right)^2+\left(K_{P\phi}^{(j)}\right)^2},
\end{aligned} \quad (157)$$

$$\begin{aligned}
E_{d[\omega_0 t]}^{(j)}(t) =& -\frac{K_{P\phi}^{(j)}}{C^{(j)^2}\left(1+K_{P\phi}^{(j)}\hat{R}_0^{(j)}\right)^2+\left(K_{P\phi}^{(j)}\right)^2}I_{d[\omega_0 t]}^{(j)}(t)\\
&+\frac{C^{(j)}K_{I\phi}^{(j)}\left(\Phi_{q[\alpha^{(j)}(t)]}^{(j)}(t)\cos(\delta^{(j)}(t))+\Phi_{d[\alpha^{(j)}(t)]}^{(j)}(t)\sin(\delta^{(j)}(t))\right)}{C^{(j)^2}\left(1+K_{P\phi}^{(j)}\hat{R}_0^{(j)}\right)^2+\left(K_{P\phi}^{(j)}\right)^2}
\end{aligned}$$

$$
\begin{aligned}
&- \frac{K_{I\phi}^{(j)} K_{P\phi}^{(j)} \left(\Phi_{q[\alpha^{(j)}(t)]}^{(j)}(t) \sin(\delta^{(j)}(t)) - \Phi_{d[\alpha^{(j)}(t)]}^{(j)}(t) \cos(\delta^{(j)}(t)) \right)}{C^{(j)2} \left(1 + K_{P\phi}^{(j)} \hat{R}_0^{(j)}\right)^2 + \left(K_{P\phi}^{(j)}\right)^2} \\
&+ \frac{E_0^{(j)} C^{(j)} K_{P\phi}^{(j)} \left(1 + K_{P\phi}^{(j)} \hat{R}_0^{(j)}\right) \cos(\delta^{(j)}(t))}{C^{(j)2} \left(1 + K_{P\phi}^{(j)} \hat{R}_0^{(j)}\right)^2 + \left(K_{P\phi}^{(j)}\right)^2} \\
&+ \frac{C^{(j)} K_{P\phi}^{(j)} \left(1 + K_{P\phi}^{(j)} \hat{R}_0^{(j)}\right) \left(Q_r^{(j)} - Q_f^{(j)}(t)\right) \cos(\delta^{(j)}(t))}{D_E^{(j)} C^{(j)2} \left(1 + K_{P\phi}^{(j)} \hat{R}_0^{(j)}\right)^2 + D_E^{(j)} \left(K_{P\phi}^{(j)}\right)^2} \\
&- \frac{\left(K_{P\phi}^{(j)}\right)^2 \sin(\delta^{(j)}(t)) \left(E_0^{(j)} + \frac{1}{D_E^{(j)}} \left(Q_r^{(j)} - Q_f^{(j)}(t)\right)\right)}{C^{(j)2} \left(1 + K_{P\phi}^{(j)} \hat{R}_0^{(j)}\right)^2 + \left(K_{P\phi}^{(j)}\right)^2}. \quad (158)
\end{aligned}
$$

Assumption 4.4 *The effect of a disturbance (load change, loss of line, loss of generator, etc.) on the system state is such that Assumptions 2.1–2.3 are satisfied, according to the formulations in Section 2.3*

Assumptions 4.1 and 4.4 are sufficient conditions for which μR0 Model-1 approximates the μHOm.

5 Microgrid Reduced-Order Model 2 (μROm2)

In this section, we further reduce the order (state-space dimension) of the μHOm to obtain μROm2.

Assumption 5.1 *For $\varepsilon_2 = 1 \times 10^{-3}$, the dynamic properties of the μHOm are such that for:*

$$
\begin{aligned}
\mathbf{z}_2(t) = \Big[& I_{q[\omega_0 t]}^{(e')}(t)\ I_{d[\omega_0 t]}^{(e')}(t)\ V_{q[\omega_0 t]}^{(j)}(t)\ V_{d[\omega_0 t]}^{(j)}(t)\ \mathbf{I}_{q[\omega_0 t]}^{(\mathscr{E})}(t)\ \mathbf{I}_{d[\omega_0 t]}^{(\mathscr{E})}(t)\ I_{q[\omega_0 t]}^{(j)}(t)\ I_{d[\omega_0 t]}^{(j)}(t) \\
& \Phi_{q[\alpha^{(j)}(t)]}^{(j)}(t)\ \Phi_{d[\alpha^{(j)}(t)]}^{(j)}(t)\ \Gamma_{q[\alpha^{(j)}(t)]}^{(j)}(t)\ \Gamma_{d[\alpha^{(j)}(t)]}^{(j)}(t)\ \Xi_{q[\alpha^{(j)}(t)]}^{(j)}(t)\ \Xi_{d[\alpha^{(j)}(t)]}^{(j)}(t) \\
& \hat{E}_{q[\omega_0 t]}^{(j)}(t)\ \hat{E}_{d[\omega_0 t]}^{(j)}(t) \Big]^T,
\end{aligned}
$$

$\mathbf{x}_2(t) = \left[\delta^{(j)}(t)\ Q_f^{(j)}(t)\ P_f^{(j)}(t) \right]^T$, *and* $\mathbf{w}_2(t) = \left[E_{q[\omega_0 t]}^{(j)}(t)\ E_{d[\omega_0 t]}^{(j)}(t) \right]$, *the dynamics of $\mathbf{z}_2(t)$ are at least $\frac{1}{\varepsilon_2}$ times faster than those of $\mathbf{x}_2(t)$, and the μHOm can be expressed compactly as follows:*

$$\dot{\mathbf{x}}_2(t) = f_2\left(\mathbf{x}_2(t), \mathbf{z}_2(t), \mathbf{w}_2(t), \varepsilon_2\right), \quad (159)$$

$$\varepsilon_2 \dot{\mathbf{z}}_2(t) = g_2\left(\mathbf{x}_2(t), \mathbf{z}_2(t), \mathbf{w}_2(t), \varepsilon_2\right), \quad (160)$$

$$\mathbf{0} = h_2\left(\mathbf{x}_2(t), \mathbf{z}_2(t), \mathbf{w}_2(t), \varepsilon_2\right). \tag{161}$$

Assumption 5.2 *Equations 159–161 are in standard form and satisfy Assumptions 2.1–2.3, according to the formulations in Section 2.3*

Assumption 5.3 *For $i = 1, 2, \ldots$, there exists $k_i^{(j)}$, $\hat{k}_i \in (0, 10)$ such that:*

$$\frac{K_{P\gamma}^{(j)} C^{(j)}}{D_\omega^{(j)} \omega_0} = k_1^{(j)} \varepsilon_2, \quad \frac{2C^{(j)}}{V_{DC} D_\omega^{(j)} \omega_0} = k_2^{(j)} \varepsilon_2, \quad \frac{2\omega_0 \varepsilon_1}{V_{DC}} = k_3^{(j)} \varepsilon_2, \quad \frac{2C^{(j)} \omega_0 \varepsilon_1}{V_{DC}} = k_4^{(j)} \varepsilon_2,$$

$$\frac{C^{(j)} K_{P\phi}^{(j)} \hat{R}_0^{(j)} \left(1 + K_{P\phi}^{(j)} \hat{R}_0^{(j)}\right)}{{C^{(j)}}^2 \left(1 + K_{P\phi}^{(j)} \hat{R}_0^{(j)}\right)^2 + \left(K_{P\phi}^{(j)}\right)^2} = k_5^{(j)} \varepsilon_2, \quad \frac{C^{(j)} K_{I\phi}^{(j)} \hat{R}_0^{(j)} \left(1 + K_{P\phi}^{(j)} \hat{R}_0^{(j)}\right)}{{C^{(j)}}^2 \left(1 + K_{P\phi}^{(j)} \hat{R}_0^{(j)}\right)^2 + \left(K_{P\phi}^{(j)}\right)^2} = k_6^{(j)} \varepsilon_2,$$

$$\frac{C^{(j)} K_{P\phi}^{(j)} \hat{R}_0^{(j)}}{{C^{(j)}}^2 \left(1 + K_{P\phi}^{(j)} \hat{R}_0^{(j)}\right)^2 + \left(K_{P\phi}^{(j)}\right)^2} = k_7^{(j)} \varepsilon_2, \quad \frac{C^{(j)} \left(1 + K_{P\phi}^{(j)} \hat{R}_0^{(j)}\right)^2}{{C^{(j)}}^2 \left(1 + K_{P\phi}^{(j)} \hat{R}_0^{(j)}\right)^2 + \left(K_{P\phi}^{(j)}\right)^2} = k_8^{(j)} \varepsilon_2,$$

$$\frac{C^{(j)} \left(1 + K_{P\phi}^{(j)} \hat{R}_0^{(j)}\right)^2 + \left(K_{P\phi}^{(j)}\right)^2}{\omega_0 K_{I\phi}^{(j)} K_{P\phi}^{(j)}} = k_9^{(j)} \varepsilon_2, \quad \frac{{C^{(j)}}^2 \left(1 + K_{P\phi}^{(j)} \hat{R}_0^{(j)}\right)^2}{K_{I\phi}^{(j)} K_{P\phi}^{(j)}} = k_{10}^{(j)} \varepsilon_2, \quad \frac{C^{(j)}}{K_{P\phi}^{(j)}} = k_{11}^{(j)} \varepsilon_2,$$

$$\frac{C^{(j)}}{K_{I\phi}^{(j)}} = k_{12}^{(j)} \varepsilon_2, \quad \frac{1}{K_{I\phi}^{(j)}} = k_{13}^{(j)} \varepsilon_2, \quad \frac{K_{P\gamma}^{(j)} K_{P\phi}^{(j)} \hat{R}_0^{(j)}}{K_{I\gamma}^{(j)}} = k_{14}^{(j)} \varepsilon_2, \quad \frac{2R_0^{(j)}}{V_{DC}^{(j)} K_{I\gamma}^{(j)}} = k_{15}^{(j)} \varepsilon_2,$$

$$\frac{C^{(j)} K_{P\phi}^{(j)} \left(1 + K_{P\phi}^{(j)} \hat{R}_0^{(j)}\right)}{{C^{(j)}}^2 \left(1 + K_{P\phi}^{(j)} \hat{R}_0^{(j)}\right)^2 + \left(K_{P\phi}^{(j)}\right)^2} = k_{16}^{(j)} \varepsilon_2, \quad \frac{C^{(j)} K_{P\phi}^{(j)}}{{C^{(j)}}^2 \left(1 + K_{P\phi}^{(j)} \hat{R}_0^{(j)}\right)^2 + \left(K_{P\phi}^{(j)}\right)^2} = k_{17}^{(j)} \varepsilon_2,$$

$$\mu^{(j)} = k_{18}^{(j)} \varepsilon_2, \quad \frac{1}{\omega_0} \mathbf{L}^{(\mathscr{E})} = \varepsilon_2 \begin{bmatrix} \hat{k}_1 & 0 & \ldots & 0 \\ 0 & \hat{k}_2 & \ldots & 0 \\ \vdots & \vdots & \ddots & \vdots \\ 0 & 0 & \ldots & \hat{k}_{|\mathscr{E}|} \end{bmatrix} = \varepsilon_2 \mathbf{K}^{(\mathscr{E})}, \text{ and } C^{(j)} < 1,\ \hat{R}_0^{(j)} < 1$$

Given Assumption 5.2, the μHOm can be approximately described by a slow model,

$$\dot{\bar{\mathbf{x}}}_2(t) = f_2\left(\bar{\mathbf{x}}_2(t), \bar{\zeta}_2\left(\bar{\mathbf{x}}_2(t)\right), \bar{v}_2\left(\bar{\mathbf{x}}_2(t)\right) + \tilde{v}_2\left(\mathbf{0}\right), 0\right), \tag{162}$$

and a fast model,

$$\frac{d\tilde{\mathbf{z}}_2(\tau_2)}{d\tau_2} = g_2\left(\bar{\mathbf{x}}_2(0), \bar{\zeta}_2\left(\bar{\mathbf{x}}_2(0)\right) + \tilde{\mathbf{z}}_2(\tau_2), \bar{v}_2\left(\bar{\mathbf{x}}_2(0)\right) + \tilde{v}_2\left(\tilde{\mathbf{z}}_2(\tau_2)\right), 0\right), \tag{163}$$

where

$$\bar{\mathbf{x}}_2(0) = \mathbf{x}_2(0) \qquad \text{and} \qquad \tilde{\mathbf{z}}_2(0) = \mathbf{z}_2(0) - \bar{\zeta}_2\left(\bar{\mathbf{x}}_2(0)\right)$$

so that:

$$\mathbf{x}_2(t) = \bar{\mathbf{x}}_2(t) + O(\varepsilon_2) \qquad \text{and} \qquad \mathbf{z}_2(0) = \tilde{\mathbf{z}}_2(\tau_2) + \bar{\zeta}_2\left(\bar{\mathbf{x}}_2(t)\right) + O(\varepsilon_2).$$

The μHOm is reduced to the expression in Eq. 162, which is independent of $\tilde{\mathbf{z}}_2(\tau_2)$. This is the so-called *Microgrid Reduced-Order Model 2 (μROm2)*.

Next, the explicit ODEs that constitute μROm2 are derived. For $i=2$, Eqs. 23–24 are expressed explicitly, and the isolated real roots for $\bar{\mathbf{z}}_i(t)$ and $\bar{\mathbf{w}}_i(t)$ are given by the following system of equations:

$$0 = q_V\left(V^{(j)}_{q[\omega_0 t]}(t), V^{(j)}_{d[\omega_0 t]}(t), I^{(e')}_{q[\omega_0 t]}(t), I^{(e')}_{d[\omega_0 t]}(t)\right), \tag{164}$$

$$0 = d_V\left(V^{(j)}_{q[\omega_0 t]}(t), V^{(j)}_{d[\omega_0 t]}(t), I^{(e')}_{q[\omega_0 t]}(t), I^{(e')}_{d[\omega_0 t]}(t)\right), \tag{165}$$

$$0 = q_I\left(V^{(j)}_{q[\omega_0 t]}(t), V^{(j)}_{d[\omega_0 t]}(t), I^{(e')}_{q[\omega_0 t]}(t), I^{(e')}_{d[\omega_0 t]}(t)\right), \tag{166}$$

$$0 = d_I\left(V^{(j)}_{q[\omega_0 t]}(t), V^{(j)}_{d[\omega_0 t]}(t), I^{(e')}_{q[\omega_0 t]}(t), I^{(e')}_{d[\omega_0 t]}(t)\right), \tag{167}$$

$$\Phi^{(j)}_{q[\alpha^{(j)}(t)]}(t) = 0, \tag{168}$$

$$\Phi^{(j)}_{d[\alpha^{(j)}(t)]}(t) = 0, \tag{169}$$

$$\begin{aligned}\Gamma^{(j)}_{q[\alpha^{(j)}(t)]}(t) = &\frac{K^{(j)}_{P\gamma}K^{(j)}_{P\phi}C^{(j)}\left(1+K^{(j)}_{P\phi}\hat{R}^{(j)}_0\right)^2\left(I^{(j)}_{q[\omega_0 t]}(t)\sin(\delta^{(j)}(t))\right)}{\left(C^{(j)2}\left(1+K^{(j)}_{P\phi}\hat{R}^{(j)}_0\right)^2+\left(K^{(j)}_{P\phi}\right)^2\right)K^{(j)}_{I\gamma}}\\ &+\frac{K^{(j)}_{P\gamma}K^{(j)}_{P\phi}C^{(j)}\left(1+K^{(j)}_{P\phi}\hat{R}^{(j)}_0\right)^2\left(I^{(j)}_{d[\omega_0 t]}(t)\cos(\delta^{(j)}(t))\right)}{\left(C^{(j)2}\left(1+K^{(j)}_{P\phi}\hat{R}^{(j)}_0\right)^2+\left(K^{(j)}_{P\phi}\right)^2\right)K^{(j)}_{I\gamma}}\\ &-\frac{K^{(j)}_{P\gamma}K^{(j)}_{P\phi}C^{(j)2}\left(1+K^{(j)}_{P\phi}\hat{R}^{(j)}_0\right)^2\left(E^{(j)}_0-\frac{1}{D^{(j)}_E}\left(Q^{(j)}_r-Q^{(j)}_f(t)\right)\right)}{\left(C^{(j)2}\left(1+K^{(j)}_{P\phi}\hat{R}^{(j)}_0\right)^2+\left(K^{(j)}_{P\phi}\right)^2\right)K^{(j)}_{I\gamma}},\end{aligned} \tag{170}$$

$$\begin{aligned}\Gamma^{(j)}_{d[\alpha^{(j)}(t)]}(t) = &-\frac{K^{(j)}_{P\gamma}K^{(j)}_{P\phi}C^{(j)}\left(1+K^{(j)}_{P\phi}\hat{R}^{(j)}_0\right)^2\left(I^{(j)}_{q[\omega_0 t]}(t)\cos(\delta^{(j)}(t))\right)}{\left(C^{(j)2}\left(1+K^{(j)}_{P\phi}\hat{R}^{(j)}_0\right)^2+\left(K^{(j)}_{P\phi}\right)^2\right)K^{(j)}_{I\gamma}}\\ &+\frac{K^{(j)}_{P\gamma}K^{(j)}_{P\phi}C^{(j)}\left(1+K^{(j)}_{P\phi}\hat{R}^{(j)}_0\right)^2\left(I^{(j)}_{d[\omega_0 t]}(t)\sin(\delta^{(j)}(t))\right)}{\left(C^{(j)2}\left(1+K^{(j)}_{P\phi}\hat{R}^{(j)}_0\right)^2+\left(K^{(j)}_{P\phi}\right)^2\right)K^{(j)}_{I\gamma}},\end{aligned} \tag{171}$$

$$\Xi^{(j)}_{q[\alpha^{(j)}(t)]}(t) = \frac{\left(K^{(j)}_{P\phi}\right)^2\left(I^{(j)}_{q[\omega_0 t]}(t)\cos(\delta^{(j)}(t)) - I^{(j)}_{d[\omega_0 t]}(t)\sin(\delta^{(j)}(t))\right)}{C^{(j)2}\left(1+K^{(j)}_{P\phi}\hat{R}^{(j)}_0\right)^2+\left(K^{(j)}_{P\phi}\right)^2}, \tag{172}$$

$$\Xi^{(j)}_{d[\alpha^{(j)}(t)]}(t) = \frac{\left(K^{(j)}_{P\phi}\right)^2 \left(I^{(j)}_{q[\omega_0 t]}(t)\sin(\delta^{(j)}(t)) + I^{(j)}_{d[\omega_0 t]}(t)\cos(\delta^{(j)}(t))\right)}{C^{(j)^2}\left(1+K^{(j)}_{P\phi}\hat{R}^{(j)}_0\right)^2 + \left(K^{(j)}_{P\phi}\right)^2}$$
$$- \frac{C^{(j)}\left(K^{(j)}_{P\phi}\right)^2 \left(E^{(j)}_0 + \frac{1}{D^{(j)}_E}\left(Q^{(j)}_r - Q^{(j)}_f(t)\right)\right)}{C^{(j)^2}\left(1+K^{(j)}_{P\phi}\hat{R}^{(j)}_0\right)^2 + \left(K^{(j)}_{P\phi}\right)^2}, \tag{173}$$

$$E^{(j)}_{q[\omega_0 t]}(t) = \frac{\left(K^{(j)}_{P\phi}\right)^2 \cos(\delta^{(j)}(t)) \left(E^{(j)}_0 + \frac{1}{D^{(j)}_E}\left(Q^{(j)}_r - Q^{(j)}_f(t)\right)\right)}{C^{(j)^2}\left(1+K^{(j)}_{P\phi}\hat{R}^{(j)}_0\right)^2 + \left(K^{(j)}_{P\phi}\right)^2}, \tag{174}$$

$$E^{(j)}_{d[\omega_0 t]}(t) = - \frac{\left(K^{(j)}_{P\phi}\right)^2 \sin(\delta^{(j)}(t)) \left(E^{(j)}_0 + \frac{1}{D^{(j)}_E}\left(Q^{(j)}_r - Q^{(j)}_f(t)\right)\right)}{C^{(j)^2}\left(1+K^{(j)}_{P\phi}\hat{R}^{(j)}_0\right)^2 + \left(K^{(j)}_{P\phi}\right)^2}, \tag{175}$$

for $G^{(j)} = \frac{R^{(j)}}{R^{(j)^2}+L^{(j)^2}}$ and $B^{(j)} = \frac{-L^{(j)}}{R^{(j)^2}+L^{(j)^2}}$,

$$I^{(j)}_{q[\omega_0 t]}(t) = G^{(j)}E^{(j)}_{q[\omega_0 t]}(t) + B^{(j)}E^{(j)}_{d[\omega_0 t]}(t) - G^{(j)}V^{(j)}_{q[\omega_0 t]}(t) - B^{(j)}V^{(j)}_{d[\omega_0 t]}(t), \tag{176}$$
$$I^{(j)}_{d[\omega_0 t]}(t) = G^{(j)}E^{(j)}_{d[\omega_0 t]}(t) - B^{(j)}E^{(j)}_{q[\omega_0 t]}(t) - G^{(j)}V^{(j)}_{d[\omega_0 t]}(t) + B^{(j)}V^{(j)}_{q[\omega_0 t]}(t), \tag{177}$$

and the network current injections are described by:

$$\mathbf{I}^{(\mathscr{V})}_{q[\omega_0 t]}(t) - \mathrm{j}\mathbf{I}^{(\mathscr{V})}_{d[\omega_0 t]}(t) = \mathbf{Y}^{(\mathscr{E})}\left(\mathbf{V}^{(\mathscr{V})}_{q[\omega_0 t]}(t) - j\mathbf{V}^{(\mathscr{V})}_{d[\omega_0 t]}(t)\right), \tag{178}$$

where

$$\mathbf{I}^{(\mathscr{V})}_{q[\omega_0 t]}(t) = \mathbf{M}^{\mathrm{T}}\mathbf{I}^{(\mathscr{E})}_{q[\omega_0 t]}(t), \tag{179}$$
$$\mathbf{Y}^{(\mathscr{E})} = \mathbf{M}^{\mathrm{T}}\left(\mathbf{G}^{(\mathscr{E})} + \mathrm{j}\mathbf{B}^{(\mathscr{E})}\right)\mathbf{M}, \tag{180}$$

with

$$\mathbf{G}^{(\mathscr{E})} = \mathbf{R}^{(\mathscr{E})}\left((\mathbf{R}^{(\mathscr{E})})^2 + (\mathbf{L}^{(\mathscr{E})})^2\right)^{-1} \quad \text{and} \quad \mathbf{B}^{(\mathscr{E})} = -\mathbf{L}^{(\mathscr{E})}\left((\mathbf{R}^{(\mathscr{E})})^2 + (\mathbf{L}^{(\mathscr{E})})^2\right)^{-1},$$

where the inverted matrices are invertible diagonal matrices. $\mathbf{Y}^{(\mathscr{E})}$ represents the bus admittance matrix of the network (see, e.g., [2]), and has the structure:

$$\begin{aligned}\text{for diagonal terms}: Y^{(i,i)} &= G^{(i,i)} + jB^{(i,i)} \\ &= (\text{sum of admittances connected to bus } i), \\ \text{and for } i \neq j: Y^{(i,j)} &= G^{(i,j)} + jB^{(i,j)} \\ &= -(\text{sum of admittances connected between bus } i \text{ and } j).\end{aligned}$$

Assumption 5.4 *For $\varepsilon_2 = 0$, the load behavior is fully captured by the so called ZIP model (see e.g. [13]) so that Eqs. 164–167 can be combined to give:*

$$V^{(j)}_{q[\omega_0 t]}(t)I^{(e')}_{q[\omega_0 t]}(t) + V^{(j)}_{d[\omega_0 t]}(t)I^{(e')}_{d[\omega_0 t]}(t) = -P^{(j)}_0 - \left|\overrightarrow{\mathbf{V}}^{(j)}_{qd0}(t)\right| P^{(j)}_1 - \left|\overrightarrow{\mathbf{V}}^{(j)}_{qd0}(t)\right|^2 P^{(j)}_2, \tag{181}$$

$$V^{(j)}_{q[\omega_0 t]}(t)I^{(e')}_{d[\omega_0 t]}(t) - V^{(j)}_{d[\omega_0 t]}(t)I^{(e')}_{q[\omega_0 t]}(t) = -Q^{(j)}_0 - \left|\overrightarrow{\mathbf{V}}^{(j)}_{qd0}(t)\right| Q^{(j)}_1 - \left|\overrightarrow{\mathbf{V}}^{(j)}_{qd0}(t)\right|^2 Q^{(j)}_2, \tag{182}$$

where $P^{(j)}_0$, $P^{(j)}_1$, $P^{(j)}_2$, $Q^{(j)}_0$, $Q^{(j)}_1$ and $Q^{(j)}_2$ denote constants for the net load at bus j.

Inverter Voltage Angle Defining the inverter voltage angle as follows

$$\hat{\theta}^{(j)}(t) := \arctan\left(\frac{-E^{(j)}_{d[\omega_0 t]}(t)}{E^{(j)}_{q[\omega_0 t]}(t)}\right), \tag{183}$$

from Eqs. 174–175, it follows that:

$$\hat{\theta}^{(j)}(t) = \delta^{(j)}(t). \tag{184}$$

Power Flow Formulation For the n-bus microgrid, let $\mathcal{N}_j$ represent the set of all buses electrically connected to bus j, including bus j, and let $\beta^{(j)} \in \{0,1\}$ be a constant such that $\beta^{(j)} = 1$ if bus j is connected to an inverter-interfaced power supply and $\beta^{(j)} = 0$ otherwise. Using Eqs. 176–178, 181 and 182, the power flow equations at bus $j = 1,2,...n$ of the network are given by:

$$\begin{aligned}
0 = {} & P^{(j)}_0 + \left|\overrightarrow{\mathbf{V}}^{(j)}_{qd0}(t)\right| P^{(j)}_1 + \left|\overrightarrow{\mathbf{V}}^{(j)}_{qd0}(t)\right|^2 P^{(j)}_2 + \beta^{(j)} G^{(j)} \left|V^{(j)}(t)\right|^2 \\
& - \beta^{(j)} \left|\overrightarrow{\mathbf{V}}^{(j)}_{qd0}(t)\right| \left|\overrightarrow{\mathbf{E}}^{(j)}_{qd0}(t)\right| \left(G^{(j)} \cos\left(\theta^{(j)}(t) - \hat{\theta}^{(j)}(t)\right) + B^{(j)} \sin\left(\theta^{(j)}(t)\right.\right. \\
& \left.\left. - \hat{\theta}^{(j)}(t)\right)\right) + \left|\overrightarrow{\mathbf{V}}^{(j)}_{qd0}(t)\right| \sum_{k \in \mathcal{N}_j} \left|\overrightarrow{\mathbf{V}}^{(k)}_{qd0}(t)\right| \left(G^{(j,k)} \cos\left(\theta^{(j)}(t) - \theta^{(k)}(t)\right)\right. \\
& \left. + B^{(j,k)} \sin\left(\theta^{(j)}(t) - \theta^{(k)}(t)\right)\right),
\end{aligned} \tag{185}$$

$$\begin{aligned}
0 = {} & Q^{(j)}_0 + \left|\overrightarrow{\mathbf{V}}^{(j)}_{qd0}(t)\right| Q^{(j)}_1 + \left|\overrightarrow{\mathbf{V}}^{(j)}_{qd0}(t)\right|^2 Q^{(j)}_2 - \beta^{(j)} B^{(j)} \left|\overrightarrow{\mathbf{V}}^{(j)}_{qd0}(t)\right|^2 \\
& - \beta^{(j)} \left|\overrightarrow{\mathbf{V}}^{(j)}_{qd0}(t)\right| \left|\overrightarrow{\mathbf{E}}^{(j)}_{qd0}(t)\right| \left(G^{(j)} \sin\left(\theta^{(j)}(t) - \hat{\theta}^{(j)}(t)\right) - B^{(j)} \cos\left(\theta^{(j)}(t)\right.\right. \\
& \left.\left. - \hat{\theta}^{(j)}(t)\right)\right) + \left|\overrightarrow{\mathbf{V}}^{(j)}_{qd0}(t)\right| \sum_{k \in \mathcal{N}_j} \left|\overrightarrow{\mathbf{V}}^{(k)}_{qd0}(t)\right| \left(G^{(j,k)} \sin\left(\theta^{(j)}(t) - \theta^{(k)}(t)\right)\right.
\end{aligned}$$

$$-B^{(j,k)}\cos\left(\theta^{(j)}(t)-\theta^{(k)}(t)\right)\Bigg). \tag{186}$$

Assumption 5.5 *The power flow equations jacobian is invertible in the domain of interest, so from the implicit function theorem, the power flow equations have isolated roots in the domain of interest. It can be shown that this implies that the reduced system of algebraic equations (Eqs. 164–167) have isolated roots, from where it follows that the μHOm is in standard form.*

Next, we reduce the system of equations by substituting Eqs 168–178 into the μH0 Model given in Eqs. 110–130, Then, μR0 Model-2 can be explicitly expressed as follows:

$$D_{\omega}^{(j)}\frac{d\hat{\theta}^{(j)}(t)}{dt}=P_r^{(j)}-P_f^{(j)}(t), \tag{187}$$

$$\begin{aligned}\frac{1}{\omega_c^{(j)}}\frac{dQ_f^{(j)}(t)}{dt}=&-B^{(j)}\left|\overrightarrow{\mathbf{V}}_{qd0}^{(j)}(t)\right|^2-\left|\overrightarrow{\mathbf{V}}_{qd0}^{(j)}(t)\right|\left|\overrightarrow{\mathbf{E}}_{qd0}^{(j)}(t)\right|\Bigg(G^{(j)}\sin\Big(\theta^{(j)}(t)\\&-\hat{\theta}^{(j)}(t)\Big)-B^{(j)}\cos\left(\theta^{(j)}(t)-\hat{\theta}^{(j)}(t)\right)\Bigg)-Q_f^{(j)}(t),\end{aligned} \tag{188}$$

$$\begin{aligned}\frac{1}{\omega_c^{(j)}}\frac{dP_f^{(j)}(t)}{dt}=&G^{(j)}\left|\overrightarrow{\mathbf{E}}_{qd0}^{(j)}(t)\right|^2-\left|\overrightarrow{\mathbf{V}}_{qd0}^{(j)}(t)\right|\left|\overrightarrow{\mathbf{E}}_{qd0}^{(j)}(t)\right|\Bigg(G^{(j)}\cos\Big(\theta^{(j)}(t)\\&-\hat{\theta}^{(j)}(t)\Big)+B^{(j)}\sin\left(\theta^{(j)}(t)-\hat{\theta}^{(j)}(t)\right)\Bigg)-P_f^{(j)}(t),\end{aligned} \tag{189}$$

and for $\mathbf{B}^{(\mathscr{E})}=-\mathbf{L}^{(\mathscr{E})}\left((\mathbf{R}^{(\mathscr{E})})^2+(\mathbf{L}^{(\mathscr{E})})^2\right)^{-1}$, $\mathbf{G}^{(\mathscr{E})}=\mathbf{R}^{(\mathscr{E})}\left((\mathbf{R}^{(\mathscr{E})})^2+(\mathbf{L}^{(\mathscr{E})})^2\right)^{-1}$, $\mathbf{I}^{(\mathscr{V})}_{q[\omega_0 t]}(t)=\mathbf{M}^{\mathrm{T}}\mathbf{I}^{(\mathscr{E})}_{q[\omega_0 t]}(t)$, $\mathbf{Y}^{(\mathscr{E})}=\mathbf{M}^{\mathrm{T}}\left(\mathbf{G}^{(\mathscr{E})}+\mathrm{j}\mathbf{B}^{(\mathscr{E})}\right)\mathbf{M}$, $G^{(j)}=\frac{R^{(j)}}{{R^{(j)}}^2+{L^{(j)}}^2}$ and $B^{(j)}=\frac{-L^{(j)}}{{R^{(j)}}^2+{L^{(j)}}^2}$, the algebraic and transcendental equations are given by:

$$\begin{aligned}0=\;&P_0^{(j)}+\left|\overrightarrow{\mathbf{V}}_{qd0}^{(j)}(t)\right|P_1^{(j)}+\left|\overrightarrow{\mathbf{V}}_{qd0}^{(j)}(t)\right|^2P_2^{(j)}+\beta^{(j)}G^{(j)}\left|\overrightarrow{\mathbf{V}}_{qd0}^{(j)}(t)\right|^2\\&-\beta^{(j)}\left|\overrightarrow{\mathbf{V}}_{qd0}^{(j)}(t)\right|\left|\overrightarrow{\mathbf{E}}_{qd0}^{(j)}(t)\right|\left(G^{(j)}\cos\left(\theta^{(j)}(t)-\hat{\theta}^{(j)}(t)\right)+B^{(j)}\sin\Big(\theta^{(j)}(t)\right.\\&\left.-\hat{\theta}^{(j)}(t)\Big)\right)+\left|\overrightarrow{\mathbf{V}}_{qd0}^{(j)}(t)\right|\sum_{k\in\mathcal{N}_j}\left|\overrightarrow{\mathbf{V}}_{qd0}^{(k)}(t)\right|\left(G^{(j,k)}\cos\left(\theta^{(j)}(t)-\theta^{(k)}(t)\right)\right.\end{aligned}$$

$$+B^{(j,k)}\sin\left(\theta^{(j)}(t)-\theta^{(k)}(t)\right)\Bigg), \tag{190}$$

$$\begin{aligned}0=\;& Q_0^{(j)}+\left|\overrightarrow{\mathbf{V}}_{qd0}^{(j)}(t)\right|Q_1^{(j)}+\left|\overrightarrow{\mathbf{V}}_{qd0}^{(j)}(t)\right|^2Q_2^{(j)}-\beta^{(j)}B^{(j)}\left|\overrightarrow{\mathbf{V}}_{qd0}^{(j)}(t)\right|^2\\ &-\beta^{(j)}\left|\overrightarrow{\mathbf{V}}_{qd0}^{(j)}(t)\right|\left|\overrightarrow{\mathbf{E}}_{qd0}^{(j)}(t)\right|\Bigg(G^{(j)}\sin\left(\theta^{(j)}(t)-\hat{\theta}^{(j)}(t)\right)-B^{(j)}\cos\left(\theta^{(j)}(t)\\ &-\hat{\theta}^{(j)}(t)\right)\Bigg)+\left|\overrightarrow{\mathbf{V}}_{qd0}^{(j)}(t)\right|\sum_{k\in\mathcal{N}_j}\left|\overrightarrow{\mathbf{V}}_{qd0}^{(k)}(t)\right|\Bigg(G^{(j,k)}\sin\left(\theta^{(j)}(t)-\theta^{(k)}(t)\right)\\ &-B^{(j,k)}\cos\left(\theta^{(j)}(t)-\theta^{(k)}(t)\right)\Bigg),\end{aligned} \tag{191}$$

$$\tag{192}$$

and

$$\left|\overrightarrow{\mathbf{E}}_{qd0}^{(j)}(t)\right|=\frac{\left(K_{P\phi}^{(j)}\right)^2\left(E_0^{(j)}+\frac{1}{D_E^{(j)}}\left(Q_r^{(j)}-Q_f^{(j)}(t)\right)\right)}{C^{(j)2}\left(1+K_{P\phi}^{(j)}\hat{R}_0^{(j)}\right)^2+\left(K_{P\phi}^{(j)}\right)^2}. \tag{193}$$

6 Microgrid Reduced-Order Model 3 (μROm3)

In this section, we further reduce the order (state-space dimension) of the μHOm to obtain μROm3.

Assumption 6.1 *For $\varepsilon_3=1\times10^{-1}$, the dynamic properties of the μHOm are such that for:*

$$\begin{aligned}\mathbf{z}_3(t)=\Big[&Q_f^{(j)}(t)\;P_f^{(j)}(t)\;I_{q[\omega_0t]}^{(e')}(t)\;I_{d[\omega_0t]}^{(e')}(t)\;V_{q[\omega_0t]}^{(j)}(t)\;V_{d[\omega_0t]}^{(j)}(t)\;\mathbf{I}_{q[\omega_0t]}^{(\mathscr{E})}(t)\;\mathbf{I}_{d[\omega_0t]}^{(\mathscr{E})}(t)\\ &I_{q[\omega_0t]}^{(j)}(t)\;I_{d[\omega_0t]}^{(j)}(t)\;\Phi_{q[\alpha^{(j)}(t)]}^{(j)}(t)\;\Phi_{d[\alpha^{(j)}(t)]}^{(j)}(t)\;\Gamma_{q[\alpha^{(j)}(t)]}^{(j)}(t)\;\Gamma_{d[\alpha^{(j)}(t)]}^{(j)}(t)\\ &\Xi_{q[\alpha^{(j)}(t)]}^{(j)}(t)\;\Xi_{d[\alpha^{(j)}(t)]}^{(j)}(t)\;\hat{E}_{q[\omega_0t]}^{(j)}(t)\;\hat{E}_{d[\omega_0t]}^{(j)}(t)\Big]^T,\end{aligned}$$

$\mathbf{x}_3(t)=\delta^{(j)}(t)$, *and* $\mathbf{w}_3(t)=\left[E_{q[\omega_0t]}^{(j)}(t)\;E_{d[\omega_0t]}^{(j)}(t)\right]^T$, *the dynamics of $\mathbf{z}_3(t)$ are at least $\frac{1}{\varepsilon_3}$ times faster than those of $\mathbf{x}_3(t)$, and the μHOm can be expressed compactly as follows:*

$$\dot{\mathbf{x}}_3(t)=f_3\left(\mathbf{x}_3(t),\mathbf{z}_3(t),\mathbf{w}_3(t),\varepsilon_3\right), \tag{194}$$

$$\varepsilon_3\dot{\mathbf{z}}_3(t)=g_3\left(\mathbf{x}_3(t),\mathbf{z}_3(t),\mathbf{w}_3(t),\varepsilon_3\right), \tag{195}$$

$$\mathbf{0}=h_3\left(\mathbf{x}_3(t),\mathbf{z}_3(t),\mathbf{w}_3(t),\varepsilon_3\right). \tag{196}$$

Assumption 6.2 *Equations 194–196 are in standard form and satisfy Assumptions 2.1–2.3, according to the formulations in Section 2.3*

Assumption 6.3 *For $i = 1,2,\ldots$, there exists $k_i^{(j)}$, $\hat{k}_i \in (0,10)$ such that:*

$$\frac{K_{P\gamma}^{(j)} C^{(j)}}{D_\omega^{(j)} \omega_0} = k_1^{(j)} \varepsilon_3, \quad \frac{2C^{(j)}}{V_{DC} D_\omega^{(j)} \omega_0} = k_3^{(j)} \varepsilon_3, \quad \frac{2\omega_0 \varepsilon_1}{V_{DC}} = k_3^{(j)} \varepsilon_3, \quad \frac{2C^{(j)} \omega_0 \varepsilon_1}{V_{DC}} = k_4^{(j)} \varepsilon_3,$$

$$\frac{C^{(j)} K_{P\phi}^{(j)} \hat{R}_0^{(j)} \left(1 + K_{P\phi}^{(j)} \hat{R}_0^{(j)}\right)}{C^{(j)^2} \left(1 + K_{P\phi}^{(j)} \hat{R}_0^{(j)}\right)^2 + \left(K_{P\phi}^{(j)}\right)^2} = k_5^{(j)} \varepsilon_3, \quad \frac{C^{(j)} K_{I\phi}^{(j)} \hat{R}_0^{(j)} \left(1 + K_{P\phi}^{(j)} \hat{R}_0^{(j)}\right)}{C^{(j)^2} \left(1 + K_{P\phi}^{(j)} \hat{R}_0^{(j)}\right)^2 + \left(K_{P\phi}^{(j)}\right)^2} = k_6^{(j)} \varepsilon_3,$$

$$\frac{C^{(j)} K_{P\phi}^{(j)} \hat{R}_0^{(j)}}{C^{(j)^2} \left(1 + K_{P\phi}^{(j)} \hat{R}_0^{(j)}\right)^2 + \left(K_{P\phi}^{(j)}\right)^2} = k_7^{(j)} \varepsilon_3, \quad \frac{C^{(j)} \left(1 + K_{P\phi}^{(j)} \hat{R}_0^{(j)}\right)^2}{C^{(j)^2} \left(1 + K_{P\phi}^{(j)} \hat{R}_0^{(j)}\right)^2 + \left(K_{P\phi}^{(j)}\right)^2} = k_8^{(j)} \varepsilon_3,$$

$$\frac{C^{(j)} \left(1 + K_{P\phi}^{(j)} \hat{R}_0^{(j)}\right)^2 + \left(K_{P\phi}^{(j)}\right)^2}{\omega_0 K_{I\phi}^{(j)} K_{P\phi}^{(j)}} = k_9^{(j)} \varepsilon_3, \quad \frac{C^{(j)^2} \left(1 + K_{P\phi}^{(j)} \hat{R}_0^{(j)}\right)^2}{K_{I\phi}^{(j)} K_{P\phi}^{(j)}} = k_{10}^{(j)} \varepsilon_3, \quad \frac{C^{(j)}}{K_{P\phi}^{(j)}} = k_{11}^{(j)} \varepsilon_3,$$

$$\frac{C^{(j)}}{K_{I\phi}^{(j)}} = k_{12}^{(j)} \varepsilon_3, \quad \frac{1}{K_{I\phi}^{(j)}} = k_{13}^{(j)} \varepsilon_3, \quad \frac{K_{P\gamma}^{(j)} K_{P\phi}^{(j)} \hat{R}_0^{(j)}}{K_{I\gamma}^{(j)}} = k_{14}^{(j)} \varepsilon_3, \quad \frac{2R_0^{(j)}}{V_{DC}^{(j)} K_{I\gamma}^{(j)}} = k_{15}^{(j)} \varepsilon_1,$$

$$\frac{C^{(j)} K_{P\phi}^{(j)} \left(1 + K_{P\phi}^{(j)} \hat{R}_0^{(j)}\right)}{C^{(j)^2} \left(1 + K_{P\phi}^{(j)} \hat{R}_0^{(j)}\right)^2 + \left(K_{P\phi}^{(j)}\right)^2} = k_{16}^{(j)} \varepsilon_3, \quad \frac{C^{(j)} K_{P\phi}^{(j)}}{C^{(j)^2} \left(1 + K_{P\phi}^{(j)} \hat{R}_0^{(j)}\right)^2 + \left(K_{P\phi}^{(j)}\right)^2} = k_{17}^{(j)} \varepsilon_3$$

$$C^{(j)^2} \left(1 + K_{P\phi}^{(j)} \hat{R}_0^{(j)}\right)^2 = k_{18}^{(j)} \varepsilon_3, \quad \frac{K_{P\gamma}^{(j)} K_{P\phi}^{(j)} C^{(j)} \left(1 + K_{P\phi}^{(j)} \hat{R}_0^{(j)}\right)^2}{\left(C^{(j)^2} \left(1 + K_{P\phi}^{(j)} \hat{R}_0^{(j)}\right)^2 + \left(K_{P\phi}^{(j)}\right)^2\right) K_{I\gamma}^{(j)}} = k_{19}^{(j)} \varepsilon_3,$$

$$\mu^{(j)} = k_{20}^{(j)} \varepsilon_3, \quad \frac{1}{\omega_c^{(j)}} = k_{21}^{(j)} \varepsilon_3, \quad \frac{1}{\omega_0} \mathbf{L}^{(\mathscr{E})} = \varepsilon_3 \begin{bmatrix} \hat{k}_1 & 0 & \ldots & 0 \\ 0 & \hat{k}_3 & \ldots & 0 \\ \vdots & \vdots & \ddots & \vdots \\ 0 & 0 & \ldots & \hat{k}_{|\mathscr{E}|} \end{bmatrix} = \varepsilon_3 \mathbf{K}^{(\mathscr{E})},$$

and $C^{(j)} < 1$, $\hat{R}_0^{(j)} < 1$

Given Assumption 6.2, the μHOm can be approximately described by a slow model,

$$\dot{\bar{\mathbf{x}}}_3(t) = f_3\left(\bar{\mathbf{x}}_3(t), \bar{\zeta}_3\left(\bar{\mathbf{x}}_3(t)\right), \bar{v}_3\left(\bar{\mathbf{x}}_3(t)\right) + \tilde{v}_3\left(\mathbf{0}\right), 0\right), \tag{197}$$

and a fast model,

$$\frac{d\tilde{\mathbf{z}}_3(\tau_3)}{d\tau_3} = g_3\left(\bar{\mathbf{x}}_3(0), \bar{\zeta}_3\left(\bar{\mathbf{x}}_3(0)\right) + \tilde{\mathbf{z}}_3(\tau_3), \bar{v}_3\left(\bar{\mathbf{x}}_3(0)\right) + \tilde{v}_3\left(\tilde{\mathbf{z}}_3(\tau_3)\right), 0\right), \tag{198}$$

where

$$\bar{\mathbf{x}}_3(0) = \mathbf{x}_3(0) \qquad \text{and} \qquad \tilde{\mathbf{z}}_3(0) = \mathbf{z}_3(0) - \bar{\zeta}_3\left(\bar{\mathbf{x}}_3(0)\right)$$

so that:

$$\mathbf{x}_3(t) = \bar{\mathbf{x}}_3(t) + O(\varepsilon_3) \qquad \text{and} \qquad \mathbf{z}_3(0) = \tilde{\mathbf{z}}_3(\tau_3) + \bar{\zeta}_3\left(\bar{\mathbf{x}}_3(t)\right) + O(\varepsilon_3).$$

The μHOm is reduced to Eq. 197, which is independent of $\tilde{\mathbf{z}}_3(\tau_3)$. Henceforth, Eq. 197 is called *Microgrid Reduced-Order Model 3 (μROm)*.

Next, the explicit ODEs that constitute μROm3 are derived. For $i = 2$, Eqs. 23–24 are expressed explicitly, and the isolated real roots for $\bar{\mathbf{z}}_i(t)$ and $\bar{\mathbf{w}}_i(t)$ are given by the following system of equations:

$$0 = q_V\left(V^{(j)}_{q[\omega_0 t]}(t), V^{(j)}_{d[\omega_0 t]}(t), I^{(e')}_{q[\omega_0 t]}(t), I^{(e')}_{d[\omega_0 t]}(t)\right), \tag{199}$$

$$0 = d_V\left(V^{(j)}_{q[\omega_0 t]}(t), V^{(j)}_{d[\omega_0 t]}(t), I^{(e')}_{q[\omega_0 t]}(t), I^{(e')}_{d[\omega_0 t]}(t)\right), \tag{200}$$

$$0 = q_I\left(V^{(j)}_{q[\omega_0 t]}(t), V^{(j)}_{d[\omega_0 t]}(t), I^{(e')}_{q[\omega_0 t]}(t), I^{(e')}_{d[\omega_0 t]}(t)\right), \tag{201}$$

$$0 = d_I\left(V^{(j)}_{q[\omega_0 t]}(t), V^{(j)}_{d[\omega_0 t]}(t), I^{(e')}_{q[\omega_0 t]}(t), I^{(e')}_{d[\omega_0 t]}(t)\right), \tag{202}$$

$$Q^{(j)}_f(t) = E^{(j)}_{q[\omega_0 t]}(t) I^{(j)}_{d[\omega_0 t]}(t) - E^{(j)}_{d[\omega_0 t]}(t) I^{(j)}_{q[\omega_0 t]}(t), \tag{203}$$

$$P^{(j)}_f(t) = E^{(j)}_{q[\omega_0 t]}(t) I^{(j)}_{q[\omega_0 t]}(t) + E^{(j)}_{d[\omega_0 t]}(t) I^{(j)}_{d[\omega_0 t]}(t), \tag{204}$$

$$\Phi^{(j)}_{q[\alpha^{(j)}(t)]}(t) = 0, \tag{205}$$

$$\Phi^{(j)}_{d[\alpha^{(j)}(t)]}(t) = 0, \tag{206}$$

$$\Gamma^{(j)}_{q[\alpha^{(j)}(t)]}(t) = 0, \tag{207}$$

$$\Gamma^{(j)}_{d[\alpha^{(j)}(t)]}(t) = 0, \tag{208}$$

$$\Xi^{(j)}_{q[\alpha^{(j)}(t)]}(t) = I^{(j)}_{q[\omega_0 t]}(t)\cos(\delta^{(j)}(t)) - I^{(j)}_{d[\omega_0 t]}(t)\sin(\delta^{(j)}(t)), \tag{209}$$

$$\begin{aligned}\Xi^{(j)}_{d[\alpha^{(j)}(t)]}(t) = {} & I^{(j)}_{q[\omega_0 t]}(t)\sin(\delta^{(j)}(t)) + I^{(j)}_{d[\omega_0 t]}(t)\cos(\delta^{(j)}(t)) \\ & - C^{(j)}\left(E^{(j)}_0 + \frac{1}{D^{(j)}_E}\left(Q^{(j)}_r - Q^{(j)}_f(t)\right)\right),\end{aligned} \tag{210}$$

$$E^{(j)}_{q[\omega_0 t]}(t) = \left(E^{(j)}_0 + \frac{1}{D^{(j)}_E}\left(Q^{(j)}_r - Q^{(j)}_f(t)\right)\right)\cos(\delta^{(j)}(t)), \tag{211}$$

$$E^{(j)}_{d[\omega_0 t]}(t) = -\left(E^{(j)}_0 + \frac{1}{D^{(j)}_E}\left(Q^{(j)}_r - Q^{(j)}_f(t)\right)\right)\sin(\delta^{(j)}(t)), \tag{212}$$

for $G^{(j)} = \frac{R^{(j)}}{{R^{(j)}}^2 + {L^{(j)}}^2}$ and $B^{(j)} = \frac{-L^{(j)}}{{R^{(j)}}^2 + {L^{(j)}}^2}$,

$$I^{(j)}_{q[\omega_0 t]}(t) = G^{(j)} E^{(j)}_{q[\omega_0 t]}(t) + B^{(j)} E^{(j)}_{d[\omega_0 t]}(t) - G^{(j)} V^{(j)}_{q[\omega_0 t]}(t) - B^{(j)} V^{(j)}_{d[\omega_0 t]}(t), \tag{213}$$

$$I^{(j)}_{d[\omega_0 t]}(t) = G^{(j)} E^{(j)}_{d[\omega_0 t]}(t) - B^{(j)} E^{(j)}_{q[\omega_0 t]}(t) - G^{(j)} V^{(j)}_{d[\omega_0 t]}(t) + B^{(j)} V^{(j)}_{q[\omega_0 t]}(t), \tag{214}$$

the network current injections are described by:

$$\mathbf{I}^{(\mathscr{V})}_{q[\omega_0 t]}(t) - \mathrm{j}\mathbf{I}^{(\mathscr{V})}_{d[\omega_0 t]}(t) = \mathbf{Y}^{(\mathscr{E})}\left(\mathbf{V}^{(\mathscr{V})}_{q[\omega_0 t]}(t) - j\mathbf{V}^{(\mathscr{V})}_{d[\omega_0 t]}(t)\right), \tag{215}$$

where $\mathbf{I}^{(\mathscr{V})}_{q[\omega_0 t]}(t)$, $\mathbf{I}^{(\mathscr{V})}_{d[\omega_0 t]}(t)$ and $\mathbf{Y}^{(\mathscr{E})}$ are defined in Eqs. 179 and 180.

Next, given Assumptions 5.4–5.5 and the formulations derived in Eqs. 183–186, we reduce the system of equations by substituting Eqs. 200–215, 185 and 186 into the μH0 Model given in Eqs. 110–130. Then, μR0 Model-3 can be explicitly expressed as follows:

For $\mathbf{B}^{(\mathscr{E})} = -\mathbf{L}^{(\mathscr{E})}\left((\mathbf{R}^{(\mathscr{E})})^2 + (\mathbf{L}^{(\mathscr{E})})^2\right)^{-1}$, $\mathbf{G}^{(\mathscr{E})} = \mathbf{R}^{(\mathscr{E})}\left((\mathbf{R}^{(\mathscr{E})})^2 + (\mathbf{L}^{(\mathscr{E})})^2\right)^{-1}$, $\mathbf{Y}^{(\mathscr{E})} = \mathbf{M}^{\mathrm{T}}\left(\mathbf{G}^{(\mathscr{E})} + \mathrm{j}\mathbf{B}^{(\mathscr{E})}\right)\mathbf{M}$, $G^{(j)} = \frac{R^{(j)}}{{R^{(j)}}^2 + {L^{(j)}}^2}$ and $B^{(j)} = \frac{-L^{(j)}}{{R^{(j)}}^2 + {L^{(j)}}^2}$,

$$D^{(j)}_{\omega}\frac{d\hat{\theta}^{(j)}(t)}{dt} = P^{(j)}_r - G^{(j)}\left|\overrightarrow{\mathbf{E}}^{(j)}_{qd0}(t)\right|^2 + \left|\overrightarrow{\mathbf{V}}^{(j)}_{qd0}(t)\right|\left|\overrightarrow{\mathbf{E}}^{(j)}_{qd0}(t)\right|\left(G^{(j)}\cos\left(\theta^{(j)}(t) - \hat{\theta}^{(j)}(t)\right) + B^{(j)}\sin\left(\theta^{(j)}(t) - \hat{\theta}^{(j)}(t)\right)\right), \tag{216}$$

and

$$\begin{aligned}
0 = {} & P^{(j)}_0 + \left|\overrightarrow{\mathbf{V}}^{(j)}_{qd0}(t)\right| P^{(j)}_1 + \left|\overrightarrow{\mathbf{V}}^{(j)}_{qd0}(t)\right|^2 P^{(j)}_2 + \beta^{(j)} G^{(j)}\left|\overrightarrow{\mathbf{V}}^{(j)}_{qd0}(t)\right|^2 \\
& - \beta^{(j)}\left|\overrightarrow{\mathbf{V}}^{(j)}_{qd0}(t)\right|\left|\overrightarrow{\mathbf{E}}^{(j)}_{qd0}(t)\right|\left(G^{(j)}\cos\left(\theta^{(j)}(t) - \hat{\theta}^{(j)}(t)\right) + B^{(j)}\sin\left(\theta^{(j)}(t) - \hat{\theta}^{(j)}(t)\right)\right) + \left|\overrightarrow{\mathbf{V}}^{(j)}_{qd0}(t)\right|\sum_{k\in\mathscr{N}_j}\left|\overrightarrow{\mathbf{V}}^{(k)}_{qd0}(t)\right|\left(G^{(j,k)}\cos\left(\theta^{(j)}(t) - \theta^{(k)}(t)\right)\right. \\
& \left. + B^{(j,k)}\sin\left(\theta^{(j)}(t) - \theta^{(k)}(t)\right)\right),
\end{aligned} \tag{217}$$

$$\begin{aligned}
0 = {} & Q^{(j)}_0 + \left|\overrightarrow{\mathbf{V}}^{(j)}_{qd0}(t)\right| Q^{(j)}_1 + \left|\overrightarrow{\mathbf{V}}^{(j)}_{qd0}(t)\right|^2 Q^{(j)}_2 - \beta^{(j)} B^{(j)}\left|\overrightarrow{\mathbf{V}}^{(j)}_{qd0}(t)\right|^2 \\
& - \beta^{(j)}\left|\overrightarrow{\mathbf{V}}^{(j)}_{qd0}(t)\right|\left|\overrightarrow{\mathbf{E}}^{(j)}_{qd0}(t)\right|\left(G^{(j)}\sin\left(\theta^{(j)}(t) - \hat{\theta}^{(j)}(t)\right) - B^{(j)}\cos\left(\theta^{(j)}(t) - \hat{\theta}^{(j)}(t)\right)\right) + \left|\overrightarrow{\mathbf{V}}^{(j)}_{qd0}(t)\right|\sum_{k\in\mathscr{N}_j}\left|\overrightarrow{\mathbf{V}}^{(k)}_{qd0}(t)\right|\left(G^{(j,k)}\sin\left(\theta^{(j)}(t) - \theta^{(k)}(t)\right)\right. \\
& \left. - B^{(j,k)}\cos\left(\theta^{(j)}(t) - \theta^{(k)}(t)\right)\right),
\end{aligned} \tag{218}$$

$$0 = \frac{1}{D_E^{(j)}} \left(Q_r^{(j)} + B^{(j)} \left| \overrightarrow{\mathbf{V}}_{qd0}^{(j)}(t) \right|^2 + \left| \overrightarrow{\mathbf{V}}_{qd0}^{(j)}(t) \right| \left| \overrightarrow{\mathbf{E}}_{qd0}^{(j)}(t) \right| \left(G^{(j)} \sin\left(\theta^{(j)}(t) - \hat{\theta}^{(j)}(t) \right) - B^{(j)} \cos\left(\theta^{(j)}(t) - \hat{\theta}^{(j)}(t) \right) \right) \right) - \left| \overrightarrow{\mathbf{E}}_{qd0}^{(j)}(t) \right| + E_0^{(j)}. \tag{219}$$

where $P_0^{(j)}, P_1^{(j)}, P_2^{(j)}, Q_0^{(j)}, Q_1^{(j)}$ and $Q_2^{(j)}$ denote constants for the net load at bus j, $\beta^{(j)} = 1$ if bus j is connected to an inverter-interfaced power supply and $\beta^{(j)} = 0$ otherwise.

7 Comparison of μHOm and μROm

In this section, the time resolution for the reduced-order models is discussed, and a comparison between the models responses is presented.

7.1 Model Time-Scale Stamp

The reduced-order models presented in Sections 4–6 are developed using singular perturbation analysis techniques, and the model-order reduction process is summarized in Fig. 6. For μROmi, where $i = 1,2,3$, the approximated fast dynamics are on a $\frac{t}{\varepsilon_i}$ seconds time-scale, where $\frac{1}{\varepsilon_i}$ is indicative of the eigenvalues of the fast dynamics. Given that the state variables associated with these fast dynamics reach an equilibrium in $5\varepsilon_i$ seconds, we choose the time resolution of μROm i to be $50\varepsilon_i$ seconds. Correspondingly, we can identify the time-scales for which each reduced-order model adequately approximates the μHOm.

Table 1: Model Time-Scale Stamps

	small parameter	*time-scale*
μROm1	$\varepsilon_1 = 1 \times 10^{-5}$	500 μs
μROm2	$\varepsilon_2 = 1 \times 10^{-3}$	50 ms
μROm3	$\varepsilon_3 = 0.1$	5 s

7.2 Test System

The test system used to validate all the models formulated above consists of two grid forming inverters connected to a network with an *RLC* load. A schematic is shown in Fig. 7 below, and the model parameters are shown in Table 2. Let $I^{(5)}_{lq[\omega_0 t]}(t) - \mathrm{j}I^{(5)}_{ld[\omega_0 t]}(t)$ denote the current across the load inductance.

The load model used in μHOm and μROm1 is given by:

$$\frac{C^{(5)}}{\omega_0}\frac{dV^{(5)}_{q[\omega_0 t]}(t)}{dt} = -\frac{1}{R^{(5)}}V^{(5)}_{q[\omega_0 t]}(t) - C^{(5)}V^{(5)}_{d[\omega_0 t]}(t) - I^{(5)}_{lq[\omega_0 t]}(t) + I^{(5)}_{q[\omega_0 t]}(t), \tag{220}$$

$$\frac{C^{(5)}}{\omega_0}\frac{dV^{(5)}_{d[\omega_0 t]}(t)}{dt} = -\frac{1}{R^{(5)}}V^{(5)}_{d[\omega_0 t]}(t) + C^{(5)}V^{(5)}_{q[\omega_0 t]}(t) - I^{(5)}_{ld[\omega_0 t]}(t) + I^{(5)}_{d[\omega_0 t]}(t), \tag{221}$$

$$\frac{L^{(5)}}{\omega_0}\frac{dI^{(5)}_{lq[\omega_0 t]}(t)}{dt} = -L^{(5)}I^{(5)}_{ld[\omega_0 t]}(t) + V^{(5)}_{q[\omega_0 t]}(t), \tag{222}$$

$$\frac{L^{(5)}}{\omega_0}\frac{dI^{(5)}_{ld[\omega_0 t]}(t)}{dt} = L^{(5)}I^{(5)}_{lq[\omega_0 t]}(t) + V^{(5)}_{d[\omega_0 t]}(t), \tag{223}$$

The load model used in μROm2 and μROm3 is given by:

$$\begin{aligned} V^{(5)}_{q[\omega_0 t]}(t) = {} & \frac{R^{(5)}}{1+\left(R^{(5)}C^{(5)}\right)^2}\left(I^{(5)}_{q[\omega_0 t]}(t) + \frac{V^{(5)}_{d[\omega_0 t]}(t)}{L^{(5)}}\right) \\ & - \frac{\left(R^{(5)}\right)^2 C^{(5)}}{1+\left(R^{(5)}C^{(5)}\right)^2}\left(I^{(5)}_{d[\omega_0 t]}(t) - \frac{V^{(5)}_{q[\omega_0 t]}(t)}{L^{(5)}}\right), \end{aligned} \tag{224}$$

$$\begin{aligned} V^{(5)}_{d[\omega_0 t]}(t) = {} & \frac{\left(R^{(5)}\right)^2 C^{(5)}}{1+\left(R^{(5)}C^{(5)}\right)^2}\left(I^{(5)}_{q[\omega_0 t]}(t) + \frac{V^{(5)}_{d[\omega_0 t]}(t)}{L^{(5)}}\right) \\ & + \frac{R^{(5)}}{1+\left(R^{(5)}C^{(5)}\right)^2}\left(I^{(5)}_{d[\omega_0 t]}(t) - \frac{V^{(5)}_{q[\omega_0 t]}(t)}{L^{(5)}}\right). \end{aligned} \tag{225}$$

A test case is considered where all four models have the same initial conditions, but at $t = 20$[s], the load resistance changes to $0.1\mathrm{k}\Omega$, the load inductance changes to

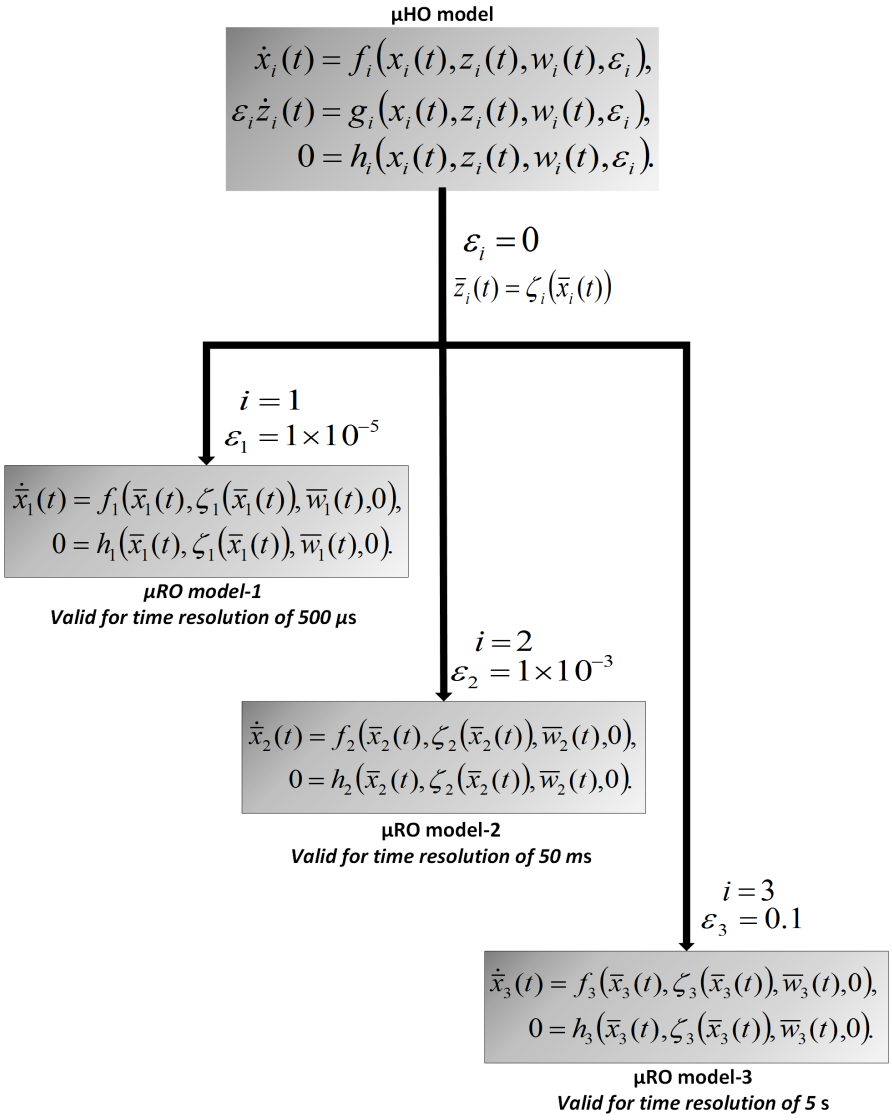

Fig. 6: Summary of Model-Order Reduction Process.

10mH and the capacitance changes to 70μF. The comparison between the models is captured in Fig. 8–11 below.

Table 2: System Parameter

	Parameter	$j=1$	$j=2$	$e=3$	$e=4$	$e'=5$
Battery	$V_{DC}^{(j)}$	900V	900V	n/a	n/a	n/a
Three-Phase Inverter	$S^{(j)}$	10kVA	12kVA	n/a	n/a	n/a
	$V_{DQ}^{(j)}$	321.0265V	321.0265V	n/a	n/a	n/a
LCL filter	$r_0^{(j)}$	0.1Ω	0.15Ω	n/a	n/a	n/a
	$l_0^{(j)}$	1.35mH	1.5mH	n/a	n/a	n/a
	$r^{(j)}$	0.03Ω	0.04Ω	n/a	n/a	n/a
	$l^{(j)}$	0.35mH	0.33mH	n/a	n/a	n/a
	$\tilde{r}_0^{(j)}$	$15\text{m}\Omega$	$16\text{m}\Omega$	n/a	n/a	n/a
	$c^{(j)}$	50μF	60μF	n/a	n/a	n/a
Inner Current Control	$\kappa_{P\gamma}^{(j)}$	10.4479	10.4479	n/a	n/a	n/a
	$\kappa_{I\gamma}^{(j)}$	6.374×10^5	6.374×10^5	n/a	n/a	n/a
Outer Voltage Control	$\kappa_{P\phi}^{(j)}$	6.1825	6.1825	n/a	n/a	n/a
	$\kappa_{I\phi}^{(j)}$	1.364×10^4	1.364×10^4	n/a	n/a	n/a
Droop Control	$D_\omega^{(j)}$	13.2629	13.2629	n/a	n/a	n/a
	$D_E^{(j)}$	2.3368	2.3368	n/a	n/a	n/a
Network	$r^{(e)}$	n/a	n/a	0.35Ω	0.4Ω	n/a
	$l^{(e)}$	n/a	n/a	1.5mH	2mH	n/a
Load	$r^{(e')}$	n/a	n/a	n/a	n/a	$0.2\text{k}\Omega$
	$l^{(e')}$	n/a	n/a	n/a	n/a	11mH
	$c^{(e')}$	n/a	n/a	n/a	n/a	64μF

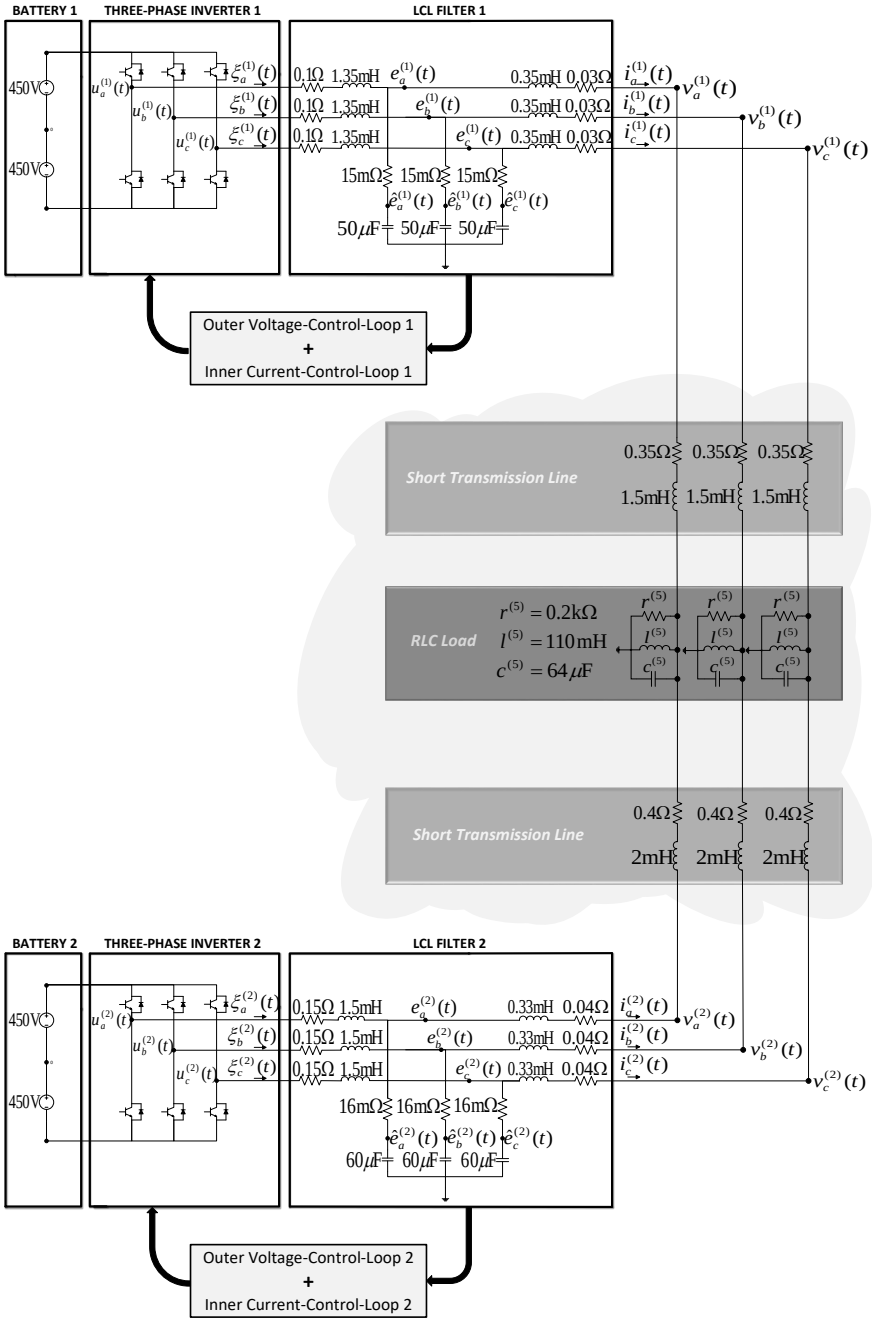

Fig. 7: Test System.

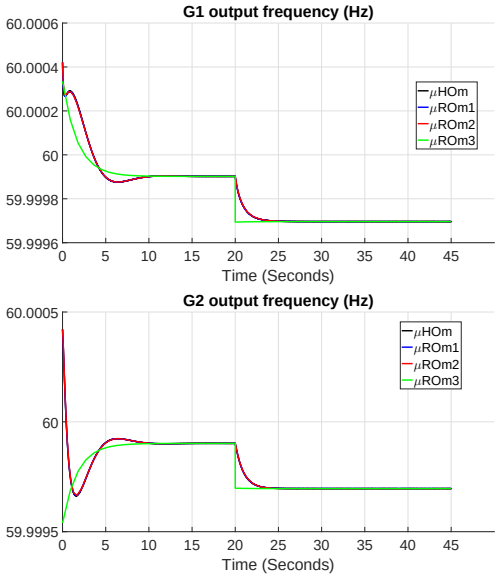

Fig. 8: Generator Output Frequency (Hz)

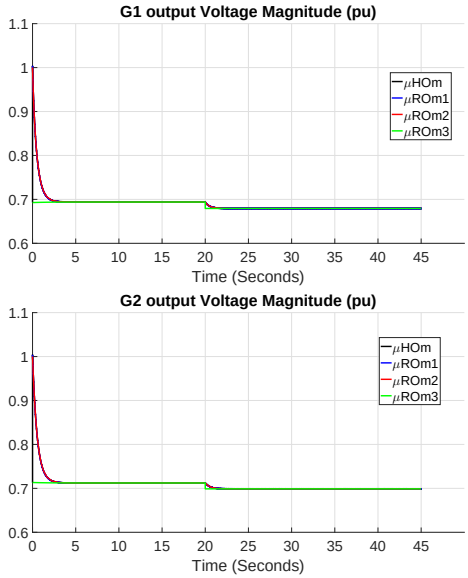

Fig. 9: Generator Output Voltage Magnitude (pu)

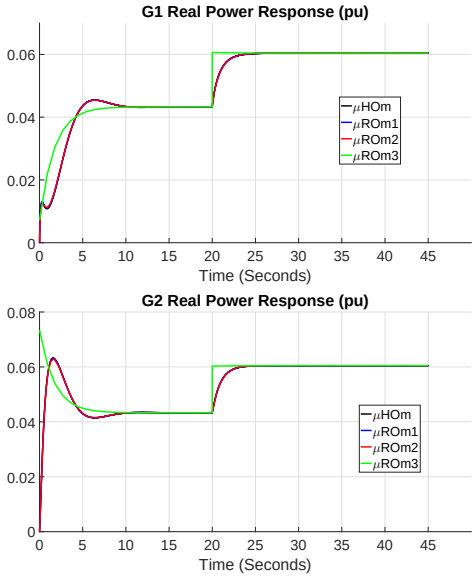

Fig. 10: Generator Output Real Power (pu)

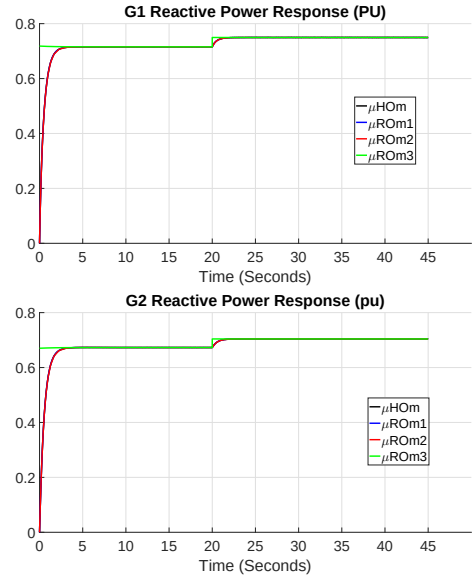

Fig. 11: Generator Output Reactive Power (pu)

References

[1] S. Anand and B. G. Fernandes. Reduced-order model and stability analysis of low-voltage dc microgrid. *IEEE Transactions on Industrial Electronics*, 60 (11):5040–5049, Nov. 2013.

[2] A.R. Bergen and V. Vittal. *Power Systems Analysis*. Prentice Hall, 2000. ISBN 9780136919902. URL https://books.google.com/books?id=4InAQwAACAAJ.

[3] A. Bidram, A. Davoudi, F. L. Lewis, and J. M. Guerrero. Distributed cooperative secondary control of microgrids using feedback linearization. *IEEE Transactions on Power Systems*, 28(3):3462–3470, Aug. 2013. ISSN 0885-8950.

[4] M.C. Chandorkar, D.M. Divan, and R. Adapa. Control of parallel connected inverters in standalone ac supply systems. *Industry Applications, IEEE Transactions on*, 29(1):136–143, 1993. ISSN 0093-9994.

[5] F. Dörfler and F. Bullo. Synchronization and transient stability in power networks and non-uniform kuramoto oscillators. In *Proceedings of the 2010 American Control Conference*, pages 930–937, June 2010.

[6] T. C. Green and M. Prodanovic. Control of inverter-based micro-grids. *Electric Power Systems Research*, 77(9):1204 – 1213, July 2007.

[7] K. Kodra, Ningfan Zhong, and Z. Gaji. Model order reduction of an islanded microgrid using singular perturbations. In *Proceedings of the 2016 American Control Conference*, pages 3650–3655, 2016.

[8] P. Kokotović, H. K. Khalil, and J. O'Reilly. *Singular Perturbation Methods in Control: Analysis and Design*. Classics in Applied Mathematics. Society for Industrial and Applied Mathematics, 1986.

[9] P.C. Krause, O. Wasynczuk, S.D. Sudhoff, S. Pekarek, Institute of Electrical, and Electronics Engineers. *Analysis of Electric Machinery and Drive Systems*. IEEE Press Series on Power Engineering. Wiley, 2013. ISBN 9781118024294. URL https://books.google.com/books?id=TVoDDQAAQBAJ.

[10] L. Luo and S. V. Dhople. Spatiotemporal model reduction of inverter-based islanded microgrids. *IEEE Transactions on Energy Conversion*, 29(4):823–832, Dec. 2014. ISSN 0885-8969.

[11] N. Pogaku, M. Prodanovic, and T. C. Green. Modeling, analysis and testing of autonomous operation of an inverter-based microgrid. *IEEE Transactions on Power Electronics*, 22(2):613–625, Mar. 2007.

[12] M. Rasheduzzaman, J. A. Mueller, and J. W. Kimball. Reduced-order small-signal model of microgrid systems. *IEEE Transactions on Sustainable Energy*, 6(4):1292–1305, Oct. 2015.

[13] P.W. Sauer and A. Pai. *Power System Dynamics and Stability*. Stipes Publishing L.L.C., 2006. ISBN 9781588746733.

[14] J. Schiffer, D. Zonetti, R. Ortega, A. M. Stankovic, T. Sezi, and J. Raisch. Modeling of microgrids - from fundamental physics to phasors and voltage sources. *CoRR*, abs/1505.00136, May 2015.

[15] A. Yazdani and R. Iravani. *Voltage-Sourced Converters in Power Systems*. Wiley, Jan. 2010.